UNIVERSITY OF CALIFORNIA, SAN DIEGO

Synthesis of Bioreversible, Phosphotriester-Modified siRNA Oligonucleotides

A dissertation in partial satisfaction of the requirements for the degree

Doctor of Philosophy

in

Biomedical Sciences

by

Bryan Richard Meade

Committee in charge:

Professor Steven F. Dowdy, Chair
Professor Jeffrey Esko
Professor Yitzhak Tor
Professor Roger Tsien
Professor Benjamin Yu

2010

The Dissertation of Bryan Richard Meade is approved, and is acceptable in quality and form for publication on microfilm and electronically:

Chair

University of California, San Diego

2010

TABLE OF CONTENTS

LIST OF FIGURES

Chapter 1

Chapter 3

Chapter 4

Chapter 5

Chapter 6

Chapter 7

ACKNOWLEDGEMENTS

First, I would like to thank my thesis advisor, mentor and friend, Dr. Steven F. Dowdy for the opportunity to not only take on a challenging and important scientific question from inception but also for instilling in me a sense of focus and drive essential for success in scientific research. The pages that follow could not have existed without his absolute and unwavering optimism. The juice was worth the squeeze.

I would also like to thank all the past members of the Dowdy Lab who I have seen come and go throughout the years. Special thanks to: Eric Snyder, for critical direction at a critical time; Jacob Gump, for constant conversation and friendship; Gary Shapiro, for constant questions and political insights; Ting-Dong Tang, for keeping the volume up and the boredom down; and all the other members that have given me a lasting memory of my time in the Dowdy Lab.

The Dowdy Laboratory, over the years, has never failed to be a dynamic and exciting place to work in, both professionally and personally. Thanks to all the current members for making the day-to-day grind of science stimulating and enjoyable. Special thanks to: Ron June, for daily updates on van maintenance; Anil Narasimha for constantly making bets he can't win; Caroline Palm-Apergi and Edwige Gros for friendship, support and bridging the alpha-beta gap; Arjen van den Berg for never failing to join me for a quick pub visit; Akiko Eguchi for putting up with the locker room chatter; and Jonathan Hagopian for friendship and support.

This thesis would not have been possible without the backbreaking teamwork in the last year. Indeed, the project would not be at all without Khirud Gogoi generating a constant stream of phosphoramidites. Thanks to Jonathan Hagopian and Arjen van den

Berg for crucial experimentation. And special thanks to Caroline Palm-Apergi for instrumental help with the Alloc-N2 deprotection strategies.

Thanks to all my friends I have made throughout all my years here, they have made San Diego a home away from home. Special thanks to Family A for putting up with more than should be expected.

Lastly, I would especially like to thank my family. I was fortunate to be raised in a very close-knit family, due primarily to a strong, loving Mother who constantly stressed the importance of family. She taught me how to think with my heart first and my head second, a life lesson to not forget. Thanks to my two wonderful Sisters, who have always been constants in inconsistent times and for all my beautiful nephews and nieces, I am convinced at least one of them will be a scientist. And finally, to my Father, who taught me the key to hard work; keep your head down, your ears open and your mouth shut. His example will forever remain the most important factor in all personal and professional success. If you want a job done right, you just do it yourself.

Chapter 4, in part, is currently being prepared for submission for publication of the material. Meade Bryan R.; Gogoi, Khirud; van den Berg, Arjen; Hagopian, Jonathan C.; Rudolph, Zachary H.; Dowdy, Steven F. The dissertation author was the primary investigator and author of this material.

Chapter 5, in part, is currently being prepared for submission for publication of the material. Gogoi, Khirud; Meade Bryan R.; van den Berg, Arjen; Hagopian, Jonathan C.; Rudolph, Zachary H.; Palm-Apergi, Caroline; Dowdy, Steven F. The dissertation author was the co-primary investigator and author of this material.

VITA

EDUCATION:

2003-2010	**Ph.D.,** Biomedical Sciences Program Department of Cellular and Molecular Medicine University of California San Diego, School of Medicine, La Jolla, CA Graduate Advisor: Professor Steven F. Dowdy, Ph.D.
1997-2001	**B.S.**, Department of Biology Saint Cloud State University, Saint Cloud, Minnesota

PROFESSIONAL EXPERIENCE:

2003-2009	*Graduate Research*, Laboratory of Steven F. Dowdy, Howard Hughes Medical Institute, Department of Cellular and Molecular Medicine, University of California San Diego, School of Medicine, La Jolla, CA. *Research Project*: Synthesis of Bioreversible, Phosphotriester-Modified siRNA Oligonucleotides.
2001-2003	*Research Technician*, Laboratory of Steven F. Dowdy, Howard Hughes Medical Institute, Department of Cellular and Molecular Medicine, University of California San Diego, School of Medicine, La Jolla, CA. *Research Project*: Synthesis of Transducible PTD-Peptides & Proteins for Cancer Therapeutics.

TEACHING:

2007	Course Coordinator, Graduate Seminars in Cancer Biology, Department of Cellular and Molecular Medicine, UC San Diego, La Jolla, CA.
2006	Teaching Assistant, Metabolic Biochemistry, Department of Biology, UC San Diego, La Jolla, CA.
1999-2001	Teaching Assistant, Biochemistry, Department of Chemistry, Saint Cloud State University, Saint Cloud, MN.

COMMITTEES:

2006	Biomedical Sciences Planning Committee, Student Representative, UC San Diego.
2005-2006	Biomedical Sciences Program Admissions Committee, UC San Diego.

RESEARCH PRESENTATIONS:

2007	*Universal Delivery of siRNAs by PTD-DRBD Fusion Proteins*, International Cell Penetrating Peptides, Telford, England.
2007	*Universal Delivery of siRNAs by PTD-DRBD Fusion Proteins*, Beyond Antibodies Conference, Carlsbad, CA.

PUBLICATIONS:

Meade BR, Gogoi K, van den Berg A, Hagopian JC, Rudolph ZH, Dowdy SF. Synthesis of Bioreversible, Phosphotriester RNA-Inducing RiboNucleic Neutral Oligonucleotides. *In preparation*.

Meade BR, Gogoi K, van den Berg A, Hagopian JC, Rudolph ZH, Palm-Apergi C, Dowdy SF. Synthesis and Structure Analysis of Bioreversible S-Acyl Thioester Containing Phosphotriester RNAi-Inducing Oligonucleotides. *In preparation.*

Meade BR, Dowdy SF. The road to therapeutic RNA interference (RNAi): Tackling the 800 pound siRNA delivery gorilla. Discov Med 2009;8:253-6.

Eguchi A, **Meade BR**, Chang YC, et al. Efficient siRNA delivery into primary cells by a peptide transduction domain-dsRNA binding domain fusion protein. Nat Biotechnol 2009;27:567-71.

Meade BR, Dowdy SF. Enhancing the cellular uptake of siRNA duplexes following noncovalent packaging with protein transduction domain peptides. Adv Drug Deliv Rev 2008;60:530-6.

Meade BR, Dowdy SF. Exogenous siRNA delivery using peptide transduction domains/cell penetrating peptides. Adv Drug Deliv Rev 2007;59:134-40.

Snyder EL, Saenz CC, Denicourt C, **Meade BR**, Cui XS, Kaplan IM, Dowdy SF. Enhanced targeting and killing of tumor cells expressing the CXC chemokine receptor 4 by transducible anticancer peptides. Cancer Res 2005;65:10646-50.

Snyder EL, **Meade BR**, Saenz CC, Dowdy SF. Treatment of terminal peritoneal carcinomatosis by a transducible p53-activating peptide. PLoS Biol 2004;2:E36.

Snyder EL, **Meade BR**, Dowdy SF. Anti-cancer protein transduction strategies: reconstitution of p27 tumor suppressor function. J Control Release 2003;91:45-51.

ABSTRACT OF THE DISSERTATION

Synthesis of Bioreversible, Phosphotriester-Modified siRNA Oligonucleotides

by

Bryan Richard Meade

Doctor of Philosophy in Biomedical Sciences

University of California, San Diego, 2010

Professor Steven F. Dowdy, Chair

The observation that synthetic siRNA molecules could induce RNAi responses following exogenous addition to human cells opened up an entirely new avenue for human disease intervention. Unfortunately, due a size of ~14,000 Da and inherent anionic character from the phosphodiester backbone, synthetic siRNA molecules fail to traverse the cellular membrane and display unfavorable pharmacokinetic patterns *in vivo*. The challenge has been to create safe and efficient delivery systems in order for siRNA therapeutics to begin to be translated into clinically-relevant settings. To date, the majority of siRNA delivery

strategies have relied on nanoparticle formulations. Due to inherent problems of nanoparticle-based delivery systems, our laboratory has sought to design soluble, monomeric siRNA delivery strategies utilizing a class of small cationic peptides termed Peptide Transduction Domains (PTDs). Unfortunately, PTD-siRNA conjugation strategies have failed in enhancing the delivery of siRNA molecules due to PTD-neutralization from the strong anionic charge of the siRNA phosphodiester. In an attempt to circumvent the anionic properties of the siRNA backbone, our laboratory began novel oligonucleotide synthesis routes to mask phosphodiester linkages with bioreversible, phosphotriester modifications. Building upon the S-Acyl-ThioEthyl (SATE) phosphotriester linkage, a cytoplasmic thioesterase sensitive linkage used for small molecule pro-drugs, we have successfully synthesized a collection of phosphodiester-neutral siRNN oligonucleotides. SATE-modified siRNN molecules were shown to be efficiently synthesized and displayed robust RNAi responses in cells in culture following cytoplasmic conversion to RNAi-compatible phosphodiesters. However, creation of PTD-siRNN conjugates with the standard SATE modifications were futile due to the extensive hydrophobicity donated from the SATE modification. In order to circumvent this hydrophobicity barrier, we synthesized a collection of Amino-SATE (N-SATE) phosphotriester siRNN containing terminal primary amines to increase the solubility of PTD-siRNN conjugates. Indeed, N-SATE siRNNs have been successfully synthesized, induce efficient RNAi responses and have succeeded in overcoming hydrophobic issues associated with SATE siRNN

oligonucleotides. Due to this increase in solubility, PTD-siRNN conjugation attempts are currently underway to determine the ability of PTD-siRNN to function as a viable siRNA delivery platform.

CHAPTER 1

INTRODUCTION

ABSTRACT

The discovery of RNA interference (RNAi) and the subsequent observation that synthetic short interfering RNA (siRNA) molecules could be used to induce sequence-specific mRNA downregulation in human cells has opened up an entirely new strategy for oligonucleotide therapeutics. Unfortunately, with a size of ~14,000 Da and extreme anionic character due to the requisite phosphodiester backbone, siRNA molecules require the aid of a delivery vector before therapeutic success can be attained. Multiple delivery systems have been developed to aid in the delivery of siRNA molecules, the majority of which utilize nanoparticle packaging schemes similar in design to nonviral delivery vehicles for antisense and gene therapy applications of the previous decade. In order to avoid inherent problems associated with these nanoparticle strategies, our laboratory has attempted to develop siRNA delivery platforms utilizing Peptide Transduction Domains (PTDs) with the goal of delivering siRNA as soluble, monomeric molecules.

INDUCTION OF RNA INTERFERENCE WITH SYNTHETIC SIRNA

The observation that long double-stranded RNA molecules (dsRNA) can lead to gene-specific silencing in *Caenorhabditis elegans* was a breakthrough observation, altering the paradigm of gene expression regulation and catapulting the idea that endogenously expressed dsRNA molecules play a functional role in gene regulation (Fire, et al. 1998). Since this initial discovery, the process of RNA interference (RNAi) has been shown to be an evolutionarily conserved mechanism spanning multiple species. In mammalian cells, it is known that endogenously expressed long dsRNA molecules undergo a multi-step processing pathway prior to activation of RNAi. The primary RNA transcript, termed pri-miRNA, is initially processed into ~70 base pair (bp) stem-loop pre-miRNA fragments by a Microprocessor complex containing the RNase III enzyme Drosha (Lee, et al. 2003). Following pre-miRNA processing and nuclear export, the RNase enzyme Dicer further processes the pre-miRNA into shorter dsRNA molecules of approximately 19 – 23 bp in length containing characteristic two nucleotide 3' overhangs (Bernstein, et al. 2001). Following this processing, these small dsRNA duplexes, termed either microRNA (miRNA) or small interfering RNA (siRNA), become the effector molecules for RNAi (Reviewed in Sontheimer, et al. 2005).

After Dicer processing, siRNA molecules become incorporated in and activate a multiprotein complex called the RNA-induced silencing complex or RISC. Recruitment and transfer of Dicer-bound siRNA to RISC is dependent

upon the transactivating response RNA-binding protein (TRBP) (Chendrimada, et al. 2005). This TRBP-mediated transfer of the siRNA passes the siRNA from the Dicer enzyme to Argonaute 2 (Ago2) (Wang, et al. 2009), the RNase component of RISC required for catalytic activity (Liu, et al. 2004). Upon incorporation into Ago2, one of the RNA strands is chosen based on the thermodynamic stability of the 5' ends (Preall, et al. 2006). The strand with the less thermodynamically stable 5' end becomes incorporated into RISC and is termed the guide strand. The alternate strand, or passenger strand, is cleaved and disassociates from the active RISC. The RISC-bound guide strand is now able to direct complementarity to mRNA transcripts shuttling from the nucleus to ribosomes for translation initiation. After guide strand directed complementation to mRNA transcripts, Ago2 down regulates gene expression by cleaving mRNA molecules and thus inhibiting translation of specific mRNA. This cleavage occurs at a specific location, at the mRNA phosphodiester adjacent to bases 10 – 11 when counting from the 5' end of the guide strand. Following mRNA cleavage, a single guide strand-loaded RISC is capable of a multiple rounds of mRNA cleavage making RISC-mediated downregulation of mRNA transcripts a powerfully catalytic event (Sontheimer, et al. 2005).

Perhaps the most significant work to occur in the years immediately following the discovery of RNAi was the observation that RNAi could be triggered within human cells following the exogenous addition of synthetic siRNA molecules (Elbashir, et al. 2001). Upon introduction into the cytoplasm of

mammalian cells, these synthetic siRNA molecules have been shown to hijack the endogenous RNAi machinery, bypass upstream processing and become incorporated into RISC, inducing RNAi against target mRNA transcripts. Not only was this observation one of the first indications that RNAi occurred in human cells but it also opened up an entirely new set of experimental tools for the world of cellular biology. This technique has since become the standard for gene function determination as well as exciting the scientific community with a new and potentially promising therapeutic strategy.

From a therapeutic prospective, siRNAs possess many positive therapeutic attributes (Tiemann, et al. 2009). Due to the catalytic nature of siRNA-loaded RISC, siRNA therapeutic strategies allow for the downregulation of specific mRNA targets at very low, picomolar concentrations. Because a multitude of disease states are caused by aberrant gene expression, siRNAs offer a potential drug candidate that could alter the progression of a wide variety of human disease conditions. Additionally, because siRNA molecules are chemically synthesized in a sequence independent manner, they can be rapidly generated against any desired target mRNA sequence with no alteration of synthetic chemistry. Moreover, siRNAs have a similar backbone composition/structure and therefore metabolism and the body's response will most likely be similar between different siRNA sequences.

However, while synthetic siRNAs hold exceptional promise in being used for the treatment of human disease, these molecules also possess significant

therapeutic drawbacks. With a size of ~14,000 Da and extreme hydrophilicity due to an 40 anionic phosphodiester charges, siRNA molecules do not traverse the cellular membrane. These same characteristics also make the pharmacokinetic properties of siRNAs unfavorable as systemic administration of naked siRNAs into the bloodstream results in rapid degradation and renal excretion within minutes following injection in murine models assaying siRNA biodistribution (Merkel, et al. 2009). Due to these fundamental problems, delivery reagents are necessary to both increase the circulation time following systemic administration as well as aid in the passage of siRNA across the cellular membrane of the target cell.

SYNTHETIC SIRNA DELIVERY STRATEGIES

Upon the discovery that synthetic siRNA molecules could induce RNAi responses, a plethora of studies began to appear in the literature showing the utility of a vast array of siRNA delivery strategies. The rapidity at which these studies began to be published was a testament to the prior decade's work on nonviral-mediated delivery systems for both gene therapy and antisense oligonucleotide therapy. Similar to the previous decade's technological advances, the vast majority of siRNA delivery systems have focused on overcoming the pharmacokinetic obstacles by encapsulating siRNA molecules within nanoparticle structures. While nanoparticle-based delivery systems are extremely variable and can have properties independent of one another, it is beyond the scope of this introduction to attempt to describe the entirety of these

comparisons. Generally speaking, nanoparticle-based delivery systems are delivery reagents that condense siRNA into particles in the optimal size range of hundreds of nanometers. The predominant packaging scheme for these nanoparticle formulations is to utilize the anionic charge of the siRNA backbone as a scaffold for electrostatic interaction with the delivery reagent. Cationic lipids, cationic polymers and cationic peptides are used with different effectiveness to engage the negatively charged phosphodiester backbone and organize large numbers of siRNA molecules into nanoparticle structures prior to cellular treatment *in vitro* or systemic administration *in vivo* (Reviewed in Whitehead, et al. 2009).

In addition to cationic motifs required for siRNA nanoparticle formation, additional motifs are also applied to these delivery reagents. A large variety of lipids, cell targeting ligands, antibodies and cell penetrating peptides, to list a few, have been covalently tethered to the cationic packaging motifs so the resulting nanoparticles that are formed will have cellular homing and delivery properties (Schroeder, et al. 2010). The resulting nanoparticles that are formed have multiple advantages. Importantly, compaction of the siRNA oligonucleotide renders them inaccessible to RNase degradation and thus, increases the half-life of the oligonuceotide *in vivo*. Additionally, the large size and hydrophobic nature of the particle increases the circulation time following systemic administration due to the size restrictions of kidney filtration and its ability to interact with serum factors. With the increased circulation time, these siRNA-containing

nanoparticles have a higher probability of not only engaging the desired target cells but also delivering the siRNA cargo across the target cell membrane. Indeed, based on these advantageous characteristics, nanoparticle-based siRNA delivery systems have been shown to work within multiple animal models of human disease (Reviewed in Tiemann, et al. 2009).

Utilizing this conventional nanoparticle-based strategy, multiple siRNA delivery strategies have been implemented including, but not limited to, antibody-protamine fusions (Song, et al. 2005; Peer, et al. 2007), polyethylenimine polymers (PEI) (Urban-Klein, et al. 2005), chitosan polymers (Howard, et al. 2006), MPG peptide (Crombez, et al. 2007), LDL-packaged cholesterol-siRNA fusions (Soutschek, et al. 2004; Wolfrum, et al. 2007), rabies virus glycoprotein (RVG)-9Arg fusion peptide (Kumar, et al. 2007), and a plethora of cationic lipid-based delivery systems (Akinc, et al. 2008; Schroeder, et al. 2010). While these published studies offer advancements for nanoparticle-based delivery of siRNA oligonucleotides, the literature landscape remains for the most part unchanged when making generalized comparisons to nucleic acid delivery systems of the previous decade.

So for all the benefits nanoparticle-based delivery systems have to offer, the question remains: are these the ideal siRNA delivery platforms as siRNA delivery technology begins its second decade? Cationic polymer and cationic lipid-based systems are known to be toxic, due to both the non-natural composition of the polymer and lipid moieties as well as the excessive cationic

charge ratio that is required for packaging. Indeed, primary cells in culture are notoriously subject to toxic responses to these delivery systems. Additionally, while particle formation is sufficient to avoid renal excretion following systemic administration in mice, the size and hydrophobicity of the circulating particles become subject to filtration by Kupffer cells, specialized macrophages located in the liver (Akinc, et al. 2009; Schroeder, et al. 2010). This biodistribution pattern is highlighted by the large number of studies that assay RNAi in the liver following systemic administration of siRNA-nanoparticle formulations (Whitehead, et al. 2009).

For the small percentage of particles that avoid filtration and reach the target tissue, there is an additional step of particle shedding that needs to occur for the siRNA to be released into the cytoplasm and subsequent RISC loading. In addition to these potential drawbacks of nanoparticle-based delivery systems, great care needs to taken during nanoparticle formulation to ensure formation of particles of an accurate size. It is generally accepted that size limitations for siRNA-nanoparticles require formation of particles <100 nm in order to avoid *in vivo* barriers including blood components, reticuloendothelial system and extacellular matrix components (Li, et al. 2007). Correct particle size requirements create a need for exacting formulation conditions including correct siRNA/vector ratios, correct time and conditions for nanoparticle formation, and assays to ensure the presence of homogenously-sized particle mixtures.

Due to these concerns as well as the dilution of published studies on nanoparticle-based formulations, our laboratory began thinking of ways in which we could generate siRNA delivery systems that avoid standard nanoparticle packaging. Nanoparticles in the 100 nm range represent molecular weights of ~100,000,000 Da while siRNA molecules themselves are a mere ~14,000 Da in size, thus bringing to mind the analogy of trying to tee-off with a golf ball that is packed inside a watermelon. We hypothesized that a synthetic siRNA molecule delivered as a single, soluble entity would not only display higher potency but would also have more favorable pharmacokinetic properties within *in vivo* model systems, bypassing multiple *in vivo* barriers that large nanoparticles are subject to. We have attempted to do so utilizing a tool for cellular delivery of macromolecules that our lab has extensive experience with: a class of small cationic peptides termed Peptide Transduction Domains (PTDs).

PEPTIDE TRANSDUCTION DOMAINS – A BRIEF HISTORY

In 1988, Frankel and Pabo observed that the exogenous addition of full-length HIV-1 TAT protein to cells in culture resulted in cell membrane penetration and trans-activation of the HIV-1 promoter (Frankel, et al. 1988). Subsequent experimentation delineated the requirements for protein translocation and defined a small basic region spanning residues 49 to 58 of HIV-1 TAT responsible for cellular uptake (Vives, et al. 1997). Concurrently, another PTD domain was derived from the third alpha helix of the Antennapedia homeodomain protein (Derossi, et al. 1994). This 16-mer peptide, termed Antp and marketed as

Penetratin, is similar to the HIV-1 TAT protein domain in that it contains a high density of basic charges crucial for mediating cellular entrance. Since these initial observations, multiple PTDs have been discovered and chimeric, synthetic peptide sequences have been derived, including transportan (Pooga, et al. 2001), HSV-1 protein VP22 (Elliot, et al. 1997), MPG (Morris, et al. 1997), and polyarginine (Futaki, et al. 2001).

PTDs have been utilized for the delivery of a wide range of cargoes, including proteins and peptides (Snyder, et al. 2005), antisense and charge neutral, peptide nucleic acids (PNA) (Gait, 2003), plasmid DNA (Eguchi, et al. 2001), liposomes (Torchilin, et al. 2001) and iron beads (Lewin, et al. 2001). The wide range of cargo size and composition accentuates the versatility that PTDs offer in the successful delivery of macromolecules across the cellular membrane. Importantly, the in vivo potential of CPPs was realized in 1999 when our laboratory described the delivery of a 120-kDa recombinant β-galactosidase protein fused to the TAT domain. Intraperitoneal administration of TAT-βgal protein resulted in the delivery into most, if not all, tissues of the mouse, including the brain, while a TAT-minus βgal resulted in little to no tissue detection (Schwarze, et al. 1999). This observation highlighted the therapeutic power of PTD-mediated delivery and opened the door for the use of small cationic peptides in the systemic delivery of information rich macromolecules.

Early studies of the uptake mechanism of PTDs suggested that the process of internalization appeared distinct from traditional forms of endocytosis.

Cell membrane translocation was not significantly inhibited by treatment at low temperatures, depletion of intracellular ATP or by various inhibitors of endocytosis (Derossi, et al. 1994; Vives, et al. 1997). However, these observations were subsequently attributed to cellular fixation artifacts and misinterpretation of flow cytometry analysis of cells treated with fluorescently labeled peptides (Richard, et al. 2003; Lundberg, et al. 2001). More recent studies have shown the importance of various forms of endocytosis on the internalization process of PTDs (Ferrari, et al. 2003; Lundberg, et al. 2003; Foerg, et al. 2005). Our own studies strongly point to a role for macropinocytosis, a specialized form of fluid phase endocytosis, in the uptake of at least one PTD, specifically TAT peptide and TAT-fused proteins (Wadia, et al. 2004; Kaplan, et al. 2005; Gump, et al. 2009). Discrepancies in the various forms of endocytosis deemed responsible for cellular entrance are most likely due to either the differences in PTDs and cell types tested or the lack of phenotypic assays used in the majority these PTD internalization studies. Nonetheless, it has become clear that PTDs utilize classical forms of endocytosis to gain access to the intracellular environment.

Of significant importance is the observation that PTDs do more than simply bind the cell surface and gain access to endosomes through constitutive endocytosis. Our laboratory has shown that PTDs rapidly induce their own uptake upon binding to the cell membrane and that this cellular uptake mechanism is independent of heparan sulfate proteoglycan binding (Gump, et al.

2010). This event most likely occurs through stimulation of intracellular signaling cascades that induce membrane ruffling and macropinocytosis (Wadia, et al. 2004). Though PTDs become internalized by endocytosis, endosomes are still, in affect, similar to the extracellular environment in that passage across the membrane has not been accomplished. The physical mechanism of translocation across the endocytic membrane is still in debate and has been attributed to inherent leakiness of certain endocytic bodies (Kawamura, et al. 2006), retrograde transport of CPP containing endosomes (Fischer, et al. 2004) and PTD-induced disruption of the endocytic cell membrane (Rothbard, et al. 2005). Whether different PTDs share a similar endocytic escape mechanism has yet to be determined.

In summary, PTDs define an extremely efficient delivery system, emphasized by their ability to allow macromolecular translocation within multiple tissues *in vivo* upon systemic administration (Schwarze, et al. 1999) and the capability of inducing cell penetration within 100% of cells of a given cell culture population (Wadia, et al. 2004). Moreover, PTDs are currently being tested in multiple phase I and II clinical trials for delivery of macromolecular peptide and protein cargo in myocardial infarct, cancer and pain (Gump, et al. 2007). Consequently, PTD-mediated delivery offers great potential for the application to synthetic siRNA therapeutics.

PTD-MEDIATED DELIVERY OF siRNA OLIGONUCLEOTIDES

The dense cationic charge of PTDs is the crucial property that gives these

peptides cell membrane interaction and translocation abilities. These cationic motifs also have a high affinity for nucleic acids and the predominant strategy that has been utilized for PTD-mediated siRNA delivery has been the noncovalent compaction of siRNA into nanoparticles using high molar excess of PTDs during nanoparticle formation. When utilized in this fashion, PTDs can be thought of as other frequently used cationic polymers such as PEI or protamine. While significantly smaller in mass, at high enough molar ratios PTDs can be sufficient to condense siRNA molecules similar to other nanoparticle scaffolding motifs (Meade, et al. 2008).

However, in order to produce soluble, monomeric siRNA delivery systems with PTDs, great care must be taken to avoid this electrostatic packaging and ensure covalent conjugation and purification of PTD-siRNA conjugates prior to cellular treatment (Meade, et al. 2007). Three early reports exist in the literature describing RNAi induction following cellular treatment with PTD-siRNA conjugates. These include covalent conjugation strategies for Penetratin-siRNA (Muratovska, et al. 2004), TAT-siRNA (Chiu, et al. 2004) and Transportan-siRNA conjugates (Davidson, et al. 2004; Muratovska, et al. 2004). Unfortunately, in our hands, these observations were not reproduced following cellular treatment with purified PTD-siRNA conjugates (See Chapter 3).

The most likely reason for this lack of reproducibility of successful siRNA delivery following PTD-siRNA conjugation is due to technical issues of ensuring solubility of PTD-siRNA conjugates during cellular treatment. Of the few reports

that have used PTD-siRNA conjugates *in vitro*, all have failed to emphasize the difficulties inherent to applying cationic peptides to the delivery of anionic cargo. In our own unpublished studies, we have demonstrated difficulties associated with keeping PTD-siRNA conjugates soluble while still maintaining the capability of gaining access to the intracellular environment for induction of RNA interference. The accessibility of the basic charges of PTDs is crucial for their interaction with the components of the cell membrane that are responsible for inducing cellular uptake (Jiang, et al. 2004). Unfortunately, charge neutralization of PTDs upon covalent attachment of anionic siRNA duplexes hinders the availability of crucial basic residues to interact with cellular membrane components critical for cellular entrance. In our hands, cellular entrance only occurs upon positively charged aggregate formation in cell culture media produced from lack of purification of PTD-siRNA from the free PTD peptide present in the conjugation reaction condition. In support of this hypothesis are two other independent groups that have reported the inability to deliver PTD-siRNA conjugates into cells (Moschos, et al. 2007; Turner, et al. 2007).

OVERCOMING THE SIRNA NEGATIVE CHARGE WITH PTD-DRBD

Following the negative results of inducing RNAi responses with PTD-siRNA conjugates, our laboratory began exploring ways in which we could overcome the anionic character of the siRNA molecule to allow for the efficiency of PTD delivery to be utilized for RNAi technology. Our first strategy involved the generation of PTD-fusion proteins with double-stranded RNA binding domains

(DRBDs) under the hypothesis that interaction of PTD-DRBD with siRNA would result in DRBD engagement of the siRNA molecule, thereby masking the negative charges of the siRNA phosphodiester backbone and allow for the fused PTD to interact with the cell surface and induce internalization (Figure 1.1A) (Eguchi, et al. 2009). We chose a small, ~65 residue DRBD domain from dsRNA-activated protein kinase (PKR), which is known to bind siRNA with high avidity (K_D~10^{-9}) along a ~12 – 16 base-pair distance on the siRNA backbone (Bevilacqua, et al. 1996; Ryter, et al. 1998). Importantly, due to these structural characteristics, multiple DRBDs can engage a single siRNA, and thus, multiple PTDs can aid in the delivery of a single siRNA molecule in a soluble fashion (Figure 1.1A).

True to our hypothesis, PTD-DRBD complexation with siRNA and subsequent cellular treatment resulted in PTD-mediated uptake and induction of RNAi responses. Typical of PTD-mediated macromolecular delivery, PTD-DRBD was able to successfully deliver multiple siRNAs in a noncytotoxic fashion into a large panel of ~20 different human cell lines *in vitro* including difficult to transfect T cells, heart and umbilical vein endothelial cells (HUVECs), and human embryonic stem cells. Indeed, in a head-to-head comparison with a common cationic lipid siRNA transfection reagent, PTD-DRBD was able to show significant delivery enhancements including >99% delivery efficiency, induction of a complete RNAi response in as little as 6 hours as assayed by quantitative RT-PCR and significantly lower off-target effects as profiled by whole-genome

microarrays (Eguchi, et al. 2009). The *in vivo* effectiveness of siRNA delivery with PTD-DRBD was also shown in a murine intranasal luciferase reporter model system (Eguchi, et al. 2009) as well as in an intracerebral glioblastoma model in a combination siRNA delivery strategy with Akt2 and EGFR siRNA (Michiue, et al. 2009).

In summary, our work with PTD-DRBD showed us that the delivery potential of PTDs can be attained for siRNA molecules assuming that the anionic character of the siRNA oligo is somehow manipulated to allow for the cationic properties of PTD peptides to be unencumbered.

CONCLUSIONS

The discovery that synthetic siRNA molecules could be used to induce RNAi responses in human cells created not only a tool for cellular biologists, but also opened up the potential for RNAi therapeutics. Unfortunately, at ~14,000 Da and extreme acidity, siRNA oligonucleotides present significant challenges as a therapeutic modality. A plethora of nanoparticle-based siRNA delivery strategies have been published translating the delivery vectors of the previous decade for antisense and gene therapy applications. In order to avoid significant *in vivo* barriers of nanoparticle-based delivery systems, our laboratory has attempted to think outside this box, developing siRNA delivery platforms that utilize the delivery properties of cationic PTDs to deliver siRNA molecules in a soluble, monomeric fashion. The use of PTD-DRBD to deliver siRNA efficiently into cells in culture and *in vivo* mouse models has shown us that the main obstacle to overcome when utilizing PTDs for soluble siRNA delivery is the anionic phosphodiester backbone charge of the siRNA molecule. In the absence of a blocking or neutralizing entity, the cationic residues of PTD peptides lack the ability to engage the cell surface and successfully deliver the siRNA oligonucleotide. However, when the acidic phosphodiester charges are appropriately masked, the delivery efficiency of PTDs is able to be translated to siRNA delivery technology.

A

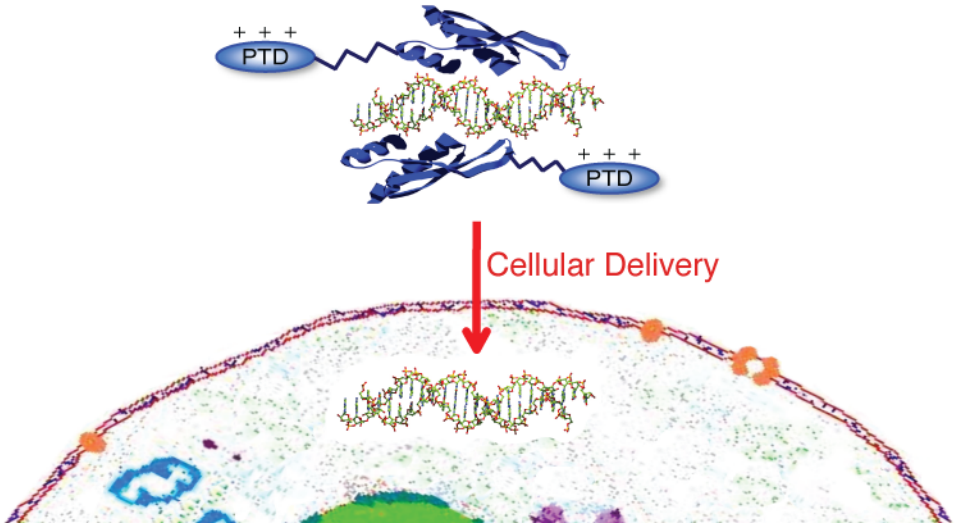

Figure 1.1. Overcoming the siRNA negative charge for PTD-mediated siRNA delivery. A) Scheme for PTD-DRBD complexing and delivery of siRNA molecules. The DRBD interaction of siRNA molecules allows for multiple PTD-DRBDs to aid in the delivery of a single siRNA molecule.

REFERENCES

Akinc A, Goldberg M, Qin J, et al. Development of lipidoid-siRNA formulations for systemic delivery to the liver. Mol Ther 2009;17:872-9.

Akinc A, Zumbuehl A, Goldberg M, et al. A combinatorial library of lipid-like materials for delivery of RNAi therapeutics. Nat Biotechnol 2008;26:561-9.

Bernstein E, Caudy AA, Hammond SM, Hannon GJ. Role for a bidentate ribonuclease in the initiation step of RNA interference. Nature 2001;409:363-6.

Bevilacqua PC, Cech TR. Minor-groove recognition of double-stranded RNA by the double-stranded RNA-binding domain from the RNA-activated protein kinase PKR. Biochemistry 1996;35:9983-94.

Chendrimada TP, Gregory RI, Kumaraswamy E, et al. TRBP recruits the Dicer complex to Ago2 for microRNA processing and gene silencing. Nature 2005;436:740-4.

Chiu YL, Ali A, Chu CY, Cao H, Rana TM. Visualizing a correlation between siRNA localization, cellular uptake, and RNAi in living cells. Chem Biol 2004;11:1165-75.

Crombez L, Charnet A, Morris MC, Aldrian-Herrada G, Heitz F, Divita G. A non-covalent peptide-based strategy for siRNA delivery. Biochem Soc Trans 2007;35:44-6.

Davidson TJ, Harel S, Arboleda VA, et al. Highly efficient small interfering RNA delivery to primary mammalian neurons induces MicroRNA-like effects before mRNA degradation. J Neurosci 2004;24:10040-6.

Derossi D, Joliot AH, Chassaing G, Prochiantz A. The third helix of the Antennapedia homeodomain translocates through biological membranes. J Biol Chem 1994;269:10444-50.

Eguchi A, Akuta T, Okuyama H, et al. Protein transduction domain of HIV-1 Tat protein promotes efficient delivery of DNA into mammalian cells. J Biol Chem 2001;276:26204-10.

Eguchi A, Meade BR, Chang YC, et al. Efficient siRNA delivery into primary cells by a peptide transduction domain-dsRNA binding domain fusion protein. Nat Biotechnol 2009;27:567-71.

Elbashir SM, Harborth J, Lendeckel W, Yalcin A, Weber K, Tuschl T. Duplexes of 21-nucleotide RNAs mediate RNA interference in cultured mammalian cells. Nature 2001;411:494-8.

Elliott G, O'Hare P. Intercellular trafficking and protein delivery by a herpesvirus structural protein. Cell 1997;88:223-33.

Ferrari A, Pellegrini V, Arcangeli C, Fittipaldi A, Giacca M, Beltram F. Caveolae-mediated internalization of extracellular HIV-1 tat fusion proteins visualized in real time. Mol Ther 2003;8:284-94.

Fire A, Xu S, Montgomery MK, Kostas SA, Driver SE, Mello CC. Potent and specific genetic interference by double-stranded RNA in Caenorhabditis elegans. Nature 1998;391:806-11.

Fischer R, Kohler K, Fotin-Mleczek M, Brock R. A stepwise dissection of the intracellular fate of cationic cell-penetrating peptides. J Biol Chem 2004;279:12625-35.

Foerg C, Ziegler U, Fernandez-Carneado J, et al. Decoding the entry of two novel cell-penetrating peptides in HeLa cells: lipid raft-mediated endocytosis and endosomal escape. Biochemistry 2005;44:72-81.

Frank F, Sonenberg N, Nagar B. Structural basis for 5'-nucleotide base-specific recognition of guide RNA by human AGO2. Nature 2010;465:818-22.

Frankel AD, Pabo CO. Cellular uptake of the tat protein from human immunodeficiency virus. Cell 1988;55:1189-93.

Futaki S, Suzuki T, Ohashi W, et al. Arginine-rich peptides. An abundant source of membrane-permeable peptides having potential as carriers for intracellular protein delivery. J Biol Chem 2001;276:5836-40.

Gait MJ. Peptide-mediated cellular delivery of antisense oligonucleotides and their analogues. Cell Mol Life Sci 2003;60:844-53.

Gump JM, June RK, Dowdy SF. Revised role of glycosaminoglycans in TAT protein transduction domain-mediated cellular transduction. J Biol Chem 2010;285:1500-7.

Howard KA, Rahbek UL, Liu X, et al. RNA interference in vitro and in vivo using a novel chitosan/siRNA nanoparticle system. Mol Ther 2006;14:476-84.

Jiang T, Olson ES, Nguyen QT, Roy M, Jennings PA, Tsien RY. Tumor imaging by means of proteolytic activation of cell-penetrating peptides. Proc Natl Acad Sci U S A 2004;101:17867-72.

Kaplan IM, Wadia JS, Dowdy SF. Cationic TAT peptide transduction domain enters cells by macropinocytosis. J Control Release 2005;102:247-53.

Kawamura KS, Sung M, Bolewska-Pedyczak E, Gariepy J. Probing the impact of valency on the routing of arginine-rich peptides into eukaryotic cells. Biochemistry 2006;45:1116-27.

Kim WJ, Christensen LV, Jo S, et al. Cholesteryl oligoarginine delivering vascular endothelial growth factor siRNA effectively inhibits tumor growth in colon adenocarcinoma. Mol Ther 2006;14:343-50.

Kumar P, Wu H, McBride JL, et al. Transvascular delivery of small interfering RNA to the central nervous system. Nature 2007;448:39-43.

Lee Y, Ahn C, Han J, et al. The nuclear RNase III Drosha initiates microRNA processing. Nature 2003;425:415-9.

Lewin M, Carlesso N, Tung CH, et al. Tat peptide-derivatized magnetic nanoparticles allow in vivo tracking and recovery of progenitor cells. Nat Biotechnol 2000;18:410-4.

Li W, Szoka FC, Jr. Lipid-based nanoparticles for nucleic acid delivery. Pharm Res 2007;24:438-49.

Liu J, Carmell MA, Rivas FV, et al. Argonaute2 is the catalytic engine of mammalian RNAi. Science 2004;305:1437-41.

Lundberg M, Johansson M. Is VP22 nuclear homing an artifact? Nat Biotechnol 2001;19:713-4.

Lundberg M, Wikstrom S, Johansson M. Cell surface adherence and endocytosis of protein transduction domains. Mol Ther 2003;8:143-50.

Manoharan M. RNA interference and chemically modified small interfering RNAs. Curr Opin Chem Biol 2004;8:570-9.

Meade BR, Dowdy SF. Exogenous siRNA delivery using peptide transduction domains/cell penetrating peptides. Adv Drug Deliv Rev 2007;59:134-40.

Meade BR, Dowdy SF. Enhancing the cellular uptake of siRNA duplexes following noncovalent packaging with protein transduction domain peptides. Adv Drug Deliv Rev 2008;60:530-6.

Merkel OM, Librizzi D, Pfestroff A, Schurrat T, Behe M, Kissel T. In vivo SPECT and real-time gamma camera imaging of biodistribution and pharmacokinetics of siRNA delivery using an optimized radiolabeling and purification procedure. Bioconjug Chem 2009;20:174-82.

Michiue H, Eguchi A, Scadeng M, Dowdy SF. Induction of in vivo synthetic lethal RNAi responses to treat glioblastoma. Cancer Biol Ther 2009;8:2306-13.

Morris MC, Vidal P, Chaloin L, Heitz F, Divita G. A new peptide vector for efficient delivery of oligonucleotides into mammalian cells. Nucleic Acids Res 1997;25:2730-6.

Moschos SA, Jones SW, Perry MM, et al. Lung delivery studies using siRNA conjugated to TAT(48-60) and penetratin reveal peptide induced reduction in gene expression and induction of innate immunity. Bioconjug Chem 2007;18:1450-9.

Muratovska A, Eccles MR. Conjugate for efficient delivery of short interfering RNA (siRNA) into mammalian cells. FEBS Lett 2004;558:63-8.

Peer D, Zhu P, Carman CV, Lieberman J, Shimaoka M. Selective gene silencing in activated leukocytes by targeting siRNAs to the integrin lymphocyte function-associated antigen-1. Proc Natl Acad Sci U S A 2007;104:4095-100.

Pooga M, Kut C, Kihlmark M, et al. Cellular translocation of proteins by transportan. FASEB J 2001;15:1451-3.

Preall JB, He Z, Gorra JM, Sontheimer EJ. Short interfering RNA strand selection is independent of dsRNA processing polarity during RNAi in Drosophila. Curr Biol 2006;16:530-5.

Richard JP, Melikov K, Vives E, et al. Cell-penetrating peptides. A reevaluation of the mechanism of cellular uptake. J Biol Chem 2003;278:585-90.

Rothbard JB, Jessop TC, Wender PA. Adaptive translocation: the role of hydrogen bonding and membrane potential in the uptake of guanidinium-rich transporters into cells. Adv Drug Deliv Rev 2005;57:495-504.

Ryter JM, Schultz SC. Molecular basis of double-stranded RNA-protein interactions: structure of a dsRNA-binding domain complexed with dsRNA. EMBO J 1998;17:7505-13.

Schroeder A, Levins CG, Cortez C, Langer R, Anderson DG. Lipid-based nanotherapeutics for siRNA delivery. J Intern Med 2010;267:9-21.

Schwarze SR, Ho A, Vocero-Akbani A, Dowdy SF. In vivo protein transduction: delivery of a biologically active protein into the mouse. Science 1999;285:1569-72.

Snyder EL, Dowdy SF. Recent advances in the use of protein transduction domains for the delivery of peptides, proteins and nucleic acids in vivo. Expert Opin Drug Deliv 2005;2:43-51.

Song E, Zhu P, Lee SK, et al. Antibody mediated in vivo delivery of small interfering RNAs via cell-surface receptors. Nat Biotechnol 2005;23:709-17.

Song JJ, Smith SK, Hannon GJ, Joshua-Tor L. Crystal structure of Argonaute and its implications for RISC slicer activity. Science 2004;305:1434-7.

Sontheimer EJ. Assembly and function of RNA silencing complexes. Nat Rev Mol Cell Biol 2005;6:127-38.

Soutschek J, Akinc A, Bramlage B, et al. Therapeutic silencing of an endogenous gene by systemic administration of modified siRNAs. Nature 2004;432:173-8.

Tiemann K, Rossi JJ. RNAi-based therapeutics-current status, challenges and prospects. EMBO Mol Med 2009;1:142-51.

Torchilin VP, Rammohan R, Weissig V, Levchenko TS. TAT peptide on the surface of liposomes affords their efficient intracellular delivery even at low temperature and in the presence of metabolic inhibitors. Proc Natl Acad Sci U S A 2001;98:8786-91.

Turner JJ, Jones S, Fabani MM, Ivanova G, Arzumanov AA, Gait MJ. RNA targeting with peptide conjugates of oligonucleotides, siRNA and PNA. Blood Cells Mol Dis 2007;38:1-7.

Urban-Klein B, Werth S, Abuharbeid S, Czubayko F, Aigner A. RNAi-mediated gene-targeting through systemic application of polyethylenimine (PEI)-complexed siRNA in vivo. Gene Ther 2005;12:461-6.

Vives E, Brodin P, Lebleu B. A truncated HIV-1 Tat protein basic domain rapidly translocates through the plasma membrane and accumulates in the cell nucleus. J Biol Chem 1997;272:16010-7.

Wadia JS, Stan RV, Dowdy SF. Transducible TAT-HA fusogenic peptide enhances escape of TAT-fusion proteins after lipid raft macropinocytosis. Nat Med 2004;10:310-5.

Wang HW, Noland C, Siridechadilok B, et al. Structural insights into RNA processing by the human RISC-loading complex. Nat Struct Mol Biol 2009;16:1148-53.

Whitehead KA, Langer R, Anderson DG. Knocking down barriers: advances in siRNA delivery. Nat Rev Drug Discov 2009;8:129-38.

Wolfrum C, Shi S, Jayaprakash KN, et al. Mechanisms and optimization of in vivo delivery of lipophilic siRNAs. Nat Biotechnol 2007;25:1149-57.

CHAPTER 2

MATERIALS AND METHODS

Phosphoramidite Synthesis

All phosporamidites were synthesized using the following scheme. An example protocol for the generation of 5'-O-(4,4'-Dimethoxytrityl)-2'-F-uridine 3'-O-[(S-pivaloyl-2-thioethyl) N,N-diisopropylphosphoramidite] is listed below:

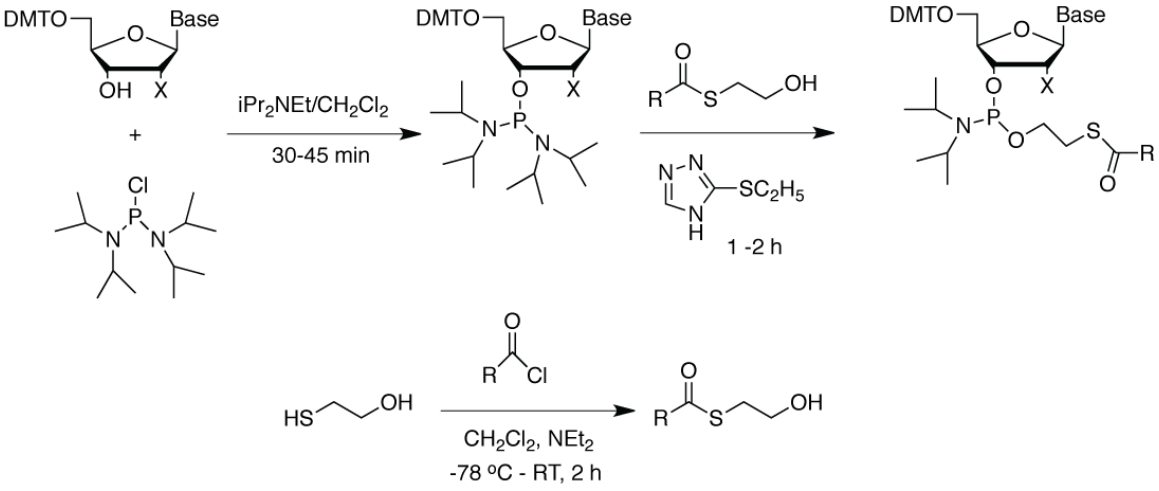

A solution of bis-(*N,N*-disiopropylamino)-chlorophosphine (1 g, 0.4 mmol) in dry CH_2Cl_2 (5 ml) was added drop-wise to a magnetically stirred cooled solution (-78 ^{0}C) of 5'-*O*-(4,4'-Dimethoxytrityl)-2'-F-uridine (2 g, 0.364 mmol)(**1**) and *N,N*-diisopropylethylamine (0.71 ml, 0.4 mmol) in dry CH_2Cl_2 (24 ml). The reaction mixture was allowed to warm to room temperature while stirring was maintained (45 min). S-(2-hydroxyethyl) thiopivaloate (0.65 g, 0.4 mmol) in 5 ml dry CH_2Cl_2 was added portion wise and stirred for 10 min. Then ethyl thiotetrazole (7.3 ml, 0.25 M solution in acetonitrile, 0.182 mmol) was added to

the reaction mixture and the reaction mixture was stirred for 1.5 hr. Then CH_2Cl_2 (60 ml) was added and the reaction mixture was washed with saturated aqueous sodium hydrogen carbonate (20 ml) and brine (2 x 20 ml) and dried over anhydrous sodium sulfate. The solvent was evaporated *in vacuo* and the residue was subjected to flash silica gel column purification on a combiflash instrument using hexane-ethyl acetate (0.5% TEA) as the solvent. The fractions containing the products were pulled together and evaporated to dryness. The foamy residue was re-dissolved in benzene, frozen and lyophilized which afforded a colorless powder (2.6 g). The yield was 85% as diastereomeric mixture.

Oligonucleotide Synthesis

All oligos were synthesized on a BioAutomation Mermade-6 oligonucleotide synthesizer (Bioautomation, Plano, TX). Oligonucleotide synthesis reagent usage was as follows: Activator = .25 M 5-(Ethylthio)-1H-Tetrazole in Acetonitrile (VWR, West Chester, PA); Cap A = 5% Phenoxyacetic anhydride in THF/Pyridine (Glen Research, Sterling, VA); Cap Mix B = 16% 1-Methylimidazole in THF (VWR); Deblock = 3% Trichloroacetic acid in DCM (VWR); Oxidizer = .02 M Iodine in THF/Pyridine/Water (70/20/10) (VWR). Commercially available dT-CE, 2'OMe-A(Pac)-CE, 2'OMe-G(iPr-Pac)-CE and 2'-O-TBMDS-U-CE phosphoramidites (Glen Research) and 2'F-C(Pac)-CE and 2'F-U-CE (R.I. Chemicals, Orange, CA) were coupled at coupling times and concentrations recommended from the manufacturer. For modifications, Infrared-800 phosphoramidite (LI-COR Biosciences, Lincoln, NE), 5'

Thiolmodifier amidite (Glen), 5'-Aldehyde modifier (Glen) and Cy3 amidite (Glen) were coupled per manufacturers recommendation. All SATE-containing phosphoramidites were coupled at 100 mM with two coupling cycles of 6 min each. Standard Q-T columns (Glen Research) were used for CPGs. Manual detritylation was accomplished by flowing 1 ml of deblock solution through the CPG column into 4 ml of 100 mM toluenesulfonic acid in anhydrous acetonitrile. Absorbance readings at 498 nm were done for DMT quantification to ensure full-length coupling.

Primary Oligonucleotide Deprotection

For all wildtype oligonucleotide deprotections, 1 ml of NH_4OH (VWR) was added to CPG for 4 hr at 65 ^oC. For all SATE containing oligos, 1 ml of 10% diisopropylamine (VWR) in methanol was added to CPG for a 4 hr deprotection at RT. After 4 hr of deprotection, oligonucleotide solutions were placed in cetntrifugal evaporator for drying. For 2'O-TBDMS deprotection, 50 nmol of RP-HPLC purified oligos were resuspended in 50 μl of anhydrous DMSO. To each oligo sample, 75 μl of triethylamine trihydrofluoride (98%) (Sigma Aldrich, St. Louis, MO) was added and reactions were left at room temperature for 4 hr. After 4 hr, oligos were precipitated by the addition of 15 μl of 3 M sodium acetate and 500 μl of 1-Butanol. Tubes were placed at -80 ^oC for 2 hr before centrifuging at 16,000 g. Oligo pellets were dissolved in 1 ml of water and desalted with NAP-10 columns (GE Healthcare, Buckingham, UK) before use.

Fmoc-N2-SATE Deprotection

Following isolation of Fmoc-N2-SATE containing oligonucleotides, RNN oligos were aliquoted into 5 nmol aliquots and lyophilized until dry. These 5 nmol aliquots were used for Fmoc-removal conditions attempts. Following treatment of Fmoc-N2-SATE oligos with 50 μl of desired deprotection condition, reaction mixtures were injected onto a rapid-gradient RP-HPLC column prior to mass spec analysis to determine Fmoc removal. Reactions mixtures attempted include 10%, 20% and 50% piperidine, piperazine, morpholine, triethylamine and diisopropylethylamine in either NMP, DMF or DCM. Reactions were assayed at time points ranging from 1 min to 1 hr depending on the strength of the base used for Fmoc removal.

Alloc-N2-SATE Deprotection

Following Alloc-N2-SATE oligo purification, oligos were transferred to tubes of 30 nmol aliquots and lyophilized until dry. To the 30 nmol oligo tube, 200 μl of DCM/MeOH mixture (5:1) was added to dissolve the oligo. To this, 102 nmol of tetrakis(triphenylphosphine)palladium was added followed by 24.6 μmol of phenylsilane. Reactions were left at RT for 10 min before injection onto RP-HPLC column with no TEAA counter ion present. Water to 80% acetonitrle gradient was run from 0 to 35 min for oligo isolation.

Oligonucleotide Purification

All oligos were purified by RP-HPLC on an Agilent 1200 Series Analytical HPLC (Agilent, Santa Clara, CA) with an Agilent Eclipse-XDB C18 column (4.6 x 150 mm). Linear gradients were run from water in .05 M triethylammonium

acetate (TEAA) to 90% acetonitrile at a flow rate of 1 ml/min. Length and steepness of gradient varied with amount of SATE groups present on oligonucleotides. For DMT-On purifications, DMT-On oligonucleotide HPLC peaks were collected and lyophilized. Detritylation was accomplished by the addition of 200 μl 80% glacial acetic for 1 hr at room temperature before re-injection onto RP-HPLC column for DMT-Off oligonucleotide isolation. Correct RP-HPLC fractions for each oligo were lyophilized or placed in a centrifugal evaporator to obtain final oligo products.

Mass Spectrometry

Oligonucleotides were analyzed by MALDI-TOF mass spec using an Applied Biosystems-DE-Pro MALDI-TOF mass spec (Applied Biosystems, Foster City, CA). 10 pmol of RNA was spotted with 1 μl of matrix from a 10 mg/ml solution of 2',4',6'-Trihydroxyacetophenone (VWR) in 50% acetonitrile/10 mM ammonium citrate.

Gel Electrophoresis

ssRNA oligos were analyzed by denaturing gel electrophoresis using 15% acrylamide/7 M Urea denaturing gels and stained with methylene blue for visualization. dsRNA oligos were hybridized by heating to 90 ^{o}C for 30 s and allowing to cool to room temperature. dsRNA analysis was performed by nondenaturing gel electrophoresis using 15% acrylamide nondenaturing gels and ethidium bromide staining for visualization.

siRNA Transfection

H1299-dGFP expressing cells were generated by infection with a lentivirus expressing Vesicular Stomatitis Virus Glycoprotein (VSVG) fused to dGFP and isolated by FACS. For transfection, cells were plated in 24-well plates at 40,000 cells/well. Prior to transfection, cells were washed twice with serum-free DMEM. 100 μl samples of corresponding siRNA concentrations in serum-free DMEM were mixed with 100 μl transfection mixture (98 μl serum-free DMEM/2 μl of Lipofectamine-2000) and left at room temperature for 30 min prior to treatments. Transfection solutions were left on cells for 8 hr before removal and the addition of DMEM with 5% FBS. Cells were trypsinized and analyzed by flow cytometry on a BD Biosciences LSRII (BD Sciences, San Jose, CA).

Preparation of ^{32}P labeled siRNA

400 pmol of guide strand was 5' labeled with 2.5 units T4 polynucletide kinase (NEB) and 200 μCi g ^{32}P-ATP (6000 Ci/mmol) in a 50 μl volume for 20 min. Reaction was inactivated for 20 min at 65 ^{o}C and free g-^{32}P-ATP was removed from the reaction mixture using Amicon Ultra 3K centrifugal filter (Milipore, Cork, Ireland). 400 pmol of passenger strand was added and annealed by heating reaction mixture to 65 ^{0}C and cooling to room temperature.

Transfection of ^{32}P labeled siRNA

400 pMol of labeled siRNA was diluted to a volume of 250 μl in Optimem-I and mixed with 250 μl Optimem-I containing 10 μl Lipofectamine-2000. After a 20 min incubation the mixture was added to 2.4 x 10^6 H1299-dGFP cells in 8 ml

DMEM containing 5% FBS and seeded in a 10 cm tissue culture dish. Cells were transfected for 12 hr and washed with PBS before medium replacement.

Argonaute 2 Co-IP

36 hr post transfection, cells were washed with ice cold PBS and lysed in 1 ml ice cold lysis buffer (20 mM Tris-Hcl (pH 7.9), 250 mM NaCl, 0.5% Triton X-100, 0.1 % DEPC, 0.5% protease inhibitor cocktail and 1% phosphatase inhibitor cocktail II (Sigma, Saint Louis, Co) for 10 min on ice. Lysates were cleared at 16,000 RCF for 10 min at 4 ^{0}C. 900 μl of cleared lysate was incubated with 100 μl of washed protein G-sepharose 4B slurry (Invitrogen, Camarillo, CA) on rotator at 4 ^{o}C. After 2 hr, beads were spun down and 850 μl of lysate was transferred to tube containing 75 μl of washed protein G-sepharose 4B slurry pre-incubated for 2 hr with 10 μl Anti human Argonaute 2 antibody (4G8,0.9 mg/ml, Wako Chemical USA, Richmond, VA) and incubated on a rotary shaker for 4 hr. Beads were washed 4 times with ice cold lysis buffer, eluted with 50 μl 7 M urea/ 0.1% bromophenol at 95 ^{0}C for 1 min. Eluate and input siRNA were counted on a scintillation counter and input counts were normalized to IP sample, except for DMB sample, of which an equal volume of eluate to SPTE sample was loaded on 15%/7 M urea PAGE. Gels were exposed to film overnight or 30 min to a phosphoimager screen at -20 ^{0}C.

5' RACE

For 5' RACE, 200 x 10^3 cells were reverse transfected with siRNA at a concentration of 100 nM using Lipofectamine-2000. Cells were harvested in

Trizol (Invitrogen, Carlsbad, Ca) 48 h post transfection. The aqueous phase was mixed with equal volume of 70% ethanol, loaded on a RNAeasy coumn (Qiagen, Valencia, CA) and RNA was prepared according to the manufacturers instruction. Three microgram RNA was ligated to 0.25 μg GeneRacer RNA oligo (Invitrogen). Ligated RNA was reverse transcribed with superscript III and oligo dT(20). cDNA was amplified with the GeneRacer 5' primer and a gene specific primer (5' TGGGCAGCGTGCCATCATCC for GFP, ATCATCCCCCTCGGGTGTAATCAGAA for GL3) using a step down PCR protocol. Second round amplification was performed using the GeneRacer 5' nested primer and a gene specific nested primer (5' ATCATCCTGCTCCTCCACCTCCGG for GFP, TCAGTGAGCCCATATCCTTGCCTGAT for GL3) at 60 ^{0}C. PCR products were analyzed on a 1.2% Agarose/TBE gel and bands of predicted size were excised, purified on S.N.A.P. columns, cloned into TOPO-PCR4 vector (Invitrogen) and sequenced or 5' RACE was performed using the Generacer kit with omission of the CIP and TAP steps.

Real time PCR

200 x 10^3 cells were reverse transfected in a 12-well plate. RNA was isolated with trizol according to the manufacturer. 10 ng of total RNA was used for real time PCR using the Taqman RNA-to-Ct 1 step kit and Taqman pre-designed probe and primers (Applied Biosystems). GFP primers were as described previously.

Serum stability

50 pMol of 5' IRdye labeled siRNA or siRNN guide strand were incubated in 50% human complement active serum (Innovative Research, Novi, Mi) at 37 ^{0}C. At indicated time points an aliquot was taken and diluted 10 fold in 7 M Urea loading buffer. Samples were heated to 95 ^{o}C for 1 min, snap cooled on dry ice and stored at -80 ^{0}C until analysis on a 15%/7 M Urea PAGE. Gels were analyzed on an Odyssey imager (LI-COR, Lincoln, NE).

CHAPTER 3

OVERCOMING THE NEGATIVE CHARGE OF siRNA

ABSTRACT

The class of small cationic peptides termed Peptide Transduction Domains (PTDs) have shown great utility in a wide variety of macromolecular delivery systems. Unfortunately, the ability for PTDs to successfully aid in the cellular delivery of siRNA oligonucleotides is hindered due to the extreme anionic character of the siRNA phosphodiester backbone. In order to generate synthetic PTD-siRNA conjugates capable of cellular delivery, we have focused our attention on charge-neutralization of the siRNA phosphodiester backbone with bioreversible groups during oligonucleotide synthesis. In order to test the hypothesis that synthetically neutral siRNA oligos can be delivered with conjugated PTD peptides, we have synthesized a series of fluorescently-labeled surrogate methylphosphotriester-neutralized oligos for PTD-siRNA cellular uptake studies. Interestingly, conjugation of PTDs to methyltriester-neutralized siRNA molecules showed positive cellular association and uptake only when the PTD-siRNA conjugate contained an overall cationic charge. This study serves as a proof of concept that phosphodiester-neutralized PTD-siRNA conjugates can be cellularly delivered and defines the degree to which future bioreversibly-neutralized PTD-siRNA conjugates need to be modified.

INTRODUCTION

Peptide Transduction Domains (PTDs) represent a class of short cationic peptides that have been shown to efficiently deliver a wide range of macromolecular cargo both *in vitro* and *in vivo* (Snyder, et al. 2005). The dense cationic charges of these peptides are essential for their engagement of the cell surface, stimulation of macroinocytosis, and trafficking and escape from endocytic vesicles (Wadia, et al. 2004). Conjugation of covalently-coupled cargo has been utilized for the cellular delivery of macromolecules ranging in size from peptides and proteins to nanoparticles and iron beads (Wadia, et al. 2002). Not surprisingly, upon the discovery that short interfering RNAs (siRNAs) could induce RNAi upon exogenous addition in human cells (Elbashir, et al. 2001), a multitude of delivery studies began to be reported utilizing the power of PTD-mediated cellular delivery for siRNA molecules.

Due to the dense cationic nature of PTDs, the majority of siRNA delivery strategies with these peptides have been through electrostatic packaging and positively-charged aggregate formation for treatment of cells in culture (Meade, et al. 2007). This nanoparticle formulation is similar in concept to traditional cationic polymers such as poly-lysine, PEI and protamine, in that when cationic peptides and polymers exist in high enough molar excess, siRNA molecules are forced to condense into positively-charged nanoparticle structures that are able to precipitate onto and engage the cell surface (Urban-Klein, et al. 2005). In our hands, great care needs to be taken for utilization of cationic peptides in this

manner as high molar excess of cationic peptides can create significant cytotoxicity for cells in culture (data not shown).

While a few studies have reported the successful delivery of PTD-siRNA conjugates (Chiu, et al. 2004; Davidson, et al. 2004; Muratovska, et al. 2004), all have failed to describe the inherent difficulties associated with conjugating cationic PTDs to anionic cargo. In our hands, covalent conjugation of PTDs directly to siRNA molecules results in conjugates that are unable to effectively bind the cell surface and stimulate cellular uptake. We hypothesized this was due to the strong anionic charge from the phosphodiester backbone of the siRNA molecule electrostatically neutralizing the cationic residues within the PTD that are crucial for cellular uptake. However, while utilizing PTD-DRBD fusion proteins, we succeeded in efficiently delivering phosphodiester-containing siRNA oligonucleotides into cells and inducing RNAi responses (Eguchi, et al. 2009). This PTD-mediated siRNA delivery strategy was dependent upon the ability of the DRBD to bind the siRNA duplex and sterically block PTD-siRNA charge neutralization.

Our work with PTD-DRBD taught us that the primary complication to be addressed with PTD-mediated siRNA delivery is the strong anionic character of the siRNA phosphodiester backbone. In the absence of some phosphodiester neutralizing or blocking entity, the basic residues within the PTD domain are electrostatically neutralized and unable to interact with the cellular membrane and induce internalization. While PTD-DRBD serves as a strong proof-of-

concept for this idea, we began thinking of ways that this same PTD delivery efficiency could be utilized on a strictly synthetic siRNA technology, thereby avoiding the use of bacterially-expressed recombinant proteins. This line of thinking led us to the idea of chemical manipulation of the siRNA phosphodiester backbone during oligonucleotide synthesis. Unfortunately, common oligonucleotide neutralizing modifications including phosphorothioates, morpholinos, peptide nucleic acids (PNA) and methylphosphonates are not tolerated for RNAi (Manoharan, 2004). This is not unsurprising considering the extent of phosphodiester interaction by Ago2 during loading and activation of RISC in RNAi (Song, et al. 2004; Frank, et al. 2010).

In order to allow for siRNA oligonucleotide neutralization while still allowing for RISC binding and RNAi induction inside cells, we began exploring various small molecule prodrug strategies that have utilized bioreversible phosphate modifications for enhancing the uptake of small molecules. Following synthesis, these small molecules have neutralizing phosphate modifications to aid in cell membrane diffusion that are then processed intracellularly, allowing for unmasking of charged phosphates and activation of the drug upon exposure to the cytoplasm (Peyrottes, et al. 2004). We sought means of bioreversibly-modifying the phosphodiester backbone with a set of criteria including modification-compatibility with common oligonucleotide synthesis strategies as well as efficiency of conversion to phosphodiesters due to the large number of neutralizing modifications that would need to be applied. We termed these

neutralized siRNA molecules small interfering RiboNucleic Neutrals (siRNNs). The end goal was a bioreversibly-neutralized siRNN oligonucletoide covalently tethered to a cationic PTD peptide that would have cell penetration properties. Theoretically, exposure to the cytoplasm would convert modified siRNN oligonucleotides into RNAi-competent siRNA molecules for efficient RNAi against target mRNAs (Figure 3.1A).

To directly test the hypothesis that synthetically neutralized siRNA molecules could be delivered following PTD-conjugation, we set up peptide/oliognucleotide conjugation strategies with surrogate siRNA molecules containing non-bioreversible, neutralizing methylphosphotriester-modifications. By covalently coupling cyanine dyes to these surrogate oligonucleotides, we were able to directly test not only the hypothesis of PTD-mediated charge neutral siRNA delivery but also to determine the degree of neutrality that needs to be achieved on a phosphodiester-neutralized PTD-siRNA conjugate to enable successful PTD cell surface engagement.

RESULTS AND DISCUSSION

For the creation of PTD-siRNA conjugates, we have utilized multiple conjugation strategies to generate stable conjugates including direct disulfide bond formation between PTD and siRNA molecules, Click chemistry conjugation reactions and bis-arylhydrazone linkages (Figure 3.2A). Due to the simplicity of the reaction conditions, the latter conjugation strategy was chosen as our primary means of peptide-siRNA conjugation. Briefly, PTDs are functionalized during solid phase synthesis with an N-terminal HydrazinoNicotinamide (HyNic) group (Figure 3.2A & 3.2B). Oligonucleotides containing aldehyde functionalities readily form stable bis-arylhydrazone bonds with PTD-HyNic peptides in aqueous buffers at pH 5.0 (Figure 3.2A) (Surfraz, et al. 2007). Similar to the previously published PTD-siRNA studies, a disulfide linkage was placed 3' to the PTD-siRNA linkage ensuring disassociation of the PTD from the siRNA oligonucleotide upon exposure to the reducing cytoplasmic environment (Figure 3.2A) (Meade, et al. 2007). Following conjugation and SDS-PAGE gel extraction of PTD-siRNA conjugates, we were able to consistently generate PTD-siRNA conjugates at >95% purity (Figure 3.2C).

The ability of these conjugates to induce RNAi responses was tested on a transduction-competent human lung carcinoma (H1299) cell line stably expressing a destabilized version of GFP. Cationic lipid transfection of a wildtype passenger and guide strand GFP siRNA duplex (P^{WT}/G^{WT}) as well as an

aldehyde-functionalized GFP wildtype siRNA sequence (Ald-P^{WT}/G^{WT}) induced efficient RNAi responses against GFP as assayed by flow cytometry at 48 hr post-transfection. Unfortunately, cellular treatment of PTD-siRNA conjugates at concentrations 100-fold that of the transfection concentrations resulted in no alteration of GFP expression (Figure 3.2D). Interestingly, cationic lipid transfection of the TAT-P^{WT}/G^{WT} conjugate resulted in a significant RNAi response indicated that the PTD-siRNA conjugate is capable of inducing RNAi responses if cellular delivery is permitted (Figure 3.2D). Additionally, cellular treatment of cyanine-dye labeled siRNA conjugates (P^{WT}/G^{WT}-Cy3) failed to show any cell surface interaction or internalization using flow cytometry analysis of Cy3 signal in non-GFP expressing H1299 cells (Figure 3.2F). Importantly, microscopy analysis of cells treated with PTD-siRNA-Cy3 conjugates displayed little to no Cy3-positive precipitation that is typical following cellular treatment of unpurified PTD-siRNA conjugation mixtures (data not shown).

The most likely reason for this lack of reproducibility of successful siRNA delivery following PTD-siRNA conjugation is due to technical issues of ensuring solubility of PTD-siRNA conjugates during cellular treatment. Of the few reports that have used covalently-linked PTD-siRNA conjugates *in vitro*, all have failed to emphasize the difficulties inherent to applying cationic peptides to the delivery of anionic cargo (Meade, et al. 2007). In our own unpublished studies, we have demonstrated difficulties associated with keeping PTD-siRNA conjugates soluble while still maintaining the capability of gaining access to the intracellular

environment for induction of RNAi. The accessibility of the basic charges of PTDs is crucial for their interaction with the components of the cell membrane that are responsible for inducing cellular uptake (Jiang, et al. 2004). Unfortunately, charge neutralization of PTDs upon covalent attachment of anionic siRNA duplexes hinders the availability of crucial basic residues to interact with cellular membrane components critical for cellular entrance. In our hands, cellular entrance only occurs upon positively charged aggregate formation in cell culture media produced from lack of purification of PTD-siRNA from the free PTD peptide present in the conjugation reaction condition. In support of this hypothesis, two other independent groups that have reported difficulties in delivering PTD-siRNA conjugates into cells (Moschos, et al. 2007; Turner, et al. 2007).

In an attempt to evolve the PTD-DRBD strategy into a strictly synthetic approach, we began thinking of ways of chemically neutralizing the siRNA phosphodiester backbone in a manner in which these phosphodiester modifications could be converted back to RNAi-compatible wild type phosphodiesters following cellular delivery. While scanning the literature for ways to accomplish this synthetically, we started experimentation using surrogate siRNA oligonucleotides neutralized with various numbers of non-bioreversible methyltriester modifications (Figure 3.3A). The goal of these sets of experiments was to determine the exact number of modifications that needed to be applied in order to achieve sufficient neutrality for PTD delivery of neutral siRNN.

Methyltriester modifications were initially chosen due to their commercial availability and ease of synthesis. Using our GFP siRNA sequence, we synthesized a collection of methyltriester containing siRNA molecules with aldehyde-modified passenger strands and cyanine dye-labeled guide strands (Figure 3.3A). For synthetic reasons, 2' modifications were applied to all nucleotides, specifically 2'-OMe purines and 2'-F pyrimdines (See 2'-OH mediated strand scission of phosphotriesters in Chapter 4). Following PTD conjugation to these neutral dsRNA molecules, flow cytometry assessment of Cy3 uptake was utilized to determine the extent of cell membrane interaction and to delineate the amount of neutrality that needed to be achieved for sufficient phosphodiester neutralization.

Due to solubility issues, complete neutrality could not be achieved for siRNA duplexes with methyltriester insertions (data not shown). Neutrality of 15x methyltriesters on both passenger and guide strand ($P_{15}^{Methyl}/G_{15}^{Methyl}$) was the maximum amount of neutrality possible while still maintaining aqueous solubility. PTD-conjugation compatible methyltriester oligonucleotides (Ald-$P_{15}^{Methyl}/G_{15}^{Methyl}$-Cy3) containing 5' aldehyde/disulfide modified passenger strands (Figure 3.3A) possess a total of 13 remaining phosphodiester groups with maximal methylphosphotriester insertions. These surrogate duplexes were covalently-conjugated through bis-arylhydrazone linkages to various PTD monomers and multimers ranging in cationic charge from +8 (TAT-HyNic), +16 (2xTAT-HyNic) and +24 (3xTAT-HyNic) (Figure 1.3C). Interestingly, treatment of

H1299 cells with methyltriester-neutralized PTD-conjugates showed positive Cy3 cell association only when the conjugate had a theoretical overall positive charge (Figure 3.3D). TAT-$P_{15}^{Methyl}/G_{15}^{Methyl}$-Cy3 conjugates displayed no enhancement of Cy3 uptake compared to $P_{15}^{Methyl}/G_{15}^{Methyl}$-Cy3 oligo only treated whereas 2xTAT-$P_{15}^{Methyl}/G_{15}^{Methyl}$-Cy3 and 3xTAT-$P_{15}^{Methyl}/G_{15}^{Methyl}$-Cy3 both showed Cy3 association in increasing intensity relative to overall charge (Figure 3.3D). Importantly, this level of Cy3 uptake is comparable to Cy3 levels obtained with cationic lipid transfection of P^{WT}/G^{WT}-Cy3 at concentrations sufficient to induce RNAi. Additionally, microscropy analysis of cells treated with PTD-$P_{15}^{Methyl}/G_{15}^{Methyl}$-Cy3 conjugates displayed endosomal staining patterns characterstic of PTD-mediated uptake (data not shown). Prior to selection of our bioreversible phosphodiester modification group, this series of experiments was crucial in determining that the degree of neutralization required is roughly that which gives a PTD-siRNN conjugate an overall positive charge when mathematically adding PTD cationic residues and anionic siRNA phosphodiesters.

CONCLUSIONS

The discovery that synthetic siRNA molecules could be used to induce RNAi in human cells created not only a tool for cellular biologists but also opened up an entirely new field of RNAi therapeutics. Unfortunately, at ~14,000 Da and extreme acidity due to 40 phosphodiester charges, siRNA oligonucleotides present significant challenges as a therapeutic modality. A plethora of nanoparticle-based delivery strategies have been published translating the delivery vectors of the previous decade for antisense and gene therapy applications (Whitehead, et al. 2009). In order to avoid significant *in vivo* barriers of nanoparticle-based delivery systems, our laboratory has attempted to think outside the box, developing siRNA delivery platforms that utilize the delivery properties of cationic PTDs and deliver the siRNA in a soluble, monomeric fashion.

The use of PTD-DRBD to deliver siRNA efficiently into cells in culture and *in vivo* mouse models has shown us that the main obstacle to overcome when utilizing PTDs for siRNA delivery is the anionic phosphodiester backbone of the siRNA molecule (Eguchi, et al. 2009). In the absence of some blocking or neutralizing entity, the cationic residues of PTD peptides lack the ability to engage the cell surface and successfully deliver the siRNA oligonucleotide. This set our laboratory on a new path to synthetically manipulate the phosphodiester backbone with charge-neutralizing bioreversible modifications as a potential pro-drug format for PTD-siRNA conjugate delivery. Interestingly, the methyltriester-

neutralized siRNA surrogates displayed cellular delivery properties only when the oligonucleotide was sufficiently neutralized where the overall charge of the PTD-siRNA conjugate was cationic. With this set of rules in hand, I began studying our first bioreversible phosphodiester-neutralizing candidate: *t*-Bu-S-Acyl-ThioEthyl (*t*-Bu-SATE) phosphotriester modifications.

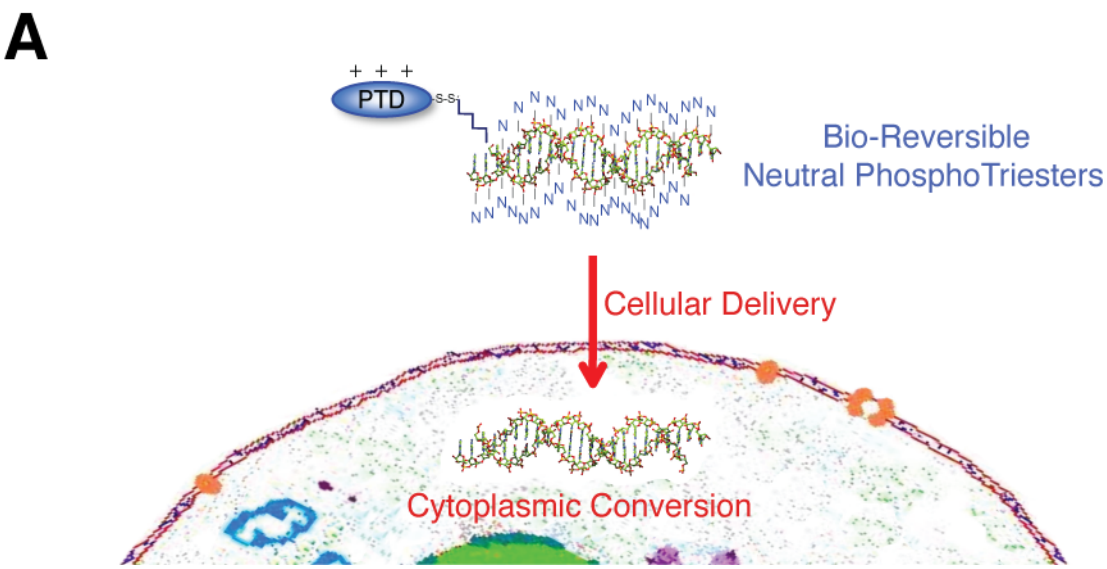

Figure 3.1. Overcoming the siRNA negative charge with PTD-siRNN conjugates. A) Scheme for PTD-siRNN cellular delivery. Bioreversible-neutralizing modifications allow for cell surface binding of the conjugated PTD peptide. Following cellular delivery, bioreversible modifications undergo conversion to RNAi-compatible phosphodiester siRNA for induction of RNAi.

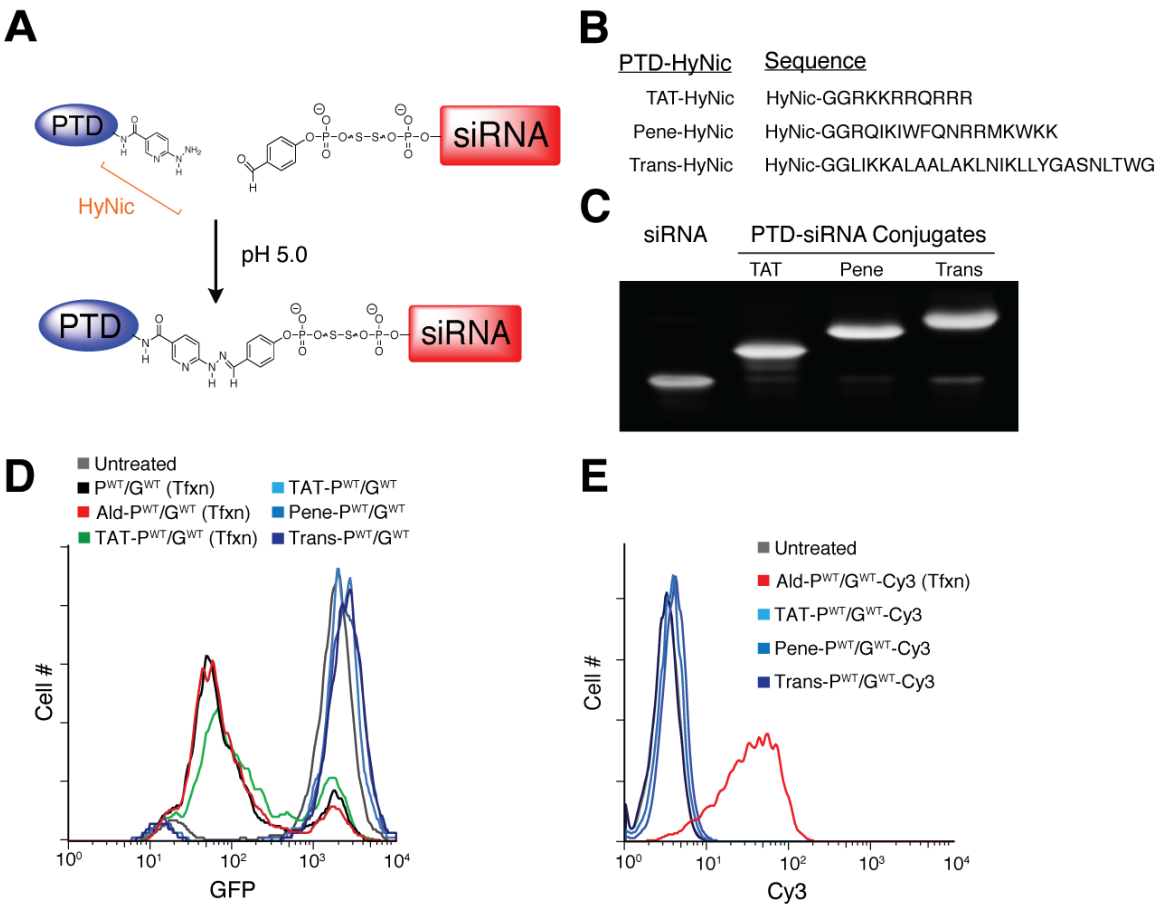

Figure 3.2. Conjugation of PTD peptides to wildtype siRNA oligonucleotides. **A**) Peptide-oligonucleotide conjugation reaction with formation of stable bis-arylhydrazone linkage with HyNic-modified PTDs and 5' aldehyde modified passenger strand oligonuceotides. Reaction occurs readily in aqueous buffers at pH 5.0. **B**) PTD-HyNic sequences used in this study. **C**) SDS-PAGE analysis of purified PTD-siRNA conjugates. 10% nondenaturing gel stained with ethidium bromide for analysis. **D**) Flow cytometry analysis of 100 nM siRNA transfected with cationic lipid (Tfxn) compared to 10 μM PTD-siRNA conjugate treatments. Cells were treated for 8 hours before GFP RNAi analysis at 48 hours post-treatment. Note no decrease in GFP values for PTD-siRNA conjugate treatments. **E**) Flow cytometry analysis of Cy3 uptake for 10 μM PTD-siRNA-Cy3 conjugates compared to 100 nM siRNA-Cy3 cationic lipid transfection (Tfxn). Analysis was done following 8 hour cellular treatment.

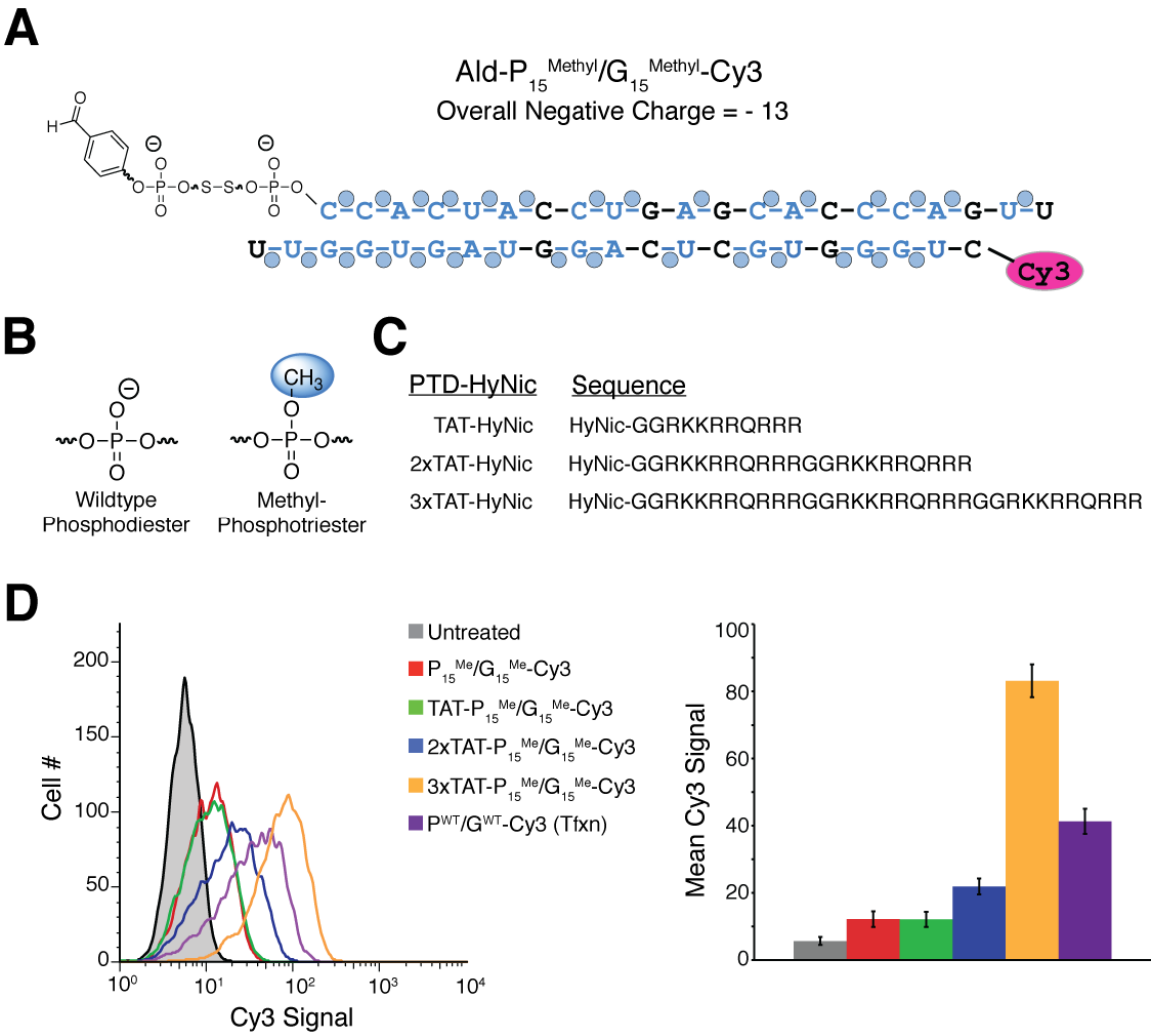

Figure 3.3. Delivery studies with PTD-siRNA methyltriester surrogate oligoncucleotides. **A**) Sequence of and insertion sites for maximum-modified Ald-$P_{15}^{Methyl}/G_{15}^{Methyl}$-Cy3 oligonucleotide. Oligo contains 13 remaining negatively charged phosphodiesters. **B**) Surrogate nonbioreversible methylphosphotriesters. **C**) PTD-HyNic sequences used in this study. Overall cationic charges: TAT-HyNic (+8), 2xTAT-HyNic (+16), 3xTAT-HyNic (+24). **D**) Flow cytometry analysis of H1299 cells treated with 10 μM PTD-$P_{15}^{Methyl}/G_{15}^{Methyl}$-Cy3 conjugates for 8 hours. Note intensify of Cy3 uptake increases with increasing overall cationic charge of the conjugate. Positive control is 100 nM siRNA-Cy3 transfection with cationic lipids (Tfxn).

REFERENCES

Chiu YL, Ali A, Chu CY, Cao H, Rana TM. Visualizing a correlation between siRNA localization, cellular uptake, and RNAi in living cells. Chem Biol 2004;11:1165-75.

Davidson TJ, Harel S, Arboleda VA, et al. Highly efficient small interfering RNA delivery to primary mammalian neurons induces MicroRNA-like effects before mRNA degradation. J Neurosci 2004;24:10040-6.

Eguchi A, Meade BR, Chang YC, et al. Efficient siRNA delivery into primary cells by a peptide transduction domain-dsRNA binding domain fusion protein. Nat Biotechnol 2009;27:567-71.

Frank F, Sonenberg N, Nagar B. Structural basis for 5'-nucleotide base-specific recognition of guide RNA by human AGO2. Nature 2010;465:818-22.

Jiang T, Olson ES, Nguyen QT, Roy M, Jennings PA, Tsien RY. Tumor imaging by means of proteolytic activation of cell-penetrating peptides. Proc Natl Acad Sci U S A 2004;101:17867-72.

Manoharan M. RNA interference and chemically modified small interfering RNAs. Curr Opin Chem Biol 2004;8:570-9.

Meade BR, Dowdy SF. Exogenous siRNA delivery using peptide transduction domains/cell penetrating peptides. Adv Drug Deliv Rev 2007;59:134-40.

Moschos SA, Jones SW, Perry MM, et al. Lung delivery studies using siRNA conjugated to TAT(48-60) and penetratin reveal peptide induced reduction in gene expression and induction of innate immunity. Bioconjug Chem 2007;18:1450-9.

Muratovska A, Eccles MR. Conjugate for efficient delivery of short interfering RNA (siRNA) into mammalian cells. FEBS Lett 2004;558:63-8.

Peyrottes S, Egron D, Lefebvre I, Gosselin G, Imbach JL, Perigaud C. SATE pronucleotide approaches: an overview. Mini Rev Med Chem 2004;4:395-408.

Snyder EL, Dowdy SF. Recent advances in the use of protein transduction domains for the delivery of peptides, proteins and nucleic acids in vivo. Expert Opin Drug Deliv 2005;2:43-51.

Song JJ, Smith SK, Hannon GJ, Joshua-Tor L. Crystal structure of Argonaute and its implications for RISC slicer activity. Science 2004;305:1434-7.

Surfraz MB, King R, Mather SJ, Biagini SC, Blower PJ. Trifluoroacetyl-HYNIC peptides: synthesis and 99mTc radiolabeling. J Med Chem 2007;50:1418-22.

Turner JJ, Jones S, Fabani MM, Ivanova G, Arzumanov AA, Gait MJ. RNA targeting with peptide conjugates of oligonucleotides, siRNA and PNA. Blood Cells Mol Dis 2007;38:1-7.

Urban-Klein B, Werth S, Abuharbeid S, Czubayko F, Aigner A. RNAi-mediated gene-targeting through systemic application of polyethylenimine (PEI)-complexed siRNA in vivo. Gene Ther 2005;12:461-6.

Wadia JS, Dowdy SF. Protein transduction technology. Curr Opin Biotechnol 2002;13:52-6.

Wadia JS, Stan RV, Dowdy SF. Transducible TAT-HA fusogenic peptide enhances escape of TAT-fusion proteins after lipid raft macropinocytosis. Nat Med 2004;10:310-5.

Whitehead KA, Langer R, Anderson DG. Knocking down barriers: advances in siRNA delivery. Nat Rev Drug Discov 2009;8:129-38.

CHAPTER 4

SYNTHESIS OF siRNN OLIGONUCLEOTIDES CONTAINING *t*-Butyl-S-ACYL-THIOETHYL (*t*-Bu-SATE) MODIFICATIONS

ABSTRACT

siRNA induced RNAi responses have great potential to treat human disease, especially cancer. However, siRNAs are ~14,000 Da double stranded 21mer RNA macromolecules that contain 40 negatively charged phosphodiesters owing to their restricted bioavailability. Current liposome and nanoparticle delivery approaches overcome this anionic charge by utilizing cationic motifs to neutralize and condense siRNAs into ~100 MDa particles. To avoid inherent problems associated with nanoparticle-based delivery strategies, I sought to synthetically generate a soluble siRNA delivery molecule by synthesizing PTD-conjugated RiboNucleic Neutral (RNN) oligonucleotides containing bioreversible, charge neutralizing *t*-Bu-S-Acyl-ThioEthyl (*t*-Bu-SATE) phosphotriester groups that, upon cellular internalization, are resolved by cytoplasmic thioesterases into charged phosphodiesters capable with the RNAi machinery. Synthetic complications of siRNN oligonucleotides require the use of ultramild oligonucleotide deprotection strategies as well as insertion of RNAi tolerated 2'-F/O-Me modifications on ribose rings adjacent to phosphotriester modifications to avoid 2'-OH nucleophilic phosphotriester attack and strand cleavage. With these two rules in mind, I have efficiently synthesized, purified and analyzed SATE

RNN oligonucleotides for biological function. Cationic lipid transfection of siRNNs into cells results in intracellular *t*-Bu-SATE cleavage, loading into Ago2, and induction of target-specific RNAi responses. While these results serve as the first example of bioreversible phosphotriester insertions on siRNA oligonucleotides, conjugation of cationic PTDs to *t*-Bu-SATE siRNN has proved futile due to the hydrophobic nature of the *t*-Bu-SATE moiety that renders these siRNN conjugates highly insoluble in physiological conditions.

INTRODUCTION

While siRNA technology represents a very promising therapeutic strategy, the use of siRNA in the intervention of human disease will require the use of a macromolecular delivery strategy to aid both with *in vivo* biodistribution and cellular delivery of siRNA oligonucleotides (Whitehead, et al. 2009). While some nanoparticle-based siRNA delivery systems have shown promise in multiple pre-clinical models (de Fougerolles, et al. 2007), our laboratory has attempted to generate soluble, non-particle forming siRNA delivery strategies in an attempt to avoid inherent problems associated with nanoparticle-based siRNA carriers (Meade, et al. 2007). We have attempted to do so utilizing a class of small cationic peptides termed Peptide Transduction Domains (PTDs). This class of peptides has been shown to deliver a plethora of macromolecules within both *in vitro* and *in vivo* settings and have also shown promising results within multiple clinical trials for the treatment of human disease (Gump, et al. 2007). The dense cationic charge of these small peptides is responsible for their ability to successfully interact with and induce internalization across the cellular membrane (Meade, et al. 2007).

Based upon our work with PTD-DRBD, it was clear that the ability of PTDs to aid in the successful delivery of siRNAs requires somehow reducing the acidity of the siRNA phophodiester backbone to allow for PTD cell surface binding and siRNA internalization. In the absence of some phosphodiester blocking entity, the anionic charge of the siRNA phosphodiester backbone neutralizes and

inactivates the cationic residues responsible for cell surface binding (Eguchi, et al. 2009). With these observations in hand, we began to think of ways that chemical manipulation of the phosphodiester backbone could lead to stable PTD-siRNA conjugates, capable of delivering siRNA molecules in the absence of recombinant PTD-fusion proteins. Due to the inability of phosphodiester-neutral siRNA to induce RNAi responses (Manoharan, et al. 2004), we decided to begin synthesizing PTD-siRNA conjugates containing neutralizing phosphodiester modifications that, following cellular delivery, undergo conversion to RNAi-compatible phosphodiesters (Figure 3.1A). This pro-drug template should, in theory, satisfy all the requirements for PTD-siRNA delivery and allow for the creation of a soluble, monomeric siRNA delivery system.

The cellular RNAi machinery requirement for the presence of internucleotide phosphodiester linkages essentially restricts all siRNA delivery approaches to require cationic motifs that electrostatically neutralize the charge to condense the siRNA. Consequently, there has been little work done on directly neutralizing the siRNA phosphodiester backbone. Indeed, addition of even closely related internucleotide phosphorothioate linkages results in a significant reduction of cellular RNAi responses (Manoharan-04). However, in theory, bioreversible siRNA charge neutralization would allow for development of novel monomeric, RNAi-inducing molecules that avoid use of particle forming, condensing delivery agents. Surprisingly, only a limited amount of literature exists for this concept.

Beaucage and colleagues developed a thermolytic thiophosphate protecting group-containing DNA oligonucleotide that is slowly reversed into a charged phosphorothioate oligonucleotide at 37 ^{O}C; however, the half-life for heat-mediated deprotection was 73 hr and the approach is restricted to a phosphorothioate linkage that is unsuitable for induction of RNAi responses (Grajkowski, et al. 2005). Additionally, McMaster and coworkers developed a nitrophenylethyl (NPE) photolabile phosphate protecting group that when singularly placed on the 5' phosphate of the siRNA guide (antisense) strand demonstrated light activated removal inside cells to induce RNAi responses (Nguyen, et al. 2006). Blidner et al. (Blidner, et al. 2008) expanded on this approach and alkylated phosphodiester linkages in a 2'-F substituted siRNA with a photolabile dimethoxynitrophenyl (DMNPE). Exposure to light in both cells in culture and in zebrafish embryos induced RNAi responses. Although this study demonstrated the ability of cellular reversal of DMNPE-phosphotriester containing siRNAs, the overall approach has several drawbacks, including alkylation of the oligonucleotide at unintended and uncontrolled sites, inefficient light removal of all DMNPE groups and the limitation for human RNAi therapeutic development as phosphotriester conversion would require light source access to the target tissue. The photolabile phosphotriester work prompted us to search for bioreversible phosphotriester protecting groups that would be converted by a cytoplasmic restricted enzyme into charged phosphodiesters. Unfortunately, to date, no bioreversible phosphotriester containing RNAs have been described.

To neutralize the phosphate charge of a mononucleotide inhibitor of HIV Reverse Transcriptase, Imbach and colleagues developed a *t*-Bu-SATE phosphotriester protecting group (Lefebvre, et al. 1995). Impressively, cleavage of the SATE phosphotriester by cytoplasmic restricted thioesterases initiated a rapid two-step decomposition process that resolved into a wild type, anionic charged phosphate (Figure 4.1A; Faraj, et al. 2009). Importantly, thioesterases are only present in the cytoplasm and organelles of cells, and extracellular esterases present in human serum cannot sufficiently process the thioester bond, thereby avoiding extracellular decomposition (Tosquellas, et al. 1998). Indeed, bioreversible SATE phosphotriester groups have been placed on a variety of mononucleotide inhibitors (Peyrottes, et al. 2004). Two groups expanded this phosphate neutralization methodology to solid phase oligonucleotide synthesis by generating *t*-Bu-SATE containing deoxy phosphoramidites and their corresponding DNA oligonucleotides (Tosquellas et al., 1998; Tosquellas, et al. 2998, Guzaev, et al. 2001). The main complication encountered by both research teams was the inherent instability of the *t*-Bu-SATE groups to standard synthetic oligonucleotide deprotection conditions. Although alternative deprotection strategies were successful at generating deoxyoligonucleotide tester sequences, to date, there are no reports of biologically relevant SATE phosphotriester oligonucleotides being tested on cells for phenotypic activity as well as no reports of SATE-containing RNA oligonucleotides.

To begin to address the siRNA delivery problem while avoiding formation

of particles, I investigated the chemical synthesis and biological properties of bioreversible, *t*-Bu-SATE phosphotriester RiboNucleic Neutrals (RNNs). Because *t*-Bu-SATE RNNs had not previously been synthesized, we focused on phosphoramidite synthesis routes, oligonucleotide synthesis conditions, orthogonal deprotection conditions, and purification strategies that maintain phosphotriester insertions. These studies defined critical RNN phosphotriester properties: 1) the thioester moiety is highly unstable to basic conditions required for oligonucleotide deprotection, thus novel deprotection strategies were generated for post-synthetic oligonucleotide processing; 2) synthesis of phosphotriester linkages adjacent to a 2'-OH on the same ribose ring resulted in nucleophillic attack and oligonucleotide strand scission, therefore it was necessary to substitute RNAi tolerated 2'-F/2'-O-Me modifications; and 3) steric hindrance across the major groove of a double-stranded siRNN molecule limits the number of SATE insertions to ~50%.

Transfection of siRNNs into cells resulted in intracellular SATE reversal, siRNA loading into Ago2, and induction of target-specific RNAi responses. In contrast, control siRNNs containing *irreversible* 3,3-dimethyl-1-butyl (DMB)-phosphotriesters were not loaded into Ago2 and did not induce RNAi responses. Additionally, highly modified *t*-Bu-SATE siRNN molecules were stable in human serum with a half-life of >24 h. While these observations represent the first report on the synthesis of an entirely new class of biologically active, RNAi-inducing bioreversible phosphotriester siRNN oligonucleotides, attempts to

conjugate t-Bu-SATE siRNNs to highly cationic peptides for soluble PTD-siRNN conjugates resulted in insurmountable problems associated with conjugate solubility.

RESULTS & DISCUSSION

Synthesis requirements for *t*-Bu-SATE oligonucleotides

Following phosphoramidite-mediated solid-phase oligonucleotide synthesis, oligonucleotides require a primary deprotection step consisting of base treatment to remove 2-cyanoethyl phosphodiester protecting groups, exocyclic amine protecting groups, and to induce the release of the oligonucleotide from the solid support (Beaucage, 2008). Generally, a strong base such as ammonium hydroxide is sufficient for these oligonucleotide deprotection requirements. In the case of *t*-Bu-SATE containing oligonucleotides, strong base treatment proved problematic due to thioester decomposition and loss of *t*-Bu-SATE insertions (Figure 4.2A). Due to this sensitivity of *t*-Bu-SATE groups during base treatment, we conducted a two-part screen using multiple primary deprotection strategies to find a condition that would fulfill oligonucleotide deprotection requirements while also maintaining *t*-Bu-SATE phosphotriester integrity.

To test *t*-Bu-SATE phosphotriester stability during oligonucleotide deprotection, we synthesized tester 20mer oligonucleotides with alternating paired deoxythymidine-cyanoethyl and deoxythymidine-(*t*-Bu-SATE) phosphoramidites ($T_{10}T_{10}^{tBu\text{-}SATE}$). For tester sequences, deoxythymidine phosphoramidites were chosen for efficiency of coupling as well as lack of nucleobase protection that could potentially confound denaturing gel and mass spectrometry analysis of oligo deprotection timepoints. As previously mentioned,

exposure of $T_{10}T_{10}^{tBu\text{-}SATE}$ DNA oligonucleotides to standard NH_4OH deprotection conditions resulted in complete decomposition and reversion of *t*-Bu-SATE phosphotriesters into wild type phosphodiesters in less than 1 hr as assayed by urea denaturing gel electrophoresis (Figure 4.2A). We next tested "ultramild" K_2CO_3/MeOH deprotection conditions that have been shown to allow efficient oligonucleotide deprotection while maintaining methyltriester insertions (Kuijpers, et al. 1990). Deprotection of the tester $T_{10}T_{10}^{tBu\text{-}SATE}$ DNA oligonucleotide in K_2CO_3/MeOH resulted in gradual *t*-Bu-SATE phosphotriester decomposition to phosphodiesters that was completed by 4 h, a window of time that is not sufficient for oligonucleotide deprotection and satisfactory *t*-Bu-SATE stability. Next, we tested various concentrations of mildly basic deprotection cocktails including piperidine, triethylamine (TEA), diethylamine (DEA), diisopropylethylamine (DIEA) and diisopropylamine (DIA). Of the various deprotection solutions assayed, we found *t*-Bu-SATE insertions remained unaffected in 10% DIA in anhydrous methanol (MeOH) for up to 8 hr (Figure 4.2A)

Additionally, time course deprotection assays for tester 20mer deoxyoligonucleotides containing 50% nucleobase-protection were done to analyze the efficiency of base deprotection in 10% DIA/MeOH as assayed by MALDI-TOF mass spectrometry (data not shown). Fortunately, the results of this set of experiments displayed satisfactory nucleobase deprotection when 'Ultramild' nucleobase protection was used including phenoxyacetal-protected

adenosine and cytosine (A^{Pac} and C^{Pac}) and isopropylphenoxyacetyl-protected guanosine ($G^{Ipr\text{-}Pac}$). Using this base deprotection assay, all phenoxyacetyl-protected oligonucleotides were sufficiently deprotected within 4 h of 10% DIA/MeOH treatment (data not shown). This deprotection strategy was used for all further phosphoramidite and oligonucleotide synthesis routes for both cyanoethyl-protected phosphodiester as well as phosphotriester insertions. Finally, due to the inability of 10% DIA/MeOH to efficiently remove oligonucleotides from the more standard succinyl-linked supports (data not shown), solid support release was optimized using a Q-linked CPG (Pon, et al. 1997) for all phosphotriester-containing oligonucleotides. Thus, sufficient deprotection requirements were met for the generation of *t*-Bu-SATE-containing oligonucleotides following solid phase oligo synthesis.

Although several groups have synthesized tester *t*-Bu-SATE containing DNA oligonucleotides, there are no reports of *t*-Bu-SATE RNA oligonucleotides. To test the ability to synthesize *t*-Bu-SATE RNA oligonucleotides, we synthesized a tester 20mer oligonucleotide containing a single Uridine-(*t*-Bu-SATE) ($U^{tBu\text{-}SATE}$) insertion at position 14 with a 2' O-*t*-butyldimethylsilyl (2'O-TBMDS) protecting group ($T_{13}U_1{}^{tBu\text{-}SATE}T_6$). The $U^{tBu\text{-}SATE}$ phosphoramidite coupled efficiently during synthesis and the tester T_{13}-$U_1{}^{tBu\text{-}SATE}$-T_6 oligonucleotide retained its *t*-Bu-SATE insertion following 10% DIA/MeOH deprotection. However, deprotection of the 2'-O-TBDMS with triethylamine trihydrofluoride (TEA.3HF) to its corresponding 2'-OH led to strand cleavage at the $U^{tBu\text{-}SATE}$ insertion site resulting in a 14 nt

oligonucleotide fragment (Figure 4.2C), suggesting that the 2'-OH performs a nucleophilic attack on the phosphotriester resulting in strand cleavage. Importantly, this result was also observed following 2'O-TBDMS deprotection in tetra-n-butylammonium fluoride (TBAF) that is indicative that 2'OH strand scission occurs independent of 2'-OH deprotection strategies (data not shown). Additionally, this observation agrees with a published report showing that post-synthetic alkylation of phosphodiesters to phosphotriesters on 2'-OH containing RNA oligonucleotides results in strand scission (Blidner, et al. 2008).

Previous RNAi studies have shown that 2'-F/2'-O-Me are highly tolerated siRNA modifications that do not impact the ability to induce a RNAi response and also protect the siRNA from RNAse degradation (Bumcrot, et al. 2006). Therefore, we synthesized T_{13}-$U_1^{tBu\text{-}SATE}$-T_6 oligonucleotides containing either a 2'-F or 2'-O-Me U at position 14. Both 2'-F or 2'-O-Me U containing T_{13}-$U_1^{tBu\text{-}SATE}$-T_6 oligonucleotides were stable before and after TEA.3HF treatment with no detectable strand cleavage observed (Figure 4.2C). Importantly, *t*-Bu-SATE RNA oligonucleotides that contained 2'-OH groups at positions other than the *t*-Bu-SATE-containing ribose ring remained intact, showing that 2'-OH-mediated strand scission only occurs while attempting to insert *t*-Bu-SATE phosphotriesters directly adjacent to 2'-OH groups (data not shown). Importantly, these observations demonstrated the ability to synthesize and deprotect *t*-Bu-SATE phosphotriester RNN oligonucleotides that incorporate 2'-F/2'-O-Me modifications.

In order to assess biological activity and bioreversibility of *t*-Bu-SATE phosphotriesters, we synthesized *t*-Bu-SATE -containing RNN oligonucleotides with $A^{tBu\text{-}SATE}$, $C^{tBu\text{-}SATE}$ and $U^{tBu\text{-}SATE}$ phosphoramidites with 2'-OMe adenosine and 2'-F cytosine and uridine. Following oligonucleotide synthesis and 10% DIA/MeOH deprotection, reverse-phase high performance liquid chromatography (RP-HPLC) and MALDI-TOF mass spectrometry were utilized for RNN oligonucleotide purification. To aid with isolation of full-length oligonucleotides, Dimethoxytrityl (DMT)-On RP-HPLC purification was used for RNN oligonucleotides containing less than 12x *t*-Bu-SATE insertions. With insertion numbers higher than 12x *t*-Bu-SATE, the DMT hydrophobicity would not dominate the hydrophobicity of the highly *t*-Bu-SATE substituted synthesis truncation products, however, RP-HPLC peak fractionation of DMT-Off oligonucleotides allowed for sufficient isolation of full length, intact SATE oligonucleotides as validated by MALDI-TOF mass spec analysis (Figure 4.2). Interestingly, RP-HPLC profiles of all SATE oligonucleotides display broad peaks indicative of SATE diastereoisomeric mixtures (Alvarez, et al. 1999) (Figure 4.2D). To date, all *t*-Bu-SATE oligonucleotide final products purified have displayed >95% full length desired *t*-Bu-SATE -containing product with only a trace amount of a single *t*-Bu-SATE reversal present (Figure 4.2E).

Biological activity and cleavage of SATE phosphotriesters

Previously, SATE phosphotriester-containing DNA oligonucleotides were not analyzed intracellularly for either cytoplasmic thioesterase cleavage of the

thioester bond or induction of any biological response. Therefore, we sought to analyze the intracellular attributes of *t*-Bu-SATE phosphotriester RNNs. Because stable installation of *t*-Bu-SATE phosphotriesters requires the presence of a 2'-F or 2'-O-Me, we first tested the consequences of 2' substitutions on overall RNAi responses. Human H1299 lung adenocarcinoma cells containing an integrated and constitutively expressed destabilized GFP reporter gene (~2 h half-life) were transfected with 0.5 nM to 100 nM 21mer GFP siRNAs containing either wild type 2'-OH or fully modified 2'-F pyrimidines and 2'-O-Me purines, and analyzed for GFP expression by flow cytometry (FACS) at 48 h (Figure 4.3A). In agreement with previously published studies (Manoharan, et al. 2004), the fully modified 2'-F/O-Me GFP siRNA induced a dose-dependent RNAi response that was near identical to wild type 2'-OH siRNAs. This observation allowed us to move forward with biological analyses using fully modified 2'-F/2'-O-Me as a template for *t*-Bu-SATE-containing siRNNs.

With the exception of 2'-F/O-Me modifications, due to strong surface contacts between the guide (G) (antisense) strand and Ago2, modifications on the siRNA guide strand are not tolerated and result in significant loss of RNAi activity (Bumcrot, et al. 2006). To analyze the biochemical and biological responses to *t*-Bu-SATE phosphotriester siRNNs, we synthesized a 21mer guide strand GFP oligonucleotide that contained either 6 bioreversible $U^{tBu\text{-}SATE}$ insertions or 6 control *irreversible* U^{DMB} insertions spread across the oligonucleotide (Figure 4.3B). Both 6x U-SATE and control 6x U-DMB guide

strands efficiently hybridized to wild type passenger (P) (sense) strands to form stable dsRNA duplexes (Figure 4.3B). Double stranded $P^{WT}/G_6^{tBu\text{-}SATE}$ siRNN, P^{WT}/G_6^{DMB} siRNN and wild type control P^{WT}/G^{WT} GFP siRNAs were transfected (0.5 to 100 nM) into GFP expressing cells and analyzed for GFP RNAi responses at 48 h post-transfection (Figure 4.3C). Impressively, $P^{WT}/G_6^{tBu\text{-}SATE}$ siRNNs induced a dose-dependent RNAi response that was near identical to wild type control P^{WT}/G^{WT} siRNAs. In contrast, P^{WT}/G_6^{DMB} siRNNs containing 6 irreversible DMB phosphotriesters did not induce an RNAi response even at the highest 100 nM concentration. Consistent with these observations, quantitative mRNA analysis by qRT-PCR showed a dose-dependent decrease of GFP mRNA levels in cells transfected with both P^{WT}/G^{WT} siRNA and $P^{WT}/G_6^{tBu\text{-}SATE}$ phosphotriester siRNN, whereas cells transfected with irreversible P^{WT}/G_6^{DMB} phosphotriester siRNNs did not show a significant change in GFP mRNA levels (Figure 4.3D). Importantly, analysis of exogenous *t*-Bu-SATE siRNN oligonucleotides during and after cationic lipid transfection showed no sign of extracellular decomposition, ensuring that the RNAi responses observed only occur following intracellular conversion (data not shown).

A hallmark of RNAi responses is the specific cleavage of target mRNA referenced between nucleotides 10-11 of the guide strand (Elbashir, et al. 2001). To capture and analyze Ago2 cleaved GFP mRNA, we performed 5' RACE analyses on GFP expressing cells transfected with $P^{WT}/G_6^{tBu\text{-}SATE}$ siRNN, P^{WT}/G_6^{DMB} siRNN and wild type control P^{WT}/G^{WT} GFP siRNAs (Figure 4.4A).

Both wild type siRNA and 6x U-SATE containing siRNNs resulted in the 5' RACE amplification of appropriately sized GFP Ago2 cleavage product cDNA fragment (189 bp) from cleaved GFP mRNA and the cleavage site specificity was confirmed by cDNA sequence analysis (Figure 4.4A & 4.4B). In contrast, 5' RACE analysis from cells transfected with irreversible 6x U-DMB containing siRNNs did not result in amplification of a specific cDNA fragment.

I hypothesized that induction of RNAi responses by phosphotriester containing oligonucleotides requires cleavage, decomposition and resolution of phosphotriesters into phosphodiester linkages for TRBP mediated loading into Ago2/RISC. To directly test this hypothesis, we ^{32}P-labeled wild type, 6x U-SATE and 6x U-DMB GFP guide strand oligonucleotides that were then duplexed to unlabeled (cold) wild type passenger strand oligonucleotides and transfected into cells. After 36 h, cells were lysed and Ago2 associated ^{32}P-labeled guide strand oligonucleotides were co-immunoprecipitated with anti-Ago2 antibodies (Figure 4.4C). Compared to input, the positive control ^{32}P-labeled wild type GFP guide strand co-immunoprecipitated with Ago2 as a full-length guide strand. Impressively, we only detected ^{32}P-labeled 6x U-(*t*-Bu-SATE) GFP guide strand associated with Ago2 that was fully reversed and now comigrated by gel electrophoresis at the same molecular weight as wild type, phosphodiester guide strand (Figure 4.4C). In contrast, we detected only background levels of control ^{32}P-labeled irreversible 6x U-DMB GFP guide strand associated with Ago2 that had not undergone intracellular cleavage. Taken together, these observations

demonstrated that *t*-Bu-SATE phosphotriester containing siRNAs are intracellularly cleaved and resolve into biologically active siRNAs, loaded into Ago2 and induce target-specific RNAi responses.

Analysis of double stranded SATE siRNNs

During the oligonucleotide synthesis oxidation step, *t*-Bu-SATE phosphotriesters will randomly resolve into either the Rp or Sp chiral configuration that eventually will protrude either into or out of the double stranded RNN major groove, respectively, and may thereby limit the number of phosphotriesters installed. Therefore, to determine if there is an upper limit to the number of *t*-Bu-SATE phosphotriesters, we synthesized and purified a series of 21mer GFP passenger strands that contained increasing numbers of *t*-Bu-SATE phosphotriesters from 4 to 16 (Figure 4.5A). Due to an increased mass and decrease of negative charge, as the number of SATE phosphotriester linkages increase the oligonucleotides migrate more slowly during denaturing gel electrophoresis in a linear fashion. However, at 14x SATE phosphotriester insertions, we begin to detect hydrophobicity problems and the decreased migration was non-linear compared to 4-12x SATE phosphotriester insertions. At 16x SATE phosphotriester insertions, we observed significant hydrophobicity issues and the oligonucleotide barely entered the gel (Figure 4.5B).

We next analyzed the ability of *t*-Bu-SATE phosphotriester containing passenger strand oligonucleotides to become double stranded with either a Cy3-labeled wild type RNA guide strand or a Cy3-labeled 9x *t*-Bu-SATE RNN guide

strand. To avoid false dsRNA interpretation, Cy3 modifications were used for guide strand oligos due to the decreased ethidium bromide intercalation with highly substititue *t*-Bu-SATE oligonucleotides (data not shown). Single stranded GFP passenger strand oligonucleotides containing between 0-16x SATE phosphotriesters were mixed at an equal molar ratio with either wild type GFP Cy3-labeled guide strand RNA oligonucleotide or 9x SATE GFP Cy3-labeled guide strand RNN oligonucleotide (Figure 4.5A), heated to 90 ^{0}C for 30 sec, cooled, subjected to native gel electrophoresis, and visualized with the Cy3 signal to determine the efficiency of double stranded RNA formation (Figure 4.5C & 4.5D). Hybridization of passenger strands containing 0 to 12 *t*-Bu-SATE phosphotriester insertions readily formed double stranded species to wild type phosphodiester guide strand. Passenger strands containing 14 and 16x *t*-Bu-SATE insertions, however, did not readily form dsRNA showing the upper limit for phosphotriester insertions for faithful dsRNA formation to wildtype guide strand oligo. In contrast, hybridization of SATE passenger strands with 0 to 9 insertions to 9x SATE GFP RNN oligonucleotide formed double stranded species, however, addition of one more *t*-Bu-SATE phosphotriester to 10x *t*-Bu-SATEs resulted in a substantial decrease in the formation of a double stranded species (Figure 4.5D). Hybridization of the 9x *t*-Bu-SATE guide strand with the 12x to 16x *t*-Bu-SATE passenger strand phosphotriester oligonucleotides showed no dsRNA formation. These observations demonstrate the ability of *t*-Bu-SATE phosphotriester oligonucleotides to form double stranded siRNNs, but also point to an upper limit

of approximately half for total *t*-Bu-SATE insertions.

Biological activity of SATE siRNNs

We next tested the ability of double stranded siRNNs containing the maximum amount of *t*-Bu-SATE modifications to induce target-specific RNAi responses. GFP expressing cells were transfected (0.5 to 100 nM) with double stranded $P_9^{tBu\text{-}SATE}/G_9^{tBu\text{-}SATE}$ GFP siRNNs, positive control wild type P^{WT}/G^{WT} GFP siRNAs and irrelevant target control $P_9^{tBu\text{-}SATE}/G_9^{tBu\text{-}SATE}$ Luciferase (Luc) siRNN and analyzed for GFP RNAi responses (Figure 4.6A). Double stranded $P_9^{tBu\text{-}SATE}/G_9^{tBu\text{-}SATE}$ GFP siRNNs induced a dose-dependent RNAi response that was near identical to positive control P^{WT}/G^{WT} GFP siRNAs. In contrast, both irrelevant target control $P_9^{tBu\text{-}SATE}/G_9^{tBu\text{-}SATE}$ Luc siRNNs and control wild type P^{WT}/G^{WT} Luc siRNAs failed to induce RNAi responses, even at the highest 100 nM concentration. Quantitative mRNA analysis by qRT-PCR showed a dose-dependent decrease of GFP mRNA levels in cells transfected with $P_9^{tBu\text{-}SATE}/G_9^{tBu\text{-}SATE}$ GFP siRNNs and positive control P^{WT}/G^{WT} GFP siRNAs, whereas cells transfected with the two irrelevant target control siRNNs and siRNAs did not show a significant change in GFP mRNA levels (Figure 4.6B). Consistent with these observations, 5' RACE analysis detected an appropriately sized GFP Ago2 cleavage product cDNA fragment (189 bp) from cells transfected with both $P_9^{tBu\text{-}SATE}/G_9^{tBu\text{-}SATE}$ GFP siRNNs and positive control P^{WT}/G^{WT} GFP siRNAs (Figure 4.6C). cDNA sequence analysis confirmed that the correct Ago2 cleavage site was present in both (Figure 4.6D). In contrast, we failed to detect an appropriate

cDNA amplification product from cells transfected with irrelevant target control $P_9^{tBu\text{-}SATE}/G_9^{tBu\text{-}SATE}$ Luc siRNN.

Lastly, we analyzed the stability of SATE phosphotriester siRNNs kinetically in human serum. We synthesized and purified 5' Infrared-dye labeled 21mer guide strands containing 2'-OH, 2'-F/2'-O-Me, and 2'-F/2'-O-Me 9x SATE phosphotriesters. IR dye-labeled oligonucleotides were incubated in 50% human serum at 37 ^{0}C, flash frozen at various time points, and analyzed by denaturing gel electrophoresis (Figure 4.6E). Consistent with previous studies, wild type 2'-OH RNA has an undetectable half-life in human serum. In contrast, inclusion of 2'-F/2'-O-Me modifications on pyrimidines and purines, respectively, resulted in an extensive increase in oligonucleotide half-life. Impressively, the 5' IR dye labeled 2'-F/2'-O-Me 9x SATE phosphotriester guide strand was even more resistant to serum-mediated degradation, and showed minimal to no degradative loss of length of SATE phosphotriesters over the 24 h exposure to human serum (Figure 4.6E). Taken together, these observations demonstrate the strong intracellular selectivity for cleavage of the thioester bond in the phosphotriester linkage by cytoplasmic thioesterases followed by loading into Ago2/RISC and induction of RNAi responses, and the inability of human serum esterases to recognize the thioester bond.

Complications of PTD Conjugation to *t*-Bu-SATE siRNNs

While cationic lipid transfection into cells in culture serves as a proof of concept for the functionality of *t*-Bu-SATE siRNN oligonucleotides, the overall

purpose for generating *t*-Bu-SATE siRNN oligonucleotides is to create monomeric PTD-siRNN conjugates that are capable of delivering siRNN oligonucleotides into cells. However, due to the limited number of *t*-Bu-SATE insertions tolerated for dsRNA formation, the aldehyde-functionalized *t*-Bu-SATE siRNN molecule still contains a strong anionic charge with 24 remaining phosphodiesters (Figure 4.7A). This requires the conjugation of highly cationic peptides due to the requirement for conjugates containing overall cationic charge for successful PTD-siRNA conjugate delivery (See Chapter 3).

Unfortunately, attempts to conjugate highly cationic peptides results in substantial insolubility of the *t*-Bu-SATE siRNN. Nondenaturing gel electrophoresis of 5 uM aliquots of P^{WT}/G^{WT} or $P_9^{tBu\text{-}SATE}/G_9^{tBu\text{-}SATE}$ centrifuged following addition of increasing amounts of 3xTAT peptide indicates siRNN insolubility at molar ratios significantly lower than those required for PTD-siRNN conjugation (Figure 4.7B). Indeed, this insolubility is independent of electrostatic precipitation as complete phosphodiester-containing P^{WT}/G^{WT} remains soluble at similar peptide ratios (Figure 4.7B). The primary complication with utilization *t*-Bu-SATE siRNN molecules for highly cationic peptide conjugation strategies is primarily due to hydrophobicity associated with the *t*-Butyl moiety. Indeed, nondenaturing gel electrophoresis of 5 uM aliquots of P^{WT}/G^{WT} or $P_9^{tBu\text{-}SATE}/G_9^{tBu\text{-}SATE}$ centrifuged following addition of increasing amounts of sodium chloride (NaCl) indicates a solubility threshold of *t*-Bu-SATE siRNN at NaCl concentrations lower than physiologically relevant levels (Figure 4.7C).

Extensive experimentation was conducted to determine conditions which favored both PTD and *t*-Bu-SATE siRNN solubility for successful conjugate formation. Indeed, success was obtained for PTD-siRNN conjugation in the presence of 60% acetonitrile and 600 mM triethylammonium acetate (data not shown). This solution was sufficient to negate the hydrophobicity of the t-Bu-SATE while still maintaining PTD solubility for successful conjugation. Isolation of the conjugate using SDS-PAGE gel extraction, gel filtration and ion-exchange chromatography all showed efficient purification of PTD-siRNN conjugates from reaction condition by-products and unreacted PTD/oligo products (data not shown). Unfortunately, attempts to utilized these purified conjugates for cellular treatment resulted in massive insolubility of the PTD-siRNN indicated by large particle formation upon dilution or resuspension in biological media (data not shown). After exhaustive experimentation, it was concluded the t-Bu-SATE siRNNs could not be utilized for PTD-siRNN conjugate delivery due to the insurmountable solubility issues in biologically relevant conditions.

CONCLUSIONS

siRNA induced RNAi responses have great potential for treating human disease, especially cancer and viral diseases (de Fougerolles, et al. 2007). However, 21mer siRNAs are heavily anionic, ~14,000 Da macromolecules with no bioavailability and require a delivery agent to enter cells (Whitehead, et al. 2009). Due to the strict requirement for intracellular recognition by TRBP's double stranded RNA binding domains, RNAi-inducing siRNAs must retain a internucleotide phosphodiester linkage backbone and are limited to 2'-OH/2'-F/2'-O-Me modifications. Consequently, the vast majority of siRNA delivery approaches have focused on liposome or nanoparticle formulations containing cationic molecules to electrostatically neutralize and condense siRNA phosphodiesters into 100-200 nm diameter nanoparticles (Whitehead, et al. 2009). Unfortunately, liposomal nanoparticle approaches suffer from inherently poor cellular delivery, low diffusion coefficients, cytotoxicity and poor pharmacokinetics restricted predominately to liver (Akinc, et al. 2009; Schroeder, et al. 2010) Thus, siRNA delivery is widely regarded as the major problem to solve for the development of RNAi therapeutics.

Our ultimate goal is to develop a monomeric, charge neutralized PTD-siRNN conjugates that do not require liposome or nanoparticle condensation for cellular delivery. Due to the strict requirement for charged phosphodiester linkages, we focused our efforts on neutralizing the phosphodiester by synthesis of bioreversible phosphotriester linkages that are selectively converted into wild

type, charged phosphodiester linkages intracellularly. After screening through several potential bioreversible phosphotriester linkages, I focused my efforts on a *t*-Bu-SATE phosphotriester-protecting group that was developed by Imbach and colleagues to mask the phosphate charge on internucleotide inhibitors of HIV Reverse Transcriptase (Lefebvre, et al. 1995).

We first developed phosphoramidite synthesis routes, optimizing oligonucleotide synthesis, and orthogonal deprotection conditions as well as advancing purification strategies to keep the sensitive phosphotriester linkages intact. These studies defined critical phosphotriester properties: 1) the thioester carbonyl is electrophilic and unstable under nucleophilic/basic oligonucleotide deprotection conditions, we therefore developed novel, milder deprotection conditions; 2) the presence of the 2'-OH group results in nucleophilic attack on the phosphotriester leading to strand cleavage, we therefore substituted the native D-ribose with RNAi tolerated 2'-F/2'-O-Me modifications; and 3) steric congestion across the major groove limits *t*-Bu-SATE incorporation to approximately half.

Cleavage of *t*-Bu-SATE phosphotriesters by cytoplasmic thioesterases initiates a two-step process resulting in rapid conversion of the neutral SATE phosphotriester to wild type charged phosphodiester (Figure 4.1A). Importantly, thioesterases are only present in the cytoplasm and organelles of cells, and extracellular esterases are unable to cleave the thioester bond, thereby avoiding extracellular decomposition (Tosquellas, et al. 1998). Indeed, we found that

siRNNs were highly resistant to serum nucleases and esterases (half-life >24 hr). Impressively, transfection of siRNNs into cells resulted in intracellular *t*-Bu-SATE cleavage, loading into Ago2, and induction of robust target-specific RNAi responses. In contrast, control siRNNs containing irreversible phosphotriester linkages were not cleaved or loaded into Ago2, and did not induce RNAi responses. Importantly, this is the first study reporting a new class of biologically active, bioreversible phosphotriester RNAi-inducing molecules and represents a critical step toward development of a monomeric, RNAi-inducing therapeutic pro-drug approach.

However, over the course of extensive experimentation, *t*-Bu-SATE siRNN oligonucleotides have posed two fundamental problems as the most likely candidates for a successful PTD-siRNN delivery strategy; 1) due to steric hindrance across the dsRNA major groove, *t*-Bu-SATE modifications can only be substituted to neutralize ~50% of the phosphodiesters of the siRNA molecule, which requires the use of highly cationic peptides to create an overall cationic charge for the conjugate (Figure 4.7A); and 2) the hydrophobic nature of the *t*-butyl moiety makes *t*-Bu-SATE siRNN molecules highly insoluble in both the presence of cationic PTDs for conjugation reactions as well as physiologically relevant salt concentrations for cellular treatment (Figure 4.7B & 4.7C). These two fundamental properties can only be solved by further chemical manipulation of the bioreversible phosphotriester modification to increase solubility and decrease the overall anionic charge of the final siRNN oligonucleotide. I

proposed two ways to accomplish this goal: 1) decrease the hydrophobicity of the terminal *t*-butyl group by methyl group reduction; or 2) increase the hydrophilicity by terminally modifying *t*-Bu-SATE groups with polar groups that allow for increased solubility in the presence of cationic peptides and biologically-relevant conditions.

Chapter 4, in part, is currently being prepared for submission for publication of the material. Meade Bryan R.; Gogoi, Khirud; van den Berg, Arjen; Hagopian, Jonathan C.; Rudolph, Zachary H.; Dowdy, Steven F. The dissertation author was the primary investigator and author of this material.

A

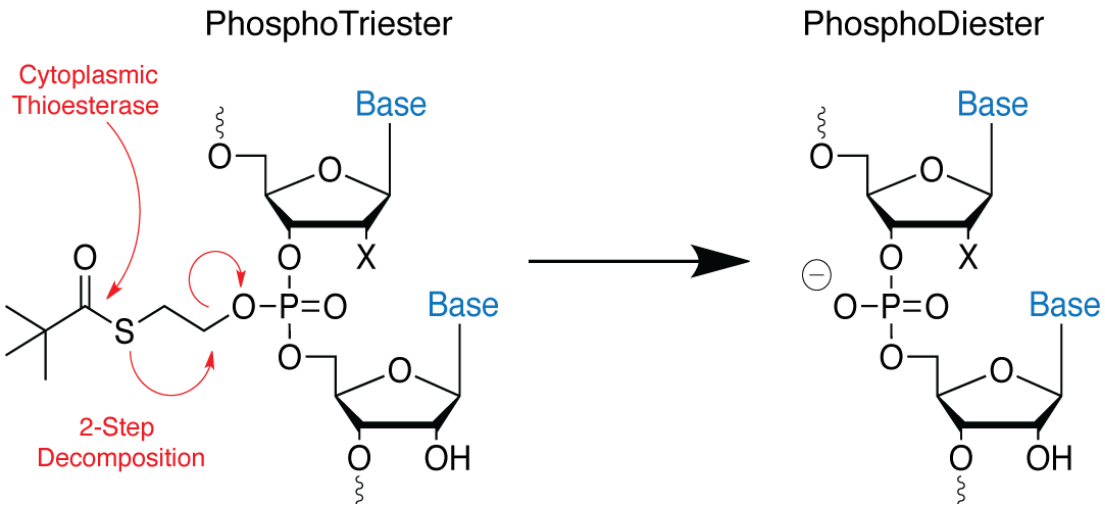

Figure 4.1. Cytoplasmic thioesterase conversion of t-Bu-SATE phosphotriesters. A) Cytoplasmic thioesterase processing of t-Bu-SATE modification induces a rapid 2-step decomposition process resulting in RNAi-compatible wildtype phosphodiester.

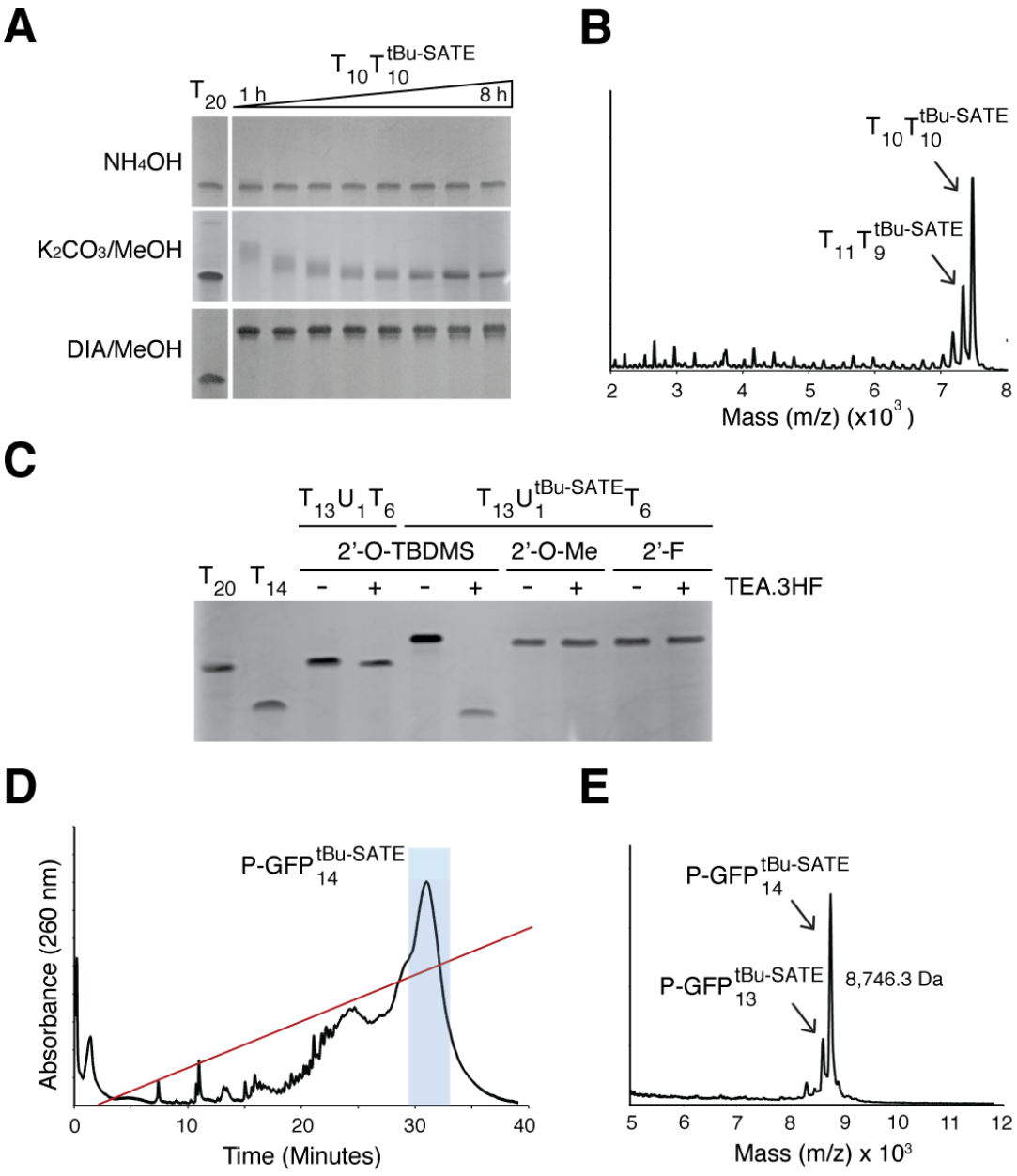

Figure 4.2. Base deprotection and purification of t-Bu-SATE siRNN oligonucleotides. A) Gel electrophoresis analysis of t-Bu-SATE phosphotriester $T_{10}T_{10}^{tBu\text{-}SATE}$ oligonucleotide exposed to various deprotection conditions over time. 15% denaturing gel, stained with methylene blue. T_{20}, reference oligonucleotide. **B)** Mass spectrometry analysis of crude deprotected $T_{10}T_{10}^{tBu\text{-}SATE}$ oligonucleotide. **C)** Comparison of 2'-OH, 2'F, 2'-O-Me modification in presence of single Uridine SATE phiosphotriester $T_{13}U_1^{tBu\text{-}SATE}T_6$ oligonucleotide. 2'-O-TBDMS deprotected by TEA.3HF addition results in strand cleavage and appearance of co-migrating band with T_{14} reference. 15% denaturing gel, stained with methylene blue. T_{20}, T_{14} reference oligonucleotides. **D)** HPLC purification and mass spectrometry of P-$GFP_{14}^{tBu\text{-}SATE}$ oligonucleotide. Red line, ACN gradient (0-80% 2'-42'), blue box isolated fraction analyzed for mass spectrometry. **E**) MALDI-TOF mass spec analysis of P-$GFP_{14}^{tBu\text{-}SATE}$ oligonucleotide. Note presence of only small amount of single t-Bu-SATE reversal product.

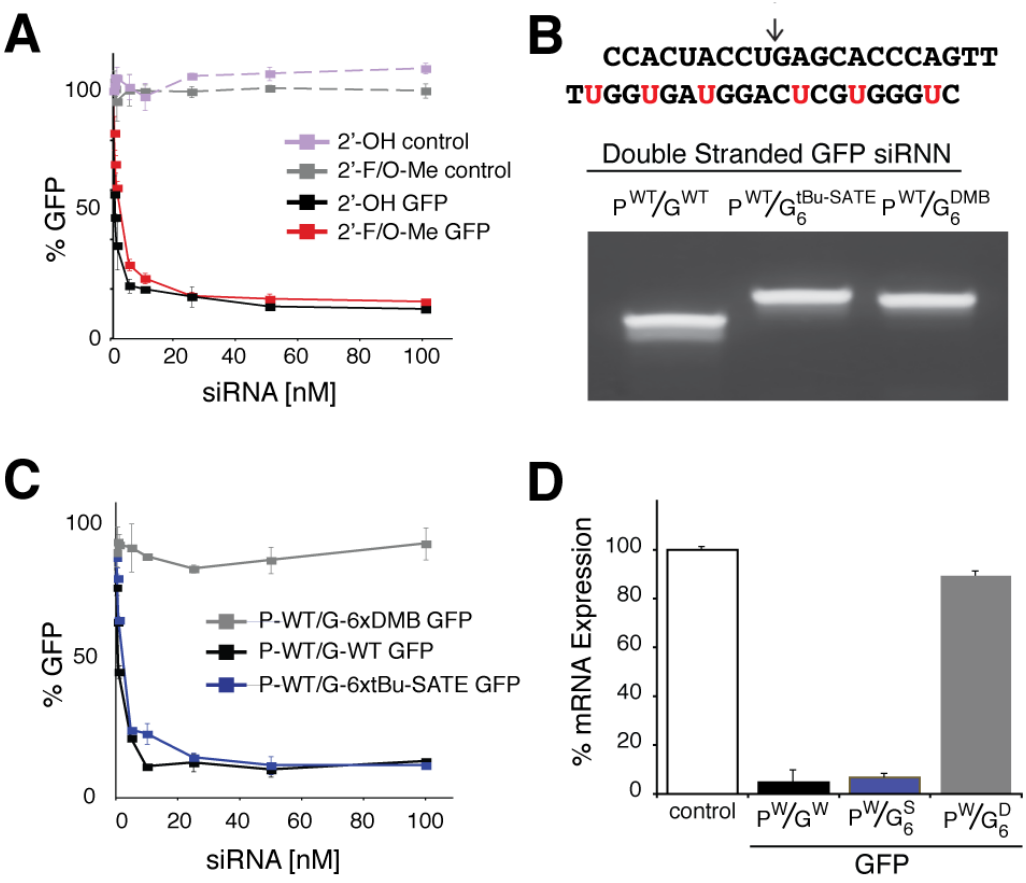

Figure 4.3. t-Bu-SATE phosphotriester oligonucleotides are cleaved *in vivo* and induce target-specific RNAi responses. A) GFP siRNAs containing 2"-OH or 2'-F/2'-O-Me targeting GFP or irrelevant control were transfected into constitutive GFP expressing cells and analyzed at day 2 for GFP expression by flow cytometry. **B)** Double stranded sequence of GFP siRNA used in this study. Passenger (P) (sense) strand 5'-3' on top, Guide (G) (antisense) strand 3'-5' on bottom. Red bases denote insertion of t-Bu-SATE phosphotriester 3' to base. Arrow indicates site of GFP mRNA cleavage by Ago2. Gel electrophoresis of double stranded oligonucleotides as indicated. 15% nondenaturing gel, stained with ethidium bromide. WT, wild type phosphodiester oligonucleotide; t-Bu-SATE, bioreversible phosphotriester; DMB, irreversible phosphotriester. **C**) GFP RNAi analysis from GFP expressing cells transfected with wild type phosphodiester passenger strand (P-WT) duplexed to wild type phosphodiester guide strand (G-WT), 6x tBu-SATE or 6x DMB phosphotriester oligonucleotides and analyzed at day 2 for GFP expression by flow cytometry. All oligonucleotides were 2'-F/2'-O-Me modified. **D**) Quantitative qRT-PCR analysis of GFP mRNA. 'S' represents t-Bu-SATE insertions; 'D' represents DMB insertions.

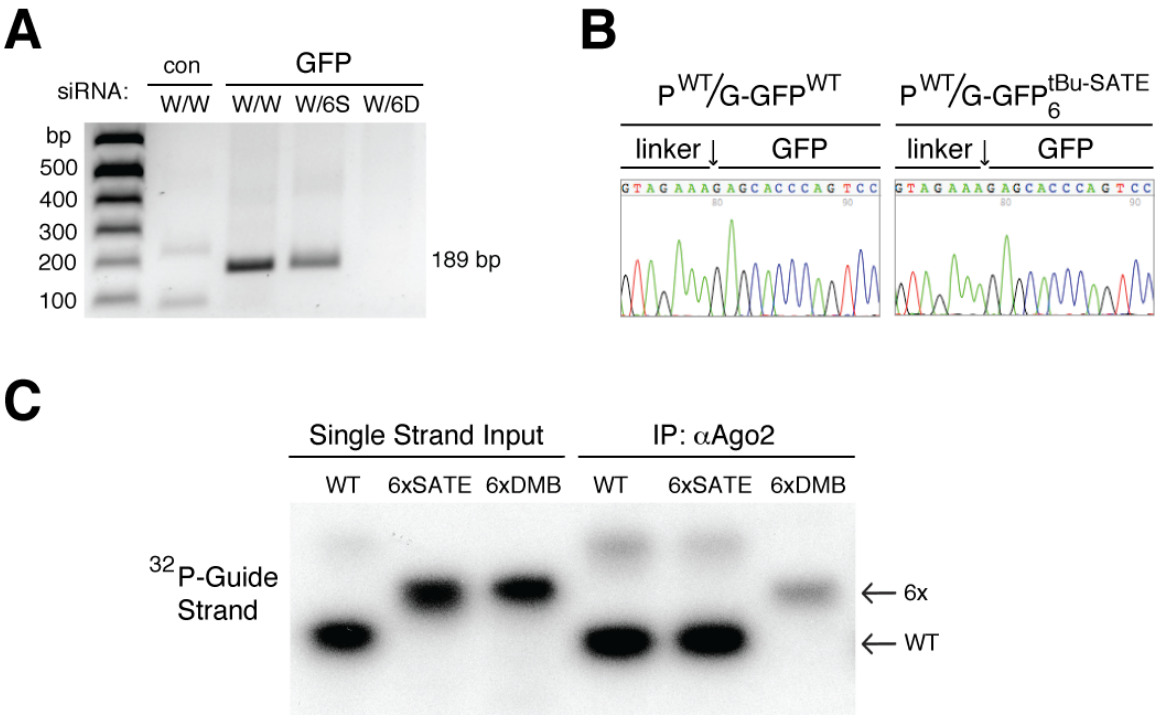

Figure 4.4. Validation of intracellular conversion and RNAi induction for t-Bu-SATE phosphotriester oligonucleotides. A) 5' RACE analysis of GFP mRNA from Figure 4.3. Control, irrelevant non-targeting siRNA. 189 bp is the correct cDNA fragment size. 'S' designated tbu-SATE insertions; 'D' designated DMB insertions **B)** cDNA sequence analysis of 5' RACE cDNA fragment. Arrow indicates correct Ago2 cleavage site. **C)** Anti-Ago2 co-immunoprecipitation from cells transfected with wild type phosphodiester passenger strand (P-WT) duplexed to 32P-labeled wild type phosphodiester guide strand (G-WT), 6x t-Bu-SATE (6xSATE) or 6x DMB phosphotriester oligonucleotides and analyzed at 30 h. Note in vivo cleavage of G-GFP-6xSATE oligonucleotide and co-migration with wild type phosphodiester oligonucleotide. 15% denaturing gel. Single strand input prior to transfection. 6x indicates position of oligonucleotide containing 6x phosphotriesters.

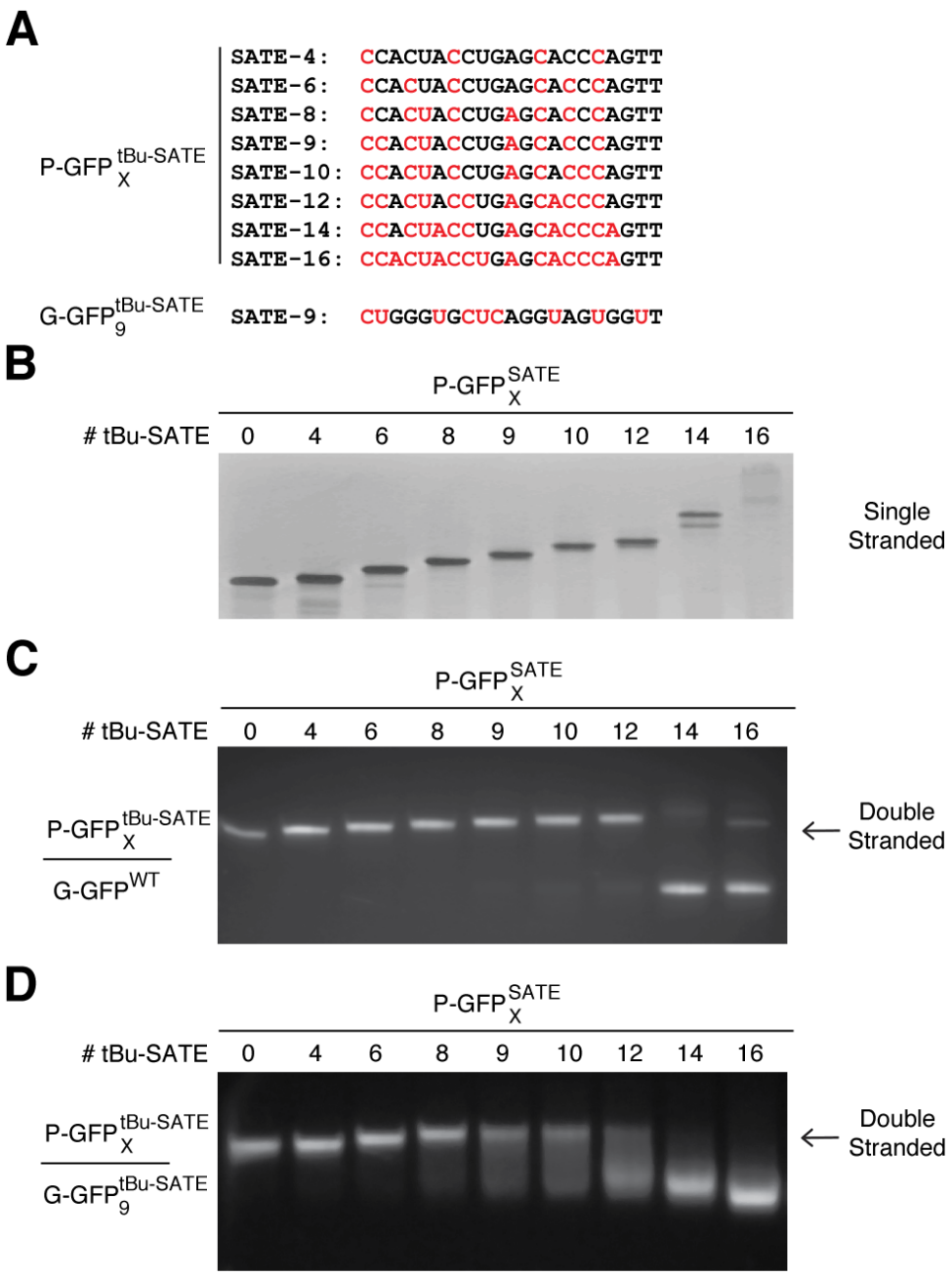

Figure 4.5. Double stranded SATE siRNN oligonucleotides. A) Number and location of tBu-SATE insertions in passenger (P) and guide (G) strand sequences indicated in red. **B)** Denaturing gel analysis of single stranded passenger strand with varying tBu-SATE insertions. Note smear of P-16xSATE due to excessive hydrophobicity. **C)** Cy3 signal of native gel of double stranded passenger strand with varying tBu-SATE insertions duplexed to wild type phosphodiester Cy3-guide strand. Note inability of double stranded P14xSATE and P16xSATE to form double stranded molecules. **D)** EtBr stained native gel of double stranded passenger strand with varying tBu-SATE insertions duplexed to 9x SATE containing phosphotriester Cy3-guide strand. Note inability of double stranded P-10xSATE and higher tBu-SATE oligonucleotides to form double stranded molecules with G-9xSATE-Cy3 oligonucleotides.

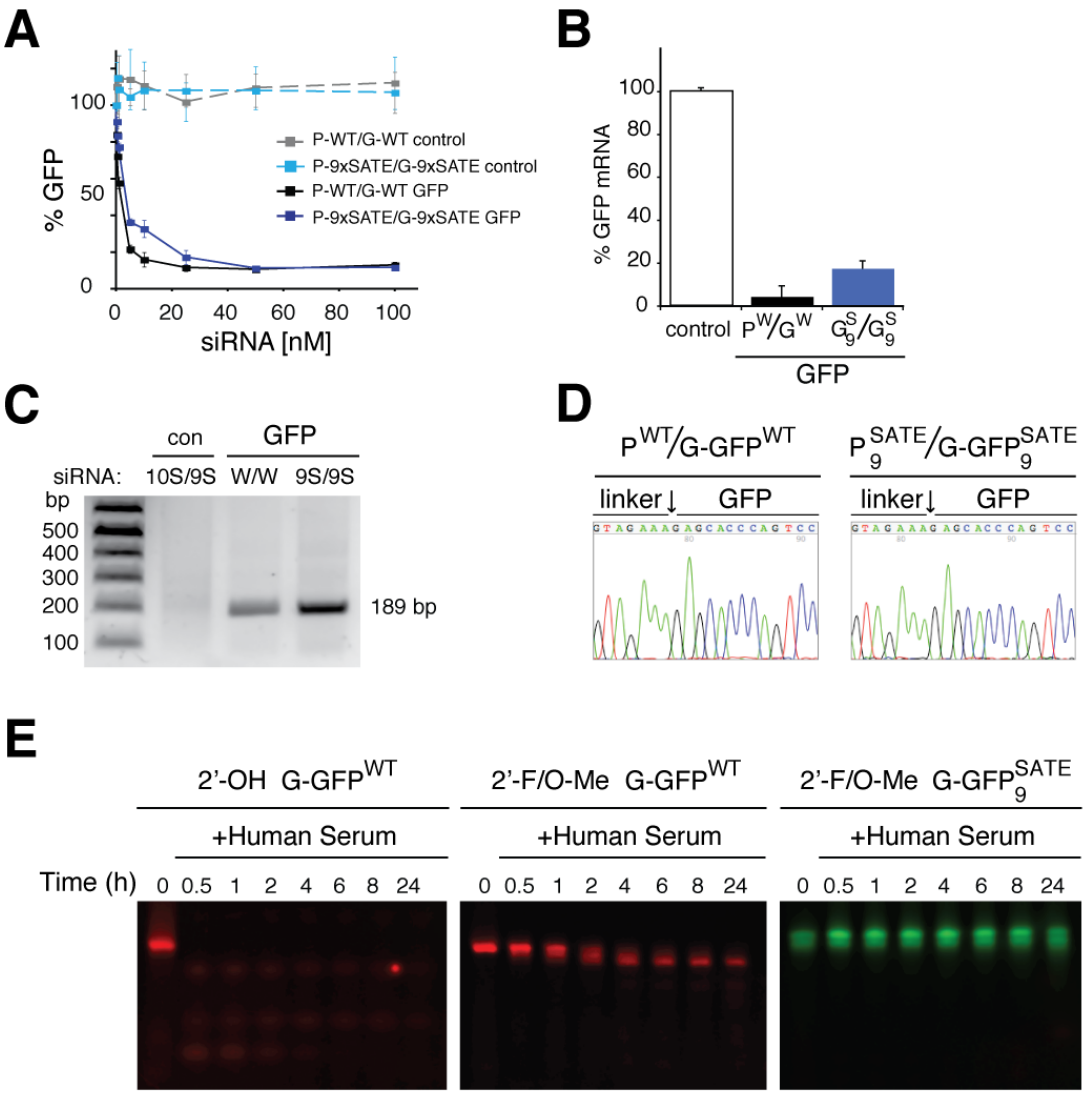

Figure 4.6. Maximally-neutralized tBu-SATE siRNNs induce RNAi responses. A) GFP RNAi analysis from GFP expressing cells transfected with wild type phosphodiester passenger and guide strands (P-WT/G-WT) GFP or control siRNAs, and tBu-SATE phosphotriester passenger and guide strands (P-9xSATE/G-9xSATE) GFP or control siRNNs and analyzed at day 2 for GFP expression by flow cytometry. All oligonucleotides were 2'- F/2'-O-Me modified. **B)** Quantitative qRT-PCR analysis of GFP mRNA from (A). **C)** 5' RACE analysis of GFP mRNA from (A). Control, irrelevant non-targeting siRNA. 189 bp is the correct cDNA fragment size. **D)** cDNA sequence analysis of 5' RACE cDNA fragment from (C). Arrow indicates correct Ago2 cleavage site. **E)** Stability analysis of dye-labeled wild type phosphodiester 2'-OH, wild type phosphodiester 2'-F/O-Me or 9xSATE phosphotriester guide strand oligonucleotides incubated in 50% human serum at 37 ^{0}C for indicated times and analyzed on a 15% denaturing gel. 0 indicates starting input. Note stability of tBu-SATE phosphotriester RNN oligonucleotide.

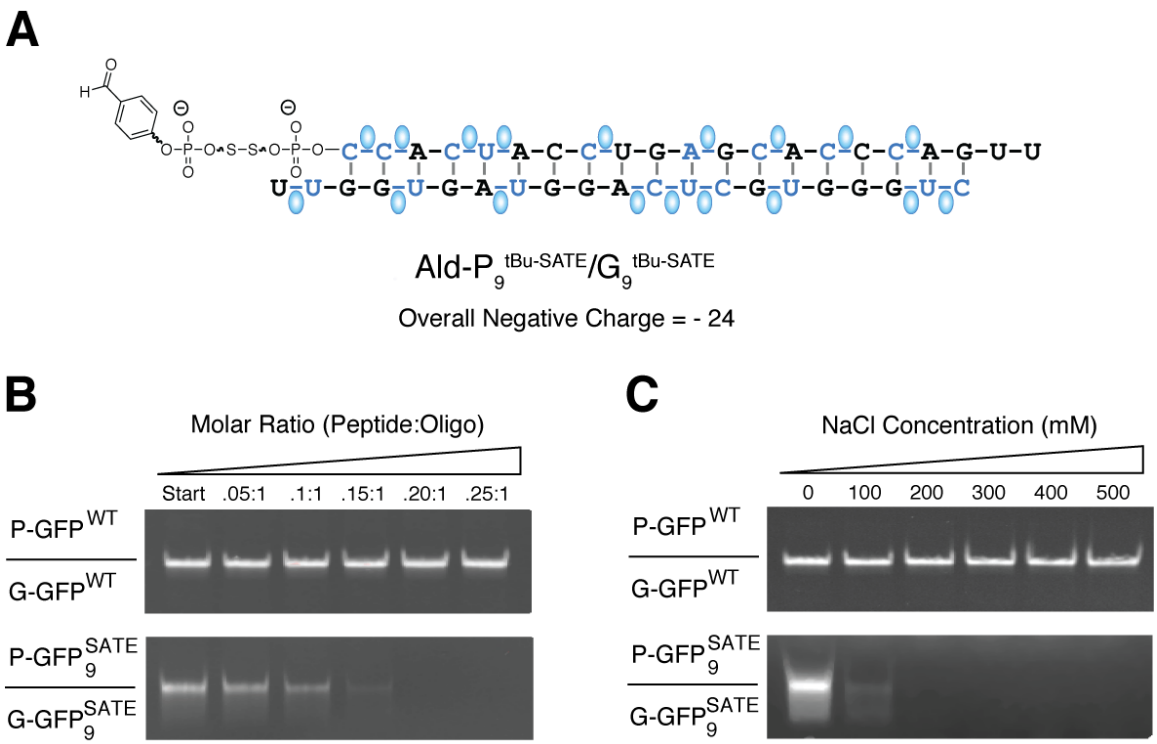

Figure 4.7. Solubility complications with tBu-SATE phosphotriester siRNNs. A) GFP siRNN sequence showing insertion sites for maximum amount of tBu-SATE modifications on aldehyde-functionalized siRNN oligo. Oligo still contains 24 phosphodiester groups. **B)** Nondenaturing gel analysis of P^{WT}/G^{WT} and $P_9^{tBu\text{-}SATE}/G_9^{tBu\text{-}SATE}$ oligos in the presence of increasing amounts of 3xTAT peptide. Note insolubility of tBu-SATE containing oligo at as little as .1:1 (Peptide:Oligo) molar ratios. **C)** Nondenaturing gel analysis of P^{WT}/G^{WT} and $P_9^{tBu\text{-}SATE}/G_9^{tBu\text{-}SATE}$ oligos in the presence of increasing amounts of NaCl. Note insolubility of tBu-SATE containing oligos in <100 mM NaCl.

REFERENCES

Akinc A, Goldberg M, Qin J, et al. Development of lipidoid-siRNA formulations for systemic delivery to the liver. Mol Ther 2009;17:872-9.

Alvarez K, Vasseur JJ, Beltran T, Imbach JL. Photocleavable protecting groups as nucleobase protections allowed the solid-phase synthesis of base-sensitive SATE-prooligonucleotides. J Org Chem 1999;64:6319-6328.

Beaucage SL. Solid-phase synthesis of siRNA oligonucleotides. Curr Opin Drug Discov Devel 2008;11:203-16.

Blidner RA, Svoboda KR, Hammer RP, Monroe WT. Photoinduced RNA interference using DMNPE-caged 2'-deoxy-2'-fluoro substituted nucleic acids in vitro and in vivo. Mol Biosyst 2008;4:431-40.

Bumcrot D, Manoharan M, Koteliansky V, Sah DW. RNAi therapeutics: a potential new class of pharmaceutical drugs. Nat Chem Biol 2006;2:711-9.

de Fougerolles A, Vornlocher HP, Maraganore J, Lieberman J. Interfering with disease: a progress report on siRNA-based therapeutics. Nat Rev Drug Discov 2007;6:443-53.

Eguchi A, Meade BR, Chang YC, et al. Efficient siRNA delivery into primary cells by a peptide transduction domain-dsRNA binding domain fusion protein. Nat Biotechnol 2009;27:567-71.

Elbashir SM, Harborth J, Lendeckel W, Yalcin A, Weber K, Tuschl T. Duplexes of 21-nucleotide RNAs mediate RNA interference in cultured mammalian cells. Nature 2001;411:494-8.

Faraj A, Placidi L, Perigaud C, et al. Intracellular metabolism of beta-L-ddAMP-bis(tbutylSATE), a potent inhibitor of hepatitis B virus replication. Nucleosides Nucleotides 1999;18:987-8.

Grajkowski A, Pedras-Vasconcelos J, Wang V, et al. Thermolytic CpG-containing DNA oligonucleotides as potential immunotherapeutic prodrugs. Nucleic Acids Res 2005;33:3550-60.

Gump JM, Dowdy SF. TAT transduction: the molecular mechanism and therapeutic prospects. Trends Mol Med 2007;13:443-8.

Guzaev AP, Bhat B, Balow G, Manoharan M. Synthesis of chimeric oligonucleotides containing internucleosidic phosphodiester and S-pivaloylthioethyl phosphotriester residues. Nucleosides Nucleotides Nucleic Acids 2001;20:1015-8.

Kuijpers WH, Huskens J, Koole LH, van Boeckel CA. Synthesis of well-defined phosphate-methylated DNA fragments: the application of potassium carbonate in methanol as deprotecting reagent. Nucleic Acids Res 1990;18:5197-205.

Lefebvre I, Perigaud C, Pompon A, et al. Mononucleoside phosphotriester derivatives with S-acyl-2-thioethyl bioreversible phosphate-protecting groups: intracellular delivery of 3'-azido-2',3'-dideoxythymidine 5'-monophosphate. J Med Chem 1995;38:3941-50.

Manoharan M. RNA interference and chemically modified small interfering RNAs. Curr Opin Chem Biol 2004;8:570-9.

Meade BR, Dowdy SF. Exogenous siRNA delivery using peptide transduction domains/cell penetrating peptides. Adv Drug Deliv Rev 2007;59:134-40.

Nguyen QN, Chavli RV, Marques JT, et al. Light controllable siRNAs regulate gene suppression and phenotypes in cells. Biochim Biophys Acta 2006;1758:394-403.

Peyrottes S, Egron D, Lefebvre I, Gosselin G, Imbach JL, Perigaud C. SATE pronucleotide approaches: an overview. Mini Rev Med Chem 2004;4:395-408.

Pon RT, Yu S. Hydroquinone-O,O'-diacetic acid ('Q-linker') as a replacement for succinyl and oxalyl linker arms in solid phase oligonucleotide synthesis. Nucleic Acids Res 1997;25:3629-35.

Schroeder A, Levins CG, Cortez C, Langer R, Anderson DG. Lipid-based nanotherapeutics for siRNA delivery. J Intern Med 2010;267:9-21.

Tosquellas G, Alvarez K, Dell'Aquila C, et al. The pro-oligonucleotide approach: solid phase synthesis and preliminary evaluation of model pro-dodecathymidylates. Nucleic Acids Res 1998;26:2069-74.

Tosquellas G, Bologna JC, Morvan F, Rayner B, Imbach JL. First synthesis of alternating SATE-phosphotriester/phosphodiester prooligonucleotides on solid support. Bioorg Med Chem Lett 1998;8:2913-8.

Whitehead KA, Langer R, Anderson DG. Knocking down barriers: advances in siRNA delivery. Nat Rev Drug Discov 2009;8:129-38.

CHAPTER 5

SYNTHESIS AND ANALYSIS OF S-ACYL-THIOETHYL (SATE) PHOSPHOTRIESTER DERIVATIVES

ABSTRACT

Successful delivery of siRNA oligonucleotides with PTD-siRNA conjugates requires the manipulation of the siRNA phosphodiester backbone to relieve the electrostatic neutralization of crucial basic residues of the PTD peptide for cell surface interaction. Our work with *t*-Bu-SATE siRNN oligonucleotides highlighted the potential to generate oligonucleotides containing phosphodiester-neutralizing modifications that revert to wildtype siRNA oligonucleotides upon exposure to the intracellular environment. Unfortunately, the ability to generate PTD-siRNN conjugates with *t*-Bu-SATE modifications presented significant problems due to the extensive hydrophobicity associated with *t*-Bu-SATE groups. In an attempt to circumvent this hydrophobicity issue, we synthesized a collection of oligonucleotides containing bioreversible SATE variations with progressive methyl group reductions distal to the thioester bond. Unfortunately, methyl group reduction distal to the *t*-Bu-SATE thioester bond resulted in thioester destabilization during oligonucleotide deprotection conditions. However, extension of the proximal S-Acyl-2-ThioEthyl (SATE) linkage to a S-Acyl-4-ThioButyl (SATB) linkage stabilized the thioester bond allowing for deprotection and purification. Transfection of bioreversible SATB phosphotriester containing

RNAi-inducing oligonucleotides into cells results in target-specific RNAi responses. However, while synthesis was accomplished for SATB siRNNs, the hydrophobicity issue still proved to be rate-limiting for successful PTD-siRNN conjugate generation.

INTRODUCTION

The discovery that synthetic siRNA molecules could be exogenously added to human cells and induce RNA interference responses spurred a rapid race to develop safe and efficient siRNA delivery strategies for therapeutic applications for human disease (de Fougerolles, et al. 2007). The majority of these delivery systems have relied on nanoparticle delivery systems that were previous developed for antisense and gene therapy applications in the prior decade (Whitehead, et al. 2009; Schroeder, et al. 2010). In order to avoid inherent problems associated with nanoparticle-based siRNA delivery strategies, our laboratory has attempted to utilize the power of Peptide Transduction Domains (PTDs) to deliver siRNA molecules as monomeric, soluble entities.

The successful delivery of siRNA with these cationic peptides can only be attained with PTD-siRNA conjugates containing neutralized phosphodiester backbone linkages on the siRNA molecule in order to avoid electrostatic neutralization of the cationic residues of the PTD required for cellular uptake (Chapter 3). Due to the strict requirement of RISC for the presence of phosphodiester linkages on the siRNA molecule (Manoharan, et al. 2004), we utilized a pro-drug format for siRNA oligonucleotide synthesis with neutralizing *t*-Bu-SATE phosphotriester modifications that are converted intracellularly to wildtype phosphodiesters and capable of inducing efficient RNAi responses (Tosquellas, et al. 1998, Peyrottes, et al. 2004).

While synthesis of these oligoncucleotides served as a strong proof-of-

concept that siRNN molecules are synthetically possible, complications arose following PTD-siRNN conjugation attempts. While PTD-siRNN *t*-Bu-SATE conjugates were generated and purified, the significant hydrophobicity of the t-butyl moiety rendered these conjugates insoluble in biologically-relevant solutions. In order to circumvent this hydrophobicity issue, we began synthesizing a collection of oligonucleotides containing SATE variations with progressive methyl reduction distal to the thioester bond (Figure 5.1A). Unfortunately, manipulation of the distal carbon content led to a decreased stability in oligonucleotide deprotection conditions employed for *t*-Bu-SATE siRNNs. Stabilization of these distal variations was accomplished by increasing the alkyl length proximal to the thioester bond, converting S-Acyl-ThioEthyl (SATE) to S-Acyl-ThioButyl (SATB) modifications. SATB siRNN oligonucleotides were efficiently synthesized and displayed similar RNAi activity compared to *t*-Bu-SATE siRNN molecules. However, synthetic stability required the increase in alkyl chain length proximal to the thioester bond for distal methyl reduction, thus the overall hydrophobicity of the SATB variations did not succeed in significantly decreasing the hydrophobicity for successful PTD-siRNN conjugation.

RESULTS AND DISCUSSION

Progressive methyl reduction distal to the thioester bond

As was accomplished for t-Bu-SATE siRNN synthesis, standard phosphoramidite and oligonucleotide synthesis routes were done for generation of full length siRNN oligonucleotides. Similar to *t*-Bu-SATE siRNN oligonucleotides, it was necessary to deprotect all SATE-containing oligonucleotides with an 'Ultramild' deprotection strategy including the use of 10% DIA/MeOH, phenoxyacetal-protected nucleobases and Q-linked solid supports (Chapter 4). All oligonucleotide deprotection requirements including nucleobase deprotection, 2-cyanoethyl phosphodiester deprotection and solid support release are accomplished within 4 hours of 10% DIA/MeOH treatment.

To investigate the structural requirement distal to the SATE thioester bond, we synthesized tester oligonucleotides containing derivative SATE phosphotriester insertions with 6x 2'F-uridines, $T_{14}U_6^{X\text{-}SATE}$, where X: methyl-SATE (Me-SATE), ethyl-SATE (Et-SATE), isopropyl-SATE (iPr-SATE) and control *t*Bu-SATE (Figure 5.1A). The $T_{14}U_6^{X\text{-}SATE}$ oligonucleotides were deprotected and analyzed for phosphotriester integrity by denaturing gel electrophoresis (Figure 5.1A). Both the $T_{14}U_6^{Me\text{-}SATE}$ and $T_{14}U_6^{Et\text{-}SATE}$ oligonucleotides showed significant decomposition over the 4 hr time course. However, the $T_{14}U_6^{iPr\text{-}SATE}$ showed some decomposition by 4 hr, but remained largely intact, whereas the $T_{14}U_6^{tBu\text{-}SATE}$ oligonucleotide remained completely intact. Due to the corresponding sensitivity to base treatment and distal methyl

group reduction, these observations suggest that the distal methyl groups contribute electrons to reduce the partial dipole moment and thereby stabilize the thioester carbonyl during nucleophilic base deprotection conditions.

To test for the ability of cellular thioesterases to cleave the distal SATE modifications, using the synthesis and deprotection protocol described above, I synthesized GFP guide (G) (antisense) strand oligonucleotides containing 6x 2'F-uridine insertions (Figure 4.3B). Previously, I determined that insertion of 6x 2'F-uridines containing irreversible DMB phosphotriesters into the GFP guide strand fails to decompose intracellulary, does not become loaded into Ago2, and does not induce an RNAi response (Chapter 4). To enrich for full-length 21mer oligonucleotides, G-GFP-$U_6^{X\text{-}SATE}$ oligonucleotides were first purified by Dimethoxytrityl (DMT)-On reverse-phase high performance liquid chromatography (RP-HPLC), followed by acidic DMT removal, a second RP-HPLC and MALDI-TOF mass spectrometry analysis (Figure 5.1B). This approach resulted in the isolation of full-length G-GFP-$U_6^{X\text{-}SATE}$ oligonucleotides with 6x intact *t*-Bu-SATE phosphotriesters and 6x intact iPr-SATE phosphotriesters (>90%) with ~10% contaminating 5x insertion oligonucleotides. However, due to substantial decomposition in 10% DIA/MeOH, 6x insertion Me-SATE and Et-SATE phosphotriester oligonucleotides were only able to be isolated as mixtures of 2-5 phosphotriester insertions (Figure 5.1C). Due to the lack of purity, I did not pursue the Me-SATE and Et-SATE phosphotriester oligonucleotides for biological analyses.

To test for the ability of cytoplasmic thioesterases to recognize the derivative SATE phosphotriesters, we hybridized the G-GFP-$U_6^{X\text{-}SATE}$ oligonucleotides to wild type passenger (P-GFP^{WT}) (sense) strands to form stable dsRNA duplexes. Human H1299 lung adenocarcinoma cells containing an integrated, constitutively expressed destabilized GFP reporter gene (~2 h half-life) were transfected with double stranded P-^{WT}/G-GFP-$U_6^{iPr\text{-}SATE}$ siRNAs, P-^{WT}/G-GFP-$U_6^{tBu\text{-}SATE}$ siRNAs, control irreversible P-^{WT}/G-GFP_6^{DMB} siRNAs and wild type control P-^{WT}/G-GFP^{WT} siRNAs and analyzed for GFP expression by flow cytometry (FACS) over a 3 day time course (Figure 5.1D). Impressively, both P-^{WT}/G-GFP-$U_6^{iPr\text{-}SATE}$ and P-^{WT}/G-GFP-$U_6^{tBu\text{-}SATE}$ siRNAs induced RNAi responses that were near identical to wild type control P-^{WT}/G-GFP^{WT} siRNAs at all time points. In contrast, P-^{WT}/G-GFP_6^{DMB} siRNAs containing six irreversible DMB phosphotriesters failed to induce an RNAi response. Likewise, transfection of negative control, irrelevant targeted P-^{WT}/G-Luc-$U_6^{tBu\text{-}SATE}$ siRNAs and P-^{WT}/G-Luc^{WT} siRNAs failed to induce a GFP RNAi response (Figure 5.1D). The reduction of the distal thioester content from *t*-Bu-SATE to IPr-SATE (Figure 5.1A) displays no alteration of thioesterase processing as transfection of 6x insertion siRNA strands shows no difference in RNAi induction. However, a single methyl reduction of the t-butyl moiety does not change the problematic hydrophobicity pattern associated with PTD-siRNN conjugate formation for *t*-Bu-SATE siRNNs (data not shown).

Alkyl chain lengthening proximal to the thioester bond

We hypothesized that the sensitivity of the Me-SATE and Et-SATE phosphotriesters was due to base-mediated attack of the thioester and decomposition of the phosphotriester similar to the 2-step decomposition reaction that occurs following thioesterase processing (Figure 5.2A). In order to slow the kinetics of this base-mediated decomposition, we hypothesized that lengthening the alkyl chain proximal to the thioester bond would result in decreased sensitivity to base-mediated decay due to less favorable by-product formation during the 2-step decomposition process (Figure 5.2A). However, this proximal thioester manipulation may also decrease the kinetics of phosphotriester conversion by intracellular thioesterases and thus, have a negative impact on RNAi responses with siRNN oligonucleotides. In order to address this issue, I synthesized proximally-modified S-Acyl-ThioPropyl and S-Acyl-ThioButyl phosphotriesters with distal *t*-butyl groups and determined RNAi induction compared to the *t*-Bu-SATE siRNN (Figure 5.2A).

To investigate the biological properties of derivative phosphotriesters proximal to the thioester bond, I synthesized and purified GFP guide strand oligonucleotides containing 6x uridine insertion G-GFP-$U_6^{tBu\text{-}SAT\text{-}X}$ oligonucleotides, with terminal *t*-butyl groups and where X: propyl (*t*Bu-SATP), butyl (*t*Bu-SATB) and control *t*Bu-SATE (Figure 5.2A). G-GFP-$U_6^{tBu\text{-}SAT\text{-}X}$ oligonucleotides were duplex to P-GFP^{WT} and analyzed by transfection into GFP expressing cells (Figure 5.2C). As previously shown, cells transfected with P-^{WT}/G-GFP-$U_6^{tBu\text{-}SATE}$ siRNAs induced RNAi responses with a similar magnitude

and kinetics as wild type control P-^{WT}/G-GFP^{WT} siRNAs. However, the extension of the bond proximal to the thioester with one additional methylene in the P-^{WT}/G-GFP-U$_6^{tBu\text{-}SAT\text{-}P}$ siRNA resulted in a dramatic reduction and incomplete RNAi response, suggesting that formation of a geometrically strained four membered ring at the second decomposition step becomes rate-limiting. Interestingly, the P-^{WT}/G-GFP-U$_6^{tBu\text{-}SAT\text{-}B}$ siRNAs induced an intermediate RNAi response at 24 and 48 hr that caught up to the wild type control siRNA by 72 hr (Figure 5.2C). These observations demonstrate the impact that the proximal thioester bond has on the kinetics of intracellular phosphotriester decomposition. It also serves as a proof of concept that the kinetics of thioesterase activation of siRNN oligonucleotides can be fine-tuned following SATE phosphotriester manipulation.

Synthesis of distal derivative SATB-phosphotriester siRNNs

To investigate the consequences of altering the distal thioester functional group for SATB phosphotriester variations, I synthesized GFP guide strand oligonucleotides containing 6x insertion G-GFP-U$_6^{X\text{-}SATB}$ oligonucleotides, with a proximal butyl group and where X: methyl-SATB (Me-SATB), ethyl-SATE (Et-SATB), isopropyl-SATE (iPr-SATB) and control *t*-Bu-SATB. In contrast to X-SATE derivative phosphotriesters, all T14-U$_6^{X\text{-}SATB}$ tester oligonucleotides displayed increased stability during oligonucleotide deprotection (Figure 5.3A). Due to this increase in stability, I was able to purify 6x phosphotriester inserted G-GFP-U$_6^{X\text{-}SATB}$ oligonucleotides for all four derivatives for RNAi studies (Figure 5.3B). G-GFP-U$_6^{X\text{-}SATB}$ oligonucleotides readily duplexed to P-GFP^{WT} strands

(Figure 5.3C). Double stranded P-^{WT}/G-GFP-U$_6^{Me\text{-}SATB}$ siRNAs, P-^{WT}/G-GFP-U$_6^{Et\text{-}SATB}$ siRNAs, P-^{WT}/G-GFP-U$_6^{iPr\text{-}SATB}$ siRNAs, P-^{WT}/G-GFP-U$_6^{tBu\text{-}SATB}$ siRNAs, control *t*-Bu-SATE P-^{WT}/G-GFP-U$_6^{tBu\text{-}SATE}$ siRNAs, control irreversible P-^{WT}/G-GFP$_6^{DMB}$ siRNAs and wild type control P-^{WT}/G-GFP^{WT} siRNAs were transfected into GFP expressing cells and analyzed for GFP expression by flow cytometry over a 3 day time course (Figure 5.3D).

Consistent with the previous analysis, P-^{WT}/G-GFP-U$_6^{tBu\text{-}SATB}$ siRNAs showed a partial and delayed RNAi response. Surprisingly, P-^{WT}/G-GFP-U$_6^{Me\text{-}SATB}$, P-^{WT}/G-GFP-U$_6^{Et\text{-}SATB}$, and P-^{WT}/G-GFP-U$_6^{iPr\text{-}SATB}$ siRNAs all showed RNAi responses with similar magnitude and kinetics as the wild type positive control P-^{WT}/G-GFP^{WT} siRNAs (Figure 5.3D). In contrast, the negative control siRNAs (irreversible P-^{WT}/G-GFP$_6^{DMB}$, irrelevant targeted P-^{WT}/G-Luc-U$_6^{tBu\text{-}SATE}$, irrelevant targeted P-^{WT}/G-GFP^{WT}) failed to induce a GFP RNAi response. The most likely explanation for the discrepancy between the reversal kinetics of *t*-Bu-SATB compared to the other SATB variations is the steric hindrance of the bulky *t*-butyl group to thioesterase access to the thioester bond. The delayed kinetics for the distal *t*-butyl modification is only apparent when the reversal kinetics of the proximal ethyl is altered by a butyl linkage. In the case of less bulky distal Me-, Et- and iPr-SATB linkages, thioesterase access to the thioester is less hindered thus increasing the overall kinetics of the decomposition reaction and allowing the butyl linkage to decompose as readily as the *t*-Bu-SATE phosphotriester. Importantly, this highlights how thioesterase activity can be modulated and how

bioreversible phosphotriester siRNA oligonucleotides can be fined tuned to meet synthetic requirements yet still maintain biological functionality.

Utilization of Me-SATB phosphotriesters for PTD-siRNN conjugates

The overall goal of the above study was an attempt to decrease the extensive hydrophobicity of *t*-Bu-SATE siRNNs to obtain siRNN molecules with sufficient hydrophilicity to maintain solubility in biologically relevant conditions following PTD conjugation. Of the multiple siRNN phosphotriesters produced, the Me-SATB represents the least hydrophobic modification that still tolerates oligonucleotide deprotection and purification conditions. In order to avoid synthesis of maximally modified Me-SATB siRNNs as was done for *t*-Bu-SATE siRNN oligonucleotides, sodium chloride (NaCl) precipitation assays were done on the previously described 6x insertion oligonucleotides comparing the solubility of wild-type phosphodiester siRNA to *t*-Bu-SATE and Me-SATB modified oligonucleotides (Figure 5.3E). Following the addition of NaCl and high speed centrifugation to siRNN oligonucleotide aliquots, spectrophotometry readings were taken on the remaining soluble fraction present to determine the solublility of siRNN oligonucleotides. Unfortunately, Me-SATB phosphotriester insertions do not significantly impact the overall hydrophobicity pattern associated with t-Bu-SATE siRNN oligonucleotides. This is not surprising considering the distal methyl group reduction necessitated an increased proximal butyl chain. Due to the correlation between solubility of siRNNs in solutions of increasing ionic

strength and PTD-siRNN conjugate solubility, the Me-SATB phosphotriester modification was not pursued further for PTD-siRNN delivery studies.

CONCLUSIONS

In order to successfully generate a soluble siRNA strategy utilizing PTD-siRNA conjugates, manipulation of the phosphodiester is necessary. In the absence of phosphodiester masking, PTD-siRNA conjugates lack the ability to engage the cell surface and induce internalization due to phosphodiester-mediated charge neutralization of crucial cationic residues of the PTD peptide (Meade, et al. 2007). In order to cirumvent this electrostatic neutralization, I began synthesizing oligonucleotides containing bioreversible, phosphodiester-modfications to extracellularly neutralize the siRNA backbone for successful PTD-siRNA delivery. Following cellular delivery, these biolabile groups decompose to generate RNAi-compatible phosphodiester-containing siRNA oligonucleotides. Initial attempts to generate siRNN molecules were accomplished with t-Bu-SATE phosphotriester groups that were efficiently synthesized and displayed favorable RNAi activity following transfection into cells in culture. Unfortunately, due to the strong hydrophobic character of the t-Bu-SATE modifications, attempts to conjugate highly cationic PTD peptides proved futile due to extreme insolubility in biologically-relevant solutions (Chapter 4).

In an attempt to overcome this hydrophobicity barrier, phosphoramidite and oligonucleotide synthesis strategies were accomplished for *t*-Bu-SATE phosphotriester derivatives with progressive methyl group reduction distal to the thioester bond (Figure 5.1A). Unfortunately, placement of less hydrophobic methyl (Me-SATE) and ethyl (Et-SATE) modifications resulted in complete

instability of the SATE group in requisite oligonucleotide basic deprotection conditions, resulting in an inability to successfully purify full-length siRNN oligonucleotides. Hypothesizing that the mechanism of base-mediated decay was similar to the multistep intracellular decomposition process, I synthesized oligonucleotides containing proximal alkyl chain lengthening between the thioester and phosphotriester bonds. Theoretically, increasing the alkyl chain length will decrease the rate of decomposition due to less favorable by-product formation (Figure 5.2A). Indeed, extension of the proximal ethyl linkage to a butyl linkage sufficiently stabilized the methyl and ethyl distal modifications for deprotection in basic conditions. Me-SATB and Et-SATB, the theoretically lowest hydrophobic SATE variations, were successfully purified and assayed for biological function. Interestingly, Me-SATB and Et-SATB displayed similar RNAi activity to compared to both wildtype and *t*-Bu-SATE containing siRNA (Figure 5.3D). However, due to the increased carbon content proximal to the thioester bond, alleviation of the t-butyl group with methyl and ethyl substitutions rendered these SATE derivatives of insufficient hydrophilicity for PTD conjugation strategies. However, while unsuccessful in generating more hydrophilic siRNN oligos, this study serves to show the extent of manipulation that can be done to the SATE phosphotriester modification while still maintaining thioesterase sensitivity and biological function.

Chapter 5, in part, is currently being prepared for submission for publication of the material. Gogoi, Khirud; Meade Bryan R.; van den Berg, Arjen;

Hagopian, Jonathan C.; Rudolph, Zachary H.; Palm-Apergi, Caroline; Dowdy, Steven F. The dissertation author was the co-primary investigator and author of this material.

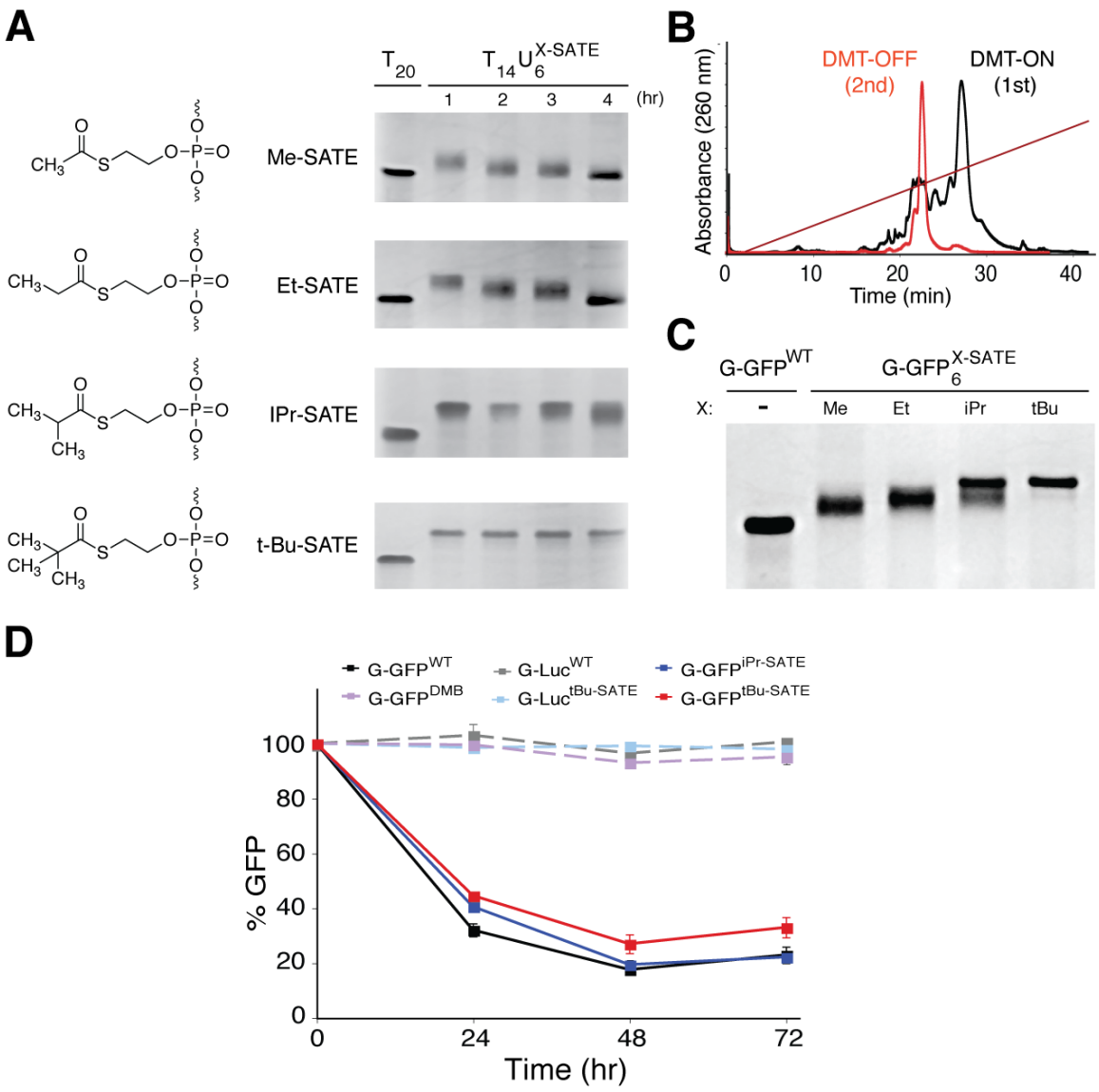

Figure 5.1. Deprotection, purification and biological function of SATE oligonucleotide variations. **A**) Denaturing gel analysis of X-SATE oligonucleotide variations in the presence of 10% DIA/MeOH for 1 to 4 hr shows the stability of *t*Bu and iPr-SATE and the sensitivity of Me-SATE and Et-SATE phosphotriesters to oligonucleotide deprotection conditions. Gels were stained with methylene blue for analysis. **B**) DMT-On RP-HPLC for phosphotriester-containing oligonucleotide purification. Follow 1st purification with DMT-On, oligos were detritylated with acetic acid prior to the 2nd purification by RP-HPLC and isolation of main peak for final products. Diagonal line indicates linear acetonitrile gradient from 0 to 40%. **C**) Denaturing gel analysis of final ssRNA products for G-GFP6 X-SATE variations. Due to stability, only iPr- and *t*Bu-SATE containing oligos were used for RNAi analysis. **D**) GFP RNAi was assessed by flow cytometry of GFP expressing cells following transfection of 100 nM siRNA containing 6x guide strand modifications. Transfection of PWT/G-GFP 6xtBu-SATE and PWT/G-GFP 6xiPr-SATE resulted in GFP RNAi responses comparable to wild-type siRNA control for 72 hr while nonreversible PWT/G-GFP 6xDMB and negative control siRNA oligos failed to induce RNAi.

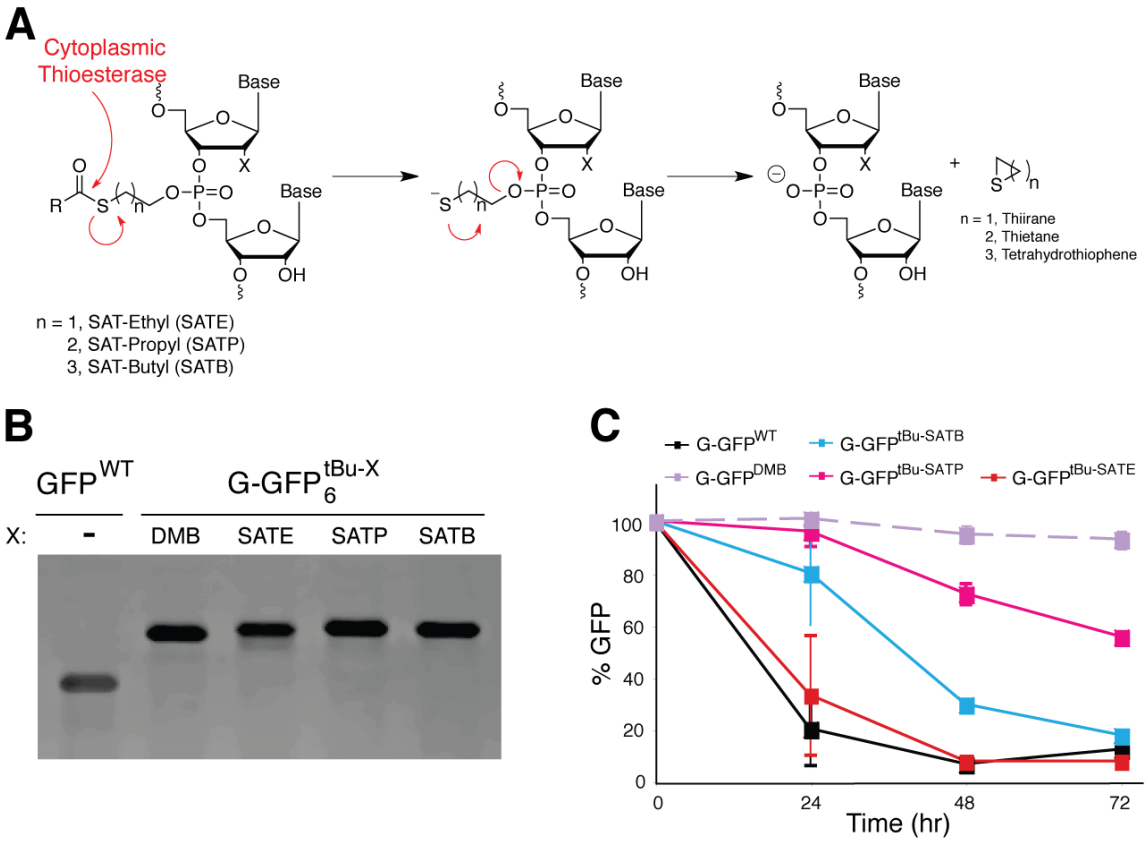

Figure 5.2. Biological activity comparison of SATE, SATP and SATB phosphotriester variations. A) Bioreversible phosphotriester groups neutralize negatively-charged siRNA phosphodiesters. Thioesterase processing results in decomposition of S-Acyl-2-ThioEthyl (SATE), S-Acyl- 3-ThioPropyl (SATP) and S-Acyl-4-ThioButyl (SATB) into wild type phosphodiester linkages. **B)** Denaturing gel analysis of purified ssRNA for 6x insertion G-GFP$_6^{tBu-X}$ oligonucleotides with S-Acyl-Thioethyl (SATE), S-Acyl-Thiopropyl (SATP) or S-Acyl-Thiobutyl (SATB) or irreversible DMB modifications. **C**) Purified G-GFP6 tBu-X oligos were hybridized to wild type GFP passenger strand (P^{WT}) and 100 nM transfection were done prior to analysis of GFP expressing cells by flow cytometry. Note the delayed kinetics of GFP RNAi for SATP and SATB-modified siRNA oligonucleotides.

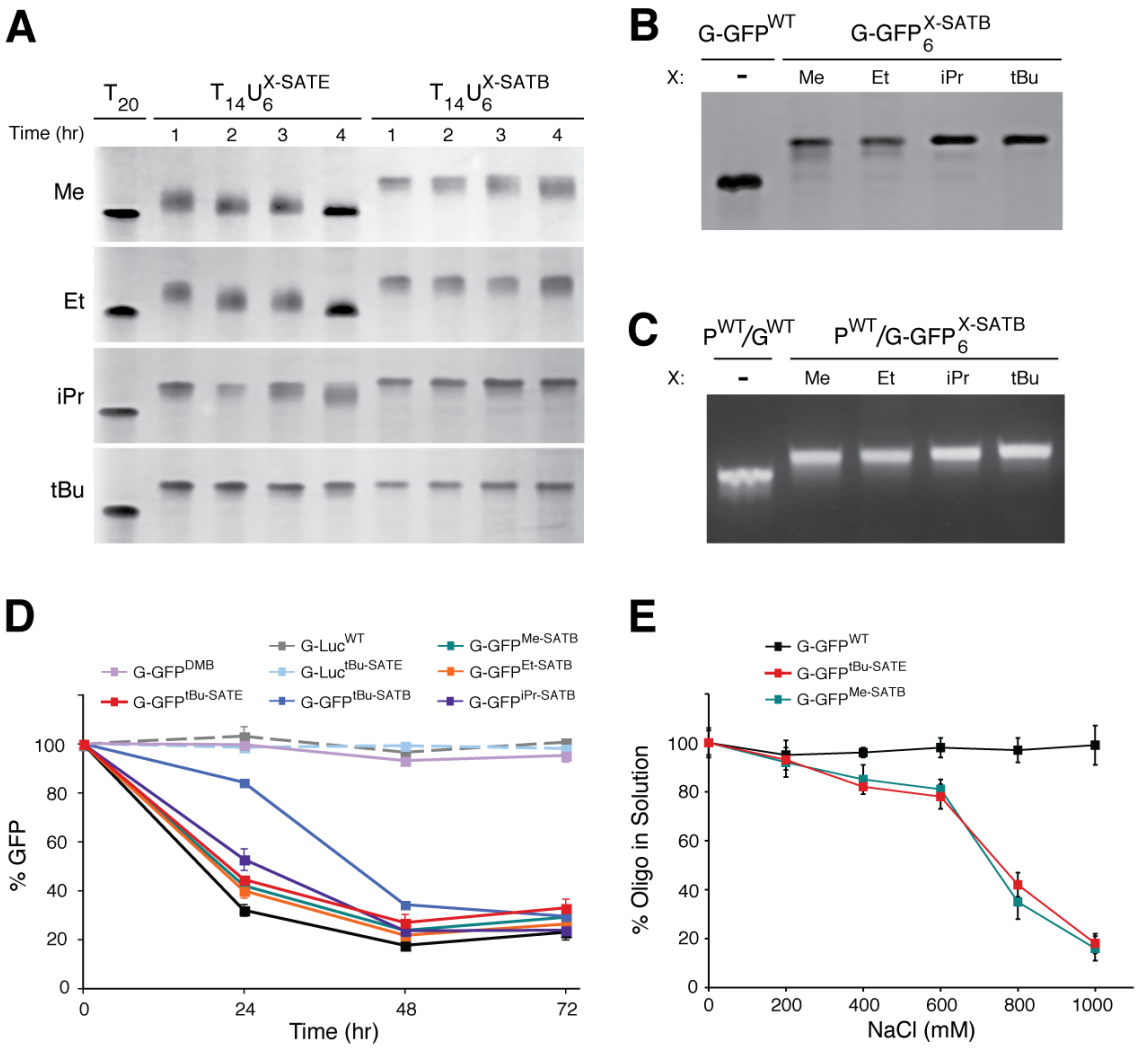

Figure 5.3. Deprotection, purification and biological function of SATB oligonucleotide variations. **A**) Denaturing gel analysis of X-SATE and X-SATB oligonucleotide stability in 10% DIA/MeOH from 1 to 4 hr. SATB modifications afford thioester stability for Me-, Et- and iPr-SATB groups compared to corresponding SATE modifications. **B**) Denaturing gel analysis of purified 6x insertion guide strand G-GFP 6x-SATB oligonucleotides. **C**) All purified 6x insertion G-GFP 6xSATB guide strands were hybridized to wild type GFP passenger strand (PWT) and analyzed by ethidium bromide stained nondenaturing gel analysis. **D**) GFP RNAi analysis of cells expressing GFP by flow cytometry at indicated times following 100 nM siRNA transfection of PWT/G-GFP 6x-SATB variations. Me-, Et- and iPr-SATB modifications displayed similar RNAi kinetics as tBu-SATE modified siRNA while tBu-SATB siRNA displayed delayed kinetics. Nonreversible PWT/G-GFP6 DMB and negative control siRNAs showed no RNAi response. **E**) NaCl precipitation experiments for solubility comparison of tBu-SATE to Me-SATB oligonucleotides. 5 μM aliquots were treated with increasing concentration of NaCl and subject to high speed centrifugation. Supernatants were quantified by 260 nm absorbance readings to calculate % of oligo remaining in solution.

REFERENCES

de Fougerolles A, Vornlocher HP, Maraganore J, Lieberman J. Interfering with disease: a progress report on siRNA-based therapeutics. Nat Rev Drug Discov 2007;6:443-53.

Manoharan M. RNA interference and chemically modified small interfering RNAs. Curr Opin Chem Biol 2004;8:570-9.

Meade BR, Dowdy SF. Exogenous siRNA delivery using peptide transduction domains/cell penetrating peptides. Adv Drug Deliv Rev 2007;59:134-40.

Peyrottes S, Egron D, Lefebvre I, Gosselin G, Imbach JL, Perigaud C. SATE pronucleotide approaches: an overview. Mini Rev Med Chem 2004;4:395-408.

Schroeder A, Levins CG, Cortez C, Langer R, Anderson DG. Lipid-based nanotherapeutics for siRNA delivery. J Intern Med 2010;267:9-21.

Tosquellas G, Alvarez K, Dell'Aquila C, et al. The pro-oligonucleotide approach: solid phase synthesis and preliminary evaluation of model pro-dodecathymidylates. Nucleic Acids Res 1998;26:2069-74.

Whitehead KA, Langer R, Anderson DG. Knocking down barriers: advances in siRNA delivery. Nat Rev Drug Discov 2009;8:129-38.

CHAPTER 6

SYNTHESIS AND ANALYSIS OF AMINO-SATE (N-SATE) siRNN OLIGONUCLEOTIDES

ABSTRACT

While siRNA technology has great potential for the intervention of human disease, the ability of siRNAs to be delivered within therapeutic applications remains the rate-limiting step for siRNA therapeutics. Attempting to harness the utility of Peptide Transduction Domains for siRNA delivery, I began a pro-drug oligonucleotide synthesis strategy involving the synthesis of neutralizing, bioreversible phophotriester-modified siRNN oligonucleotides for PTD-siRNN conjugate delivery. Previously I have shown the successful synthesis and characterization of a variety of siRNN oligonucleotides building upon the S-Acyl ThioEthyl (SATE) phosphotriester moiety. While SATE-containing siRNNs were synthesized and displayed favorable RNAi activity *in vitro*, insurmountable solubility issues were encountered due to siRNN hydrophobicity. In an attempt to negate this hydrophobicity, I have synthesized a collection of Amino-SATE (N-SATE) siRNN olignucleotides containing terminal primary amines on the SATE phosphotriester modification. Synthesis and deprotection of N-SATE siRNN oligonucleotides was successful after selection of appropriate orthogonal amine protecting groups required during siRNN oligonucleotide synthesis. Following amine deprotection, N-SATE siRNNs displayed efficient RNAi responses *in vitro*

and significantly higher aqueous solubility compared to their SATE siRNN counterparts. Current work is underway to determine the cellular deliverability of PTD-siRNN N-SATE oligonucleotide conjugates as a viable siRNA therapeutic approach.

INTRODUCTION

Since the discovery that synthetic siRNA molecules could be administered to human cells *in vitro* and induce RNA interference (RNAi) responses, a plethora of studies have appeared highlighting the potential of these synthetic oligonucleotides in therapeutic applications (Elbashir, et al. 2001; de Fougerolles, et al. 2007). Unfortunately, with a size of ~14,000 Da and extreme anionic character from the requisite phosphodiester backbone, naked siRNA oligonucleotides possess unfavorable cellular delivery and pharmacokinetic properties (Whitehead, et al. 2009). Over the last decade, significant attempts have been made to minimize these negative attributes by utilizing nanoparticle-based delivery systems to complex siRNA molecules to aid in there delivery across the cellular membrane and alter their pharmacokinetic properties *in vivo* (Schroeder, et al. 2010). However, while some success has been attained, nanoparticle delivery systems have their own set of complications including notorious cytotoxicity to primary cells in culture and filtration to the spleen and liver following *in vivo* systemic administration (Akinc, et al. 2009; Schroeder, et al. 2010). In order to potentially overcome these limitations, our laboratory has attempted to device soluble, non-nanoparticle forming siRNA delivery strategies utilizing a class of small cationic peptides termed Peptide Transduction Domains (PTDs).

Following covalent conjugation, PTDs have been shown to deliver a wide range of macromolecular cargo (Snyder, et al. 2005). Unfortunately, covalent

conjugation of PTD peptides to siRNA oligonucleotides results in an inability of the PTD domain to interact with the cell surface and induce internalization (Chapter 3). This negative result is due to the anionic charge of the conjugated siRNA phosphodiester backbone neutralizing the cationic residues of the PTD required for cell surface interaction (Meade, et al. 2007). In order to circumvent this problem and allow for successful PTD-mediated siRNA delivery, masking or manipulation of the phosphodiester backbone is necessary. Indeed, covering the siRNA molecule with dsRNA binding domains fused to PTD domains (PTD-DRBD) alleviated this phosphodiester neutralizing effect and allowed for successful *in vitro* and *in vivo* siRNA delivery (Eguchi, et al. 2009).

In order to generate a PTD-siRNA delivery strategy independent of bacterially-expressed recombinant proteins, I began strategies to neutralize the siRNA phosphodiester backbone during oligonucleotide synthesis to generate phosphodiester-neutral PTD-siRNA conjugates. However, the siRNA phosphodiester linkages are critical for their recognition by the RNA-induced silencing complex (RISC) and induction of RNAi responses (Manoharan, 2004). Thus I began synthesizing siRNA oligonucleotides with neutral, bioreverisble phosphotriester insertions, termed short interfering RiboNucleic Neutral (siRNN) oligonucleotides, capable of alleviating PTD-charge neutralization extracellularly. Theoretically, exposure to the cytoplasmic environment following cellular delivery would induce conversion of these neutralizing modifications to RNAi-compatible siRNA molecules.

Our initial attempts focused on phosphoramidite and oligonucleotide synthesis routes for S-Acyl-ThioEthyl (SATE) modifications, a bioreversible phosphate protection group utilized for small molecule pro-drug therapeutics and with limited success, neutralized antisense oligonucleotide synthesis (Tosquellas, et al. 1998; Peyrottes, et al. 2004). Exposure of the SATE-protected phosphodiesters to cytoplasmic thioesterases initiates a rapid two-step decomposition process resulting in conversion to charged, biologically-active phosphodiesters (Figure 4.1A). Our work with SATE siRNN oligonucleotides delineated the requirements for oligonucleotide synthesis including the use of 'Ultramild' oligonucleotide deprotection conditions to ensure stability of SATE modifications, replacement of SATE-adjacent 2' OH groups with RNAi-compatible 2'-F/2'-OMe modifications to prevent internucleotide strand scission, and a threshold value of SATE insertions of ~50% due to structural requirements for double-stranded siRNA formation.

With this set of criteria in hand, I successfully synthesized a collection of SATE containing oligonucleotides and assayed their ability to undergo intracellular conversion and induce efficient RNAi responses. Importantly, transfection of SATE-containing siRNN molecules into cells resulted in rapid intracellular decomposition and RNAi responses comparable to wildtype siRNA in both dose and duration of response (Chapter 4.6A). Due to the limitation of ~50% insertions, PTD conjugation required the use of highly cationic peptides in order to create stable PTD-siRNN conjugates containing an overall cationic

charge (Chapter 3). Unfortunately, attempts to conjugate these cationic PTDs to SATE-containing siRNN molecules resulted in significant hydrophobicity issues due to the SATE-modifications during both the PTD-siRNN conjugation reaction as well as following addition to cells in biologically-relevant solutions.

In an attempt to overcome these solubility drawbacks, we have designed phosphoramidite and oligonucleotide synthesis routes for the introduction of more polar groups into the SATE phosphotriester modification. One of these modifications, the Amino-SATE (N-SATE), involves placement of a primary amine distal to the thioester bond on the SATE modification to not only increase aqueous solubility but also increase the overall cationic character of the siRNN molecule (Figure 6.1A). Indeed, due to insolubility issues of SATE-containing prodrugs of AZT, insertion of terminal primary amines on the SATE moiety have been shown to increase aqueous solubility of the small molecule compounds (Villard, et al. 2008). Relative to anionic charge, insertion of N-SATE phosphotriesters should serve as a two-for-one modification; decreasing the anionic charge by neutralizing a phosphodiester while also introducing a cationic primary amine. Theoretically, the maximally-modified N-SATE siRNN should require conjugation to less cationic peptides than the SATE siRNNs to attain an overall cationic conjugate charge due to the positive charges donated by the N-SATE primary amines.

Synthesis of N-SATE siRNN oligonucleotides requires the use of orthogonal primary amine protecting groups to prevent unwanted side-chain

reactions during solid phase oligonucleotide synthesis. Additionally, due to the instability of the SATE moiety, primary amine deprotection strategies must also be compatible with SATE integrity during deprotection. Our first attempt to generate N-SATE siRNN oligonucleotides involved phosphoramidite and oligonucleotide synthesis routes with 9-fluorenylmethyloxycarbonyl (Fmoc)-protected N-SATEs. Isolation of full length Fmoc-N-SATE siRNN was successful but primary amine deprotection resulted in significant decomposition of the SATE group and an inability to successfully isolate primary amine-containing N-SATE siRNN. Fortunately, synthesis of allyloxycarbonyl (Alloc)-protected N-SATEs resulted in full-length Alloc-N-SATE siRNN isolation and successful primary amine deprotection following palladium catalysis. Maximum insertion N-SATE GFP siRNNs were successfully synthesized, purified and assayed for biological function. Similar to other SATE-modified siRNN oligonucleotides, N-SATE siRNN oligos induced efficient RNAi responses, comparable in magnitude and duration to the phosphodiester-containing wildtype siRNA controls. As hypothesized, sodium chloride precipitation experiments displayed significantly higher aqueous solubility for the N-SATE siRNN compared to previously synthesized SATE siRNN oligonucleotides. Due to this increase in solubility, PTD-siRNN conjugation attempts are currently underway to determine the ability of PTD-siRNN to function as a viable siRNA delivery platform.

RESULTS AND DISCUSSION

Synthesis and deprotection of Fmoc-N-SATE oligonucleotides

In order to successfully generate N-SATE siRNN oligonucleotides, orthogonal primary amine-protecting groups are needed to prevent unwanted side-chain reactions from occurring during solid phase oligonucleotide synthesis. Our first protecting group candidate was 9-fluorenylmethyloxycarbonyl (Fmoc) (Figure 6.1A), a common amine protection strategy employed for N-terminal protection during solid phase peptide synthesis (Carpino, et al. 1972). Initially, two different variations of the N-SATE were attempted and were designated N1-SATE and N2-SATE based on the distance of the primary amine from the parent t-Bu-SATE moiety (Figure 6.1A). Following Fmoc-N-SATE phosphoramidite synthesis, standard oligonucleotide synthesis routes were employed for generation of full-length oligonucleotides. Similar to other SATE-containing RNNs, 'Ultramild' oligonucleotide deprotection was carried out in 10% DIA/MeOH for 4 hours to remove phenoxyacetal nucleobase protection, 2-cyanoethyl phosphodiester protection and to induce release of the oligonucleotide from the solid support (Chapter 4).

To simplify analysis of Fmoc-N-SATE stability during oligonucleotide deprotection, T20 tester oligonucleotides were synthesized with 3x Fmoc-N1-SATE or 3x Fmoc-N2-SATE insertions ($T_{17}U_3^{\text{Fmoc-N-SATE}}$) and subject to 10% DIA/MeOH for 4 hours (Figure 6.1B). Interestingly, the presence of the Fmoc-protected N-SATE group significantly decreased the stability of the SATE group

to the 'Ultramild' deprotection condition in comparison to the complete stability of the *t*-Bu-SATE modification within the same treatment time (Figure 4.2A). Importantly, this sensitivity was more pronounced for the Fmoc-N1-SATE compared to the Fmoc-N2-SATE indicating that the distance of the amine group from the thioester plays a role in base-mediated destabilization (Figure 6.1B). However, a sufficient amount of full-length Fmoc-N2-SATE-containing oligo was still present following primary deprotection. Due to the large hydrophobic nature of the Fmoc-N2-SATE modification, RP-HPLC can distinguish the different Fmoc-N-SATE reversal products from the crude oligo deprotection mixture and it was used to isolate the desired T_{17}-$U_3^{\text{Fmoc-N2-SATE}}$ product (Figure 6.1C & 6.1D). Indeed, full length Fmoc-N2-SATE containing oligonucleotides were isolated at >95% purity (Figure 6.1D & 6.1E).

Following purification of the Fmoc-N2-SATE containing oligonucleotide, a secondary deprotection step is necessary to generate the primary amine-containing oligonucleotide product (Figure 6.1A). Standard Fmoc group removal uses base deprotection with primary or secondary amines to liberate the Fmoc protecting group (Fields, 1995). Unfortunately, SATE modifications are highly susceptible to base-mediated decomposition (Figure 4.2A) and thus, analysis of Fmoc removal and N-SATE decomposition were monitored simultaneously. Unfortunately, MALDI-TOF mass spec analysis of T_{17}-$U_3^{\text{Fmoc-N2-SATE}}$ treated with common Fmoc-deprotection solutions, including various concentrations of piperidine, morpholine or piperazine in polar and nonpolar solvents, resulted in

significant N-SATE decomposition with kinetics equivalent to Fmoc-removal. Attempts to overcome N-SATE decomposition and slow down the kinetics of the reaction with tertiary amines such as diisopropylethylamine (DIEA) or triethylamine (TEA) showed that while it was possible to slow down the rates of Fmoc-removal and N-SATE reversal, the relative kinetics of the two reactions remained unchanged. This is most likely due to the enhanced base sensitivity of the N2-SATE following Fmoc-removal and thus, an acceleration of N-SATE decomposition as the Fmoc-deprotection reaction proceeds. Indeed, the extremely heterogenous mixture of oligonucleotide products during all Fmoc-deprotection conditions attempted made isolation of full-length N2-SATE oligonucleotides futile (Figure 6.1F).

Synthesis and analysis of Alloc-N-SATE siRNN oligonucleotides

To avoid N-SATE decomposition during the primary amine deprotection conditions as was evident for the Fmoc-N-SATE modifications, I sought alternative primary amine protecting group strategies that avoid use of basic solutions for amine deprotection. At the top of the list was amine-protection with allyloxycarbonyl (Alloc)-protecting groups which undergo deprotection in the presence of tetrakis(triphenylphosphine)palladium catalyst to yield the desired primary amine (Figure 6.2A; Zorn, et al. 2001). As described previously, standard phosphoramidite and oligonucleotide synthesis routes were undertaken to generate Alloc-N-SATE containing RNN oligonucleotides in sufficient yields.

Similar to Fmoc-N-SATEs, primary deprotection of Alloc-N-SATE oligonucleotides in 10% DIA/MeOH resulted in some reversal of Alloc-N-SATE modifications (Figure 6.2B). As was the case for the Fmoc-N-SATE variations, the Alloc-N1-SATE displayed a higher sensitivity to 10% DIA/MeOH deprotection than the Alloc-N2-SATE modification, thus only Alloc-N2-SATE oligonucleotides were further processed. Typical of phosphotriester-containing oligonucleotides, RP-HPLC purification of G-GFP_9 $^{Alloc\text{-}N2\text{-}SATE}$ oligonucleotide resulted in a broad peak distribution indicative of diastereomeric oligo mixtures (Alvarez, et al. 1999). However, careful fractionation allowed for the successful isolation of the desired full-length oligo product independent of Alloc-N2-SATE reversal products present in the crude oligo mixture (Figure 6.2C & 6.2D). Indeed, MALDI-TOF mass spec analysis confirmed the existence of only a small amount of single-reversal Alloc-N2-SATE product remaining (Figure 6.2E).

Following Alloc-On isolation, palladium-catalyzed deprotection was accomplished with tetrakis(triphenylphosphine)palladium and phenylsilane in a dicholoromethane/methanol solvent mixture. Direct RP-HPLC injection of the reaction mixture following palladium deprotection resulted in efficient separation of RNN oligonucleotide from palladium and phenylsilane reagents (Figure 6.3A). MALDI-TOF mass spec analysis of the oligonucleotide peak fractions identified the main oligo product as fully deprotected G-$GFP_9^{N2\text{-}SATE}$ oligonucleotide with some single N2-SATE reversal present (Figure 6.3B). Thus, palladium-catalyzed deprotection of Alloc-protected amines results in successful N2-SATE generation

in the absence of significant N2-SATE decomposition. Interestingly, denaturing gel analysis of purified G-GFP$_9^{N2\text{-}SATE}$ oligonucleotides indicates an increased mobility in the electrophoretic gel compared to the start Alloc-protected oligonucleotide. This decreased mass yet increase in electrophoretic migration is indicative of the presence of positively-charged amine modifications on the siRNN backbone (Figure 6.3C).

Following synthesis of both 9x N2-SATE insertion guide and passenger strands for GFP siRNN, the oligos were analyzed for their ability to form faithful dsRNA molecules. By nondenaturing gel electrophoresis, P-GFP$_9^{N2\text{-}SATE}$ and G-GFP$_9^{N2\text{-}SATE}$ were able to form dsRNA as assayed by gel migration and ethidium bromide intercalation (Figure 6.3D). Similar to *t*-Bu-SATE modified siRNN oligos, attempts to increase the number of insertions led to a significant decrease in dsRNA formation, and thus nonfunctional siRNN duplexes, displaying the limitation of insertion number for N-SATE modifications (data not shown). To assay RNAi activity, double stranded P^{WT}/G^{WT}, P$_9^{N2\text{-}SATE}$/G^{WT}, P^{WT}/ G$_9^{N2\text{-}SATE}$ and P$_9^{N2\text{-}SATE}$/ G$_9^{N2\text{-}SATE}$ GFP or negative control Luciferase (Luc) siRNAs were transfected into GFP expressing cells and analyzed for GFP expression by flow cytometry over a 3 day time course (Figure 6.3D). Impressively, the presence of the primary amine at the terminal end of the SATE modification did little to inhibit thioesterase processing as all GFP siRNN variations tested displayed similar kinetics to phosphodiester-containing GFP siRNA. To the best of our knowledge

this serves as the first example of siRNA oligonucleotide synthesis and validation of intracellular conversion of cationic, bioreversible phosphotriester modifications.

Increasing the solubility of siRNN with N-SATE modifications

Problems associated with previous SATE siRNNs has been due to extreme insolubility in aqueous conditions, creating significant problems for both PTD conjugation reactions and cellular treatment. The synthesis of N-SATE siRNN oligonucleotides was directed towards solving this issue by the installment of primary amines on the terminal ends of the SATE phosphotriester to enhance solubility in biologically relevant solutions. To assay the solubility of N-SATE siRNN oligos, aliquots of $P_9^{N2\text{-}SATE}$/ $G_9^{N2\text{-}SATE}$ GFP siRNN molecules were subject to increasing concentrations of sodium chloride (NaCl) followed by high-speed centrifugation. Following centrifugation, supernatants were analyzed by spectrophotometer absorbance readings (data not shown) and nondenaturing gel electrophoresis to analyze the amount of N-SATE siRNN olignucleotide in solution (Figure 6.4A). Interestingly, alteration of the SATE modification with terminal primary amines allows for solubility of siRNN molecules to concentrations greater than 500 mM NaCl, almost 5-fold more than the ionic strength of physiological conditions while t-Bu-SATE modified siRNN oligonucleotides fail to remain soluble in 100 mM NaCl (Figure 6.4A).

The solubility of siRNN oligonucleotides in solutions of increasing ionic strength correlates to their ability to handle solubility in PTD conjugation reaction conditions, subsequent purification and cellular treatment in a soluble form.

While more work needs to yet be done, initial attempts to conjugate PTD-HyNic peptides to Aldehyde-functionalized N-SATE siRNN oligonucleotides has proven successful and have allowed for conjugation and SDS-PAGE gel extraction of conjugates at greater than 80% purity (Figure 6.3B). Thus, success was accomplished in the synthesis of N-SATE phosphotriester modifications for the enhancement of overall solubility for siRNN oligonucleotides.

Cellular treatment of PTD-siRNN N-SATE conjugates

While utilizing our methyltriester surrogate siRNA oligonucleotides for delivery studies (Chapter 3), I defined the ability of PTD-siRNA conjugates to be successful at cellular association and uptake when the overall charge of the PTD-siRNA conjugate was cationic. In addition to the increased solubility that N-SATE modifications provide, they also donate a cationic primary amine to the siRNN thus altering the overall charge of the siRNN molecule prior to PTD conjugation. The theoretical overall charge of a conjugation competent Ald-$P_9^{N2\text{-}SATE}$/ $G_9^{N2\text{-}SATE}$ siRNN is (–) 6, thus conjugation of PTDs with greater than 6 cationic charges should theoretically result in some enhancement of cellular delivery. Unfortunately, thus far, TAT and 2xTAT N-SATE siRNN conjugates with theoretical charges of (+) 2 and + (10) respectively, have failed to show any RNAi responses upon cellular treatment (data not shown). Attempts are underway to conjugate more highly charged PTD peptides to N-SATE siRNN in an attempt to overpower the remaining phosphodiesters for cellular delivery.

Unfortunately, N-SATE modifications do not display the same stability to human serum as t-Bu-SATE modifications, leading to complete decomposition of the siRNN oligonucleotide in less than 4 hours at 37 ^{o}C (Figure 6.4C). Addtionally, analysis of N-SATE siRNN stability in biological media such as DMEM, MEM and RPMI at 37 ^{o}C has displayed unfortunate results, as N-SATE phosphotriesters appear to undergo spontaneous reversal in these selected medias. Interestingly, this decomposition does not occur in water or PBS (pH 7.2), even when these solutions are heated to 37 ^{o}C for an extended period of time (data not shown). As of now, it is unclear whether or not the lack of RNAi response from TAT and 2xTAT-$P_9^{N2\text{-}SATE}$/ $G_9^{N2\text{-}SATE}$ conjugates is due to insufficient amount of cationic charge of the overall conjugate or extracellular decomposition of the N-SATE modifications leading to an inability of the PTD-siRNN conjugates to possess significant cationic charge long enough for cell surface binding. Current studies are underway to determine what is present in biological media that is enhancing N-SATE decay as well as engineering minimal nutrient media to determine cellular viability in conditions that N-SATEs remain stable.

CONCLUSIONS

Since the discovery of RNAi and the observation that synthetic siRNA molecules could lead to sequence specific mRNA downregulation in human cells, the race has been on to develop safe and efficient siRNA delivery strategies for therapeutic applications (Elbashir, et al. 2001; Whitehead, et al. 2009). In avoidance of the traditional nanoparticle-based delivery systems, our laboratory has sought to develop novel, monomeric siRNA delivery strategies following the covalent conjugation to cationic PTD peptides. Our studies have indicated a requirement for phosphodiester neutralization to allow for successful PTD-siRNA conjugate cell surface binding and cellular uptake. This has led us down a path of novel oligonucleotide synthesis conditions to develop a pro-drug template for phosphodiester-neutralizing modifications for PTD-siRNN delivery.

The development of successful PTD-siRNN delivery strategies has been hindered due to the extensive hydrophobicity associated with previously synthesized bioreversible SATE phosphotriester modified siRNN oligonucleotides. Indeed, the *t*-Bu-SATE modifications, while displaying significant stability during oligonucleotide deprotection and purification, have difficulty remaining soluble in physiological salt concentrations and have proven unusable for PTD-siRNN conjugate formation. In an attempt to alleviate difficulties encountered with the more tradiational SATE modifications, we set up phosphoramidite and oligonucleotide synthesis conditions to generate SATE modifications containing terminal primary amines to aid in both the aqueous

solubility properties of the siRNN as well as increasing the cationic characteristic of the siRNN molecule.

Synthesis of these Amino-SATE (N-SATE) modifications requires the use of orthogonal protecting group strategies for the terminal primary amines. After scanning multiple amine protecting groups, assaying both stability during required oligonucleotide deprotection conditions as well as SATE stability following amine deprotection, I settled on the Alloc-N2-SATE phosphotriester modification. Alloc-N2-SATE oligonucleotides were successfully synthesized and deprotected to generate siRNN containing cationic primary amines at each SATE insertion site. Theoretically, placement of primary amines on the SATE group alters the total charge of the siRNA in a 2-fold manner, decreasing the phosphodiester charge due to phosphotriester insertion and adding a cationic primary amine to increase the overall cationic character of the molecule. Unfortunately, PTD conjugation of N-SATE siRNN molecules has resulted in lack of RNAi response induction following cellular treatment. Currently, attempts are underway to conjugate N-SATE siRNN to more highly cationic PTD multimers to generate more positively-charged conjugates for successful PTD-siRNN delivery.

Of immediate concern is the instability of the N-SATE modifications following addition to human serum and biological media. While serum instability may be due to serum esterase processing of the thioester bond, decomposition in physiologic media is more concerning. Indeed, small molecule prodrug strategies using N-SATE modified AZT have also reported the instability of this

modification in biological media. The reported half-life for this N-SATE decomposition was ~6 minutes in RPMI media while the half-life in water was ~6 days (Villard, et al. 2008). While considerably more work needs to be done, I have shown stability of N-SATE siRNN in water and phosphate buffers (pH 7.0) for up to 24 hours at 37 ^{o}C. However, addition of N-SATE siRNN to media including DMEM, MEM and RPMI have led to significant decomposition with siRNN molecules losing ~50% of their N-SATE modifications in as little as 2 hours (data not shown). Current experimentation is underway to determine what components of biological media are leading to hydrolysis of the thioester bond. Additionally, minimal nutrient media is being engineered to ensure N-SATE siRNN stability and cellular viability during PTD-siRNN treatment conditions.

Importantly, all N-SATE phosphoramidites utilized in Chapter 6 were synthesized by Khirud Gogoi. The conditions for palladium-mediated deprotetction of Alloc-N-SATE oligonucleotides were worked out by Caroline Palm-Apergi. All N-SATE oligonucleotides were synthesized and processed through primary deprotection by Zachary Rudolph. All cellular treatments and flow cytometry analysis for GFP RNAi response assessment were performed by Jonathan Hagopian and Arjen van den Berg.

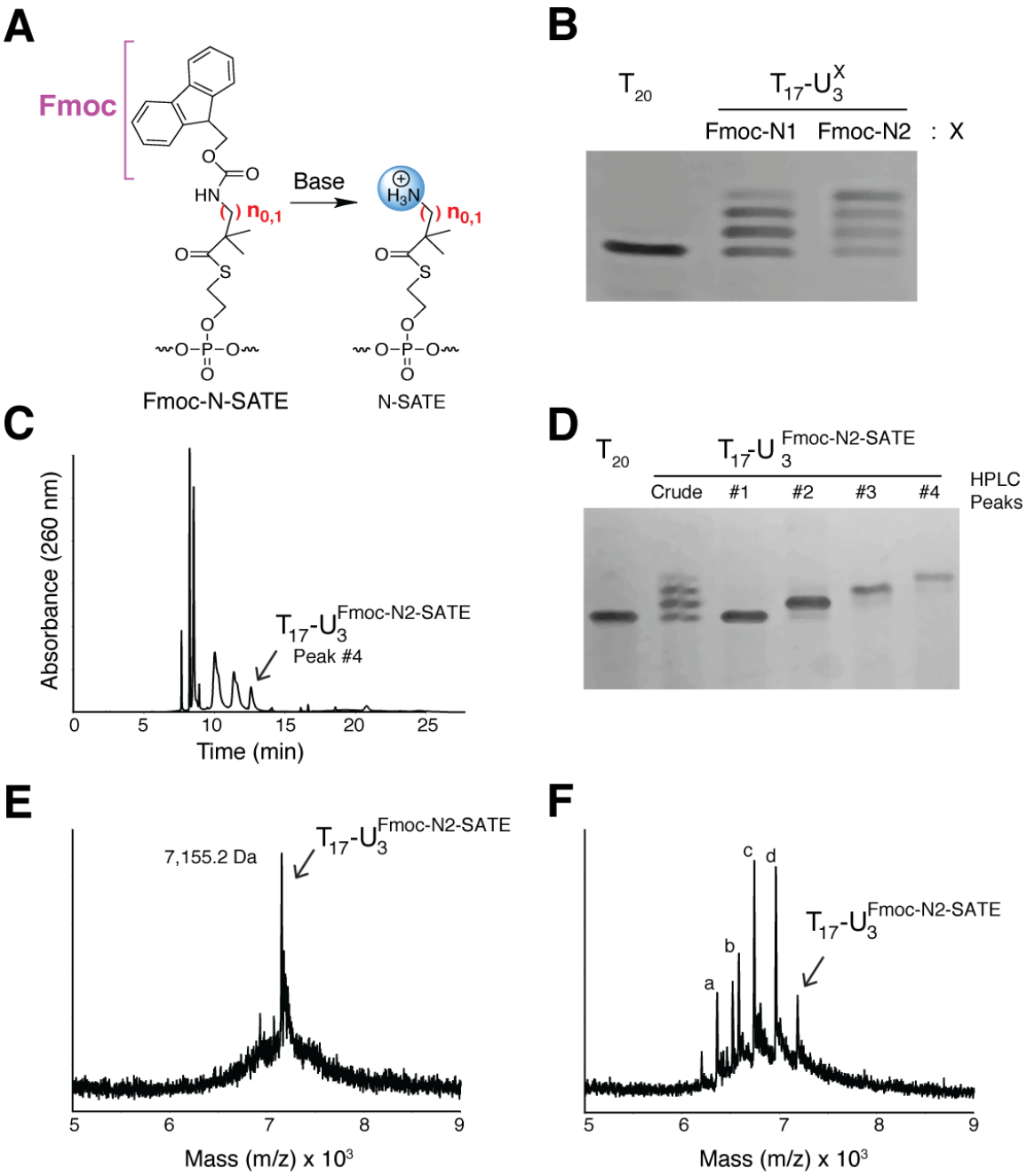

Figure 6.1. Synthesis and deprotection of Fmoc-N2-SATE oligonucleotides. A) Fmoc-N-SATE and deprotected N-SATE structure (n_0 = N1-SATE; n_1 = N2-SATE). **B)** Urea denaturing gel analysis of T17-U3Fmoc-N1 and Fmoc-N2 oligos after 4 hour deprotection in 10% DIA/MeOH. **C)** RP-HPLC purification of T17-U3Fmoc-N2-SATE. **D)** Urea denaturing gel anlaysis of RP-HPLC fractions (Note Peak #4 contains isolated T17-U3Fmoc-N2-SATE). **E)** MALDI-TOF mass spec analysis of T17-U3Fmoc-N2-SATE HPLC Peak #4 (Mass Expected = 7,143 Da; Mass Obtained = 7,155 Da). **F)** MALDI-TOP mass spec example of Fmoc-deprotection time point after 5 minutes in 10% morpholine in DMF. (Peaks a-d) represent masses for various products of Fmoc-deprotection, Fmoc-N2-SATE reversal and N2-SATE reversal species.

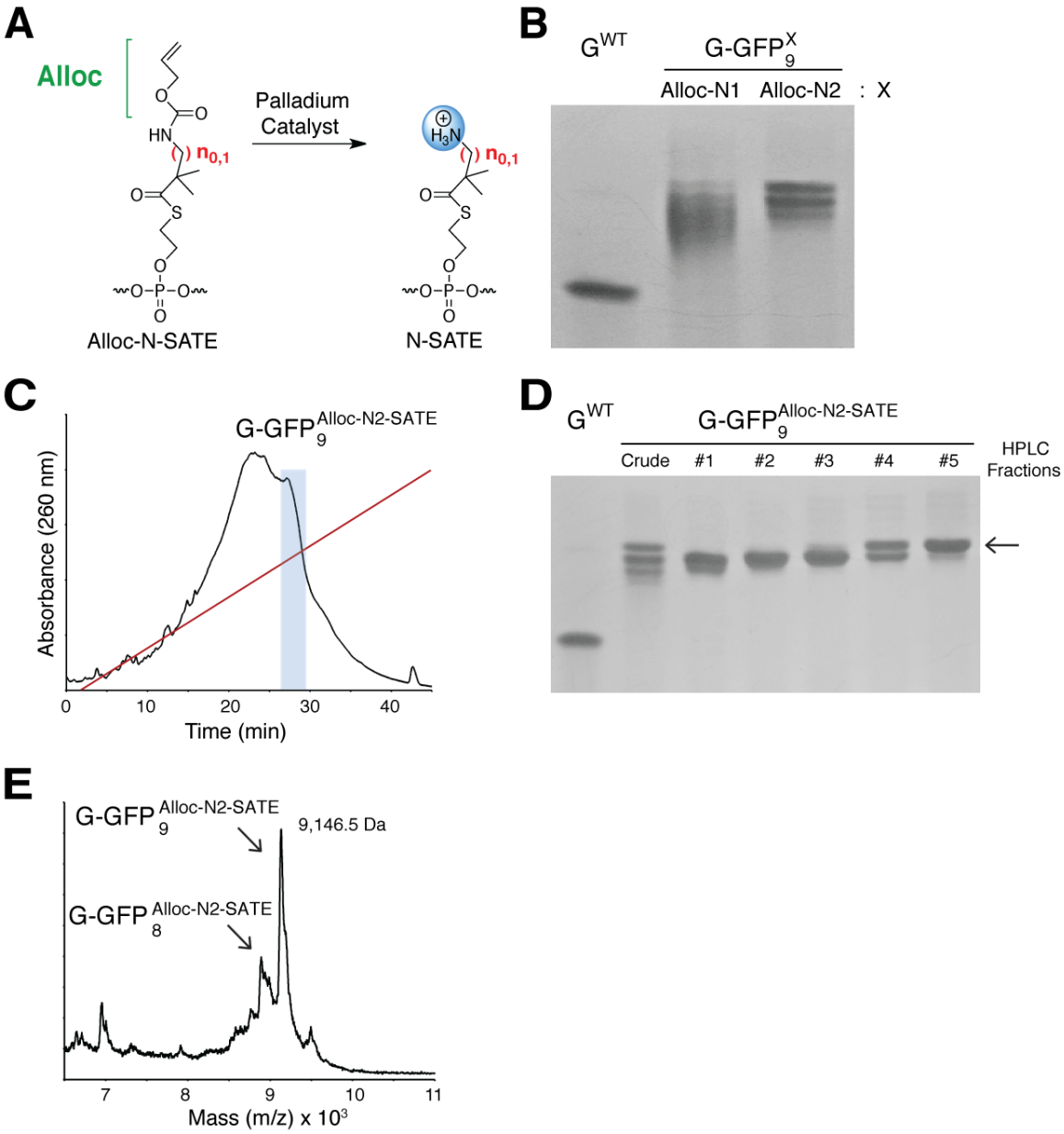

Figure 6.2. Synthesis of Alloc-N-SATE siRNN oligonucleotides. **A**) Structure of Alloc-N-SATE and N-SATE phoshotriesters. n_0 = N1-SATEs; n_1 = N2-SATE. **B**) Urea denaturing gel analysis of G-GFP$_9^{\text{Alloc-N-SATE}}$ decomposition following 4 hours in 10% DIA/MeOH. Gel was methylene blue stained for analysis. **C**) RP-HPLC profile for G-GFP$_9^{\text{Alloc-N2-SATE}}$. Red line indicates 0% - 80% acetonitrile gradient. Blue shading represents full-length oligo location. **D**) Urea denaturing gel analysis of G-GFP$_9^{\text{Alloc-N-SATE}}$ RP-HPLC fractions. Aarow indications full length G-GFP$_9^{\text{Alloc-N-SATE}}$ in HPLC Fraction #5. **E**) MALDI-TOF mass spec analysis of final product for G-GFP$_9^{\text{Alloc-N-SATE}}$ oligonucleotide (Expected mass = 9,144 Da; Observed mass = 9,146.5 Da). Note presence of single Alloc-N2-SATE reversal product present.

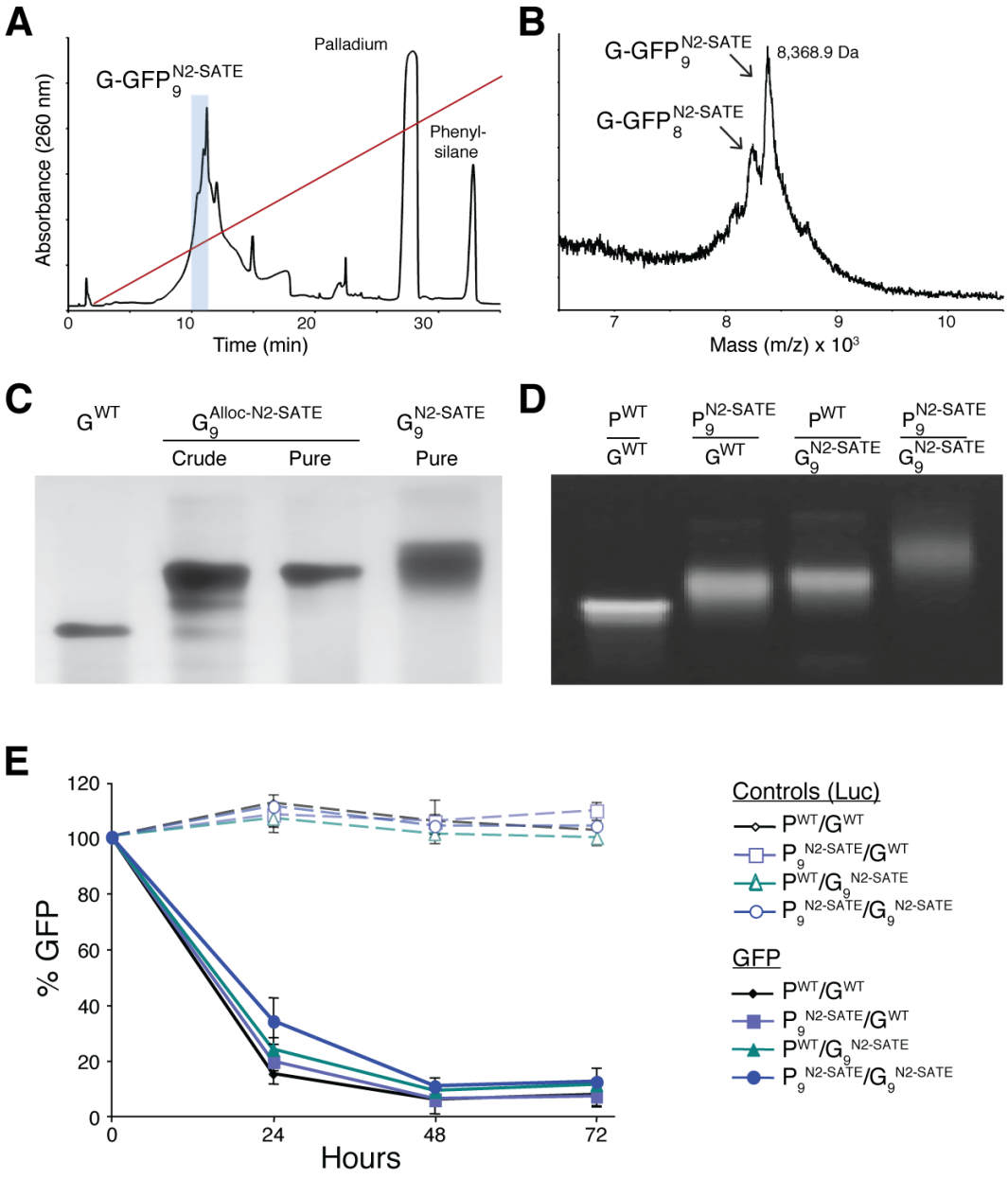

Figure 6.3. Primary amine deprotection and biological activity of N2-SATE siRNNs. **A**) RP-HPLC trace of G-GFP$_9^{\text{Alloc-N-SATE}}$ following amine deprotection in palladium/phenylsilane mixture. Red line indicated 0 – 80% acetonitrile gradient. Highly hydrophobic peaks for palladium and phenylsilane indicate sufficient separation of reactants from siRNN oligo products. **B**) MALDI-TOF mass spec analysis of final product for G-GFP$_9^{\text{N2-SATE}}$ siRNN. Note presence of single reversal N2-SATE product present. **C**) Urea denaturing gel analysis of G-GFP$_9^{\text{N2-SATE}}$ siRNN oligo at different stages of deprotection. Gel was methylene blue stained for analysis. Note increase in electrophorectic migration following Alloc-deprotection indicating presence of intact primary amines. **D**) Nondenaturing gel analysis of N-SATE GFP siRNN oligonucleotides forming dsRNA. Gel was ethidium bromidE stained for analysis. **E**) GFP RNAi analysis of cells expressing GFP by flow cytometry at indicated times following 100 nM siRNA transfection of indicated siRNNs.

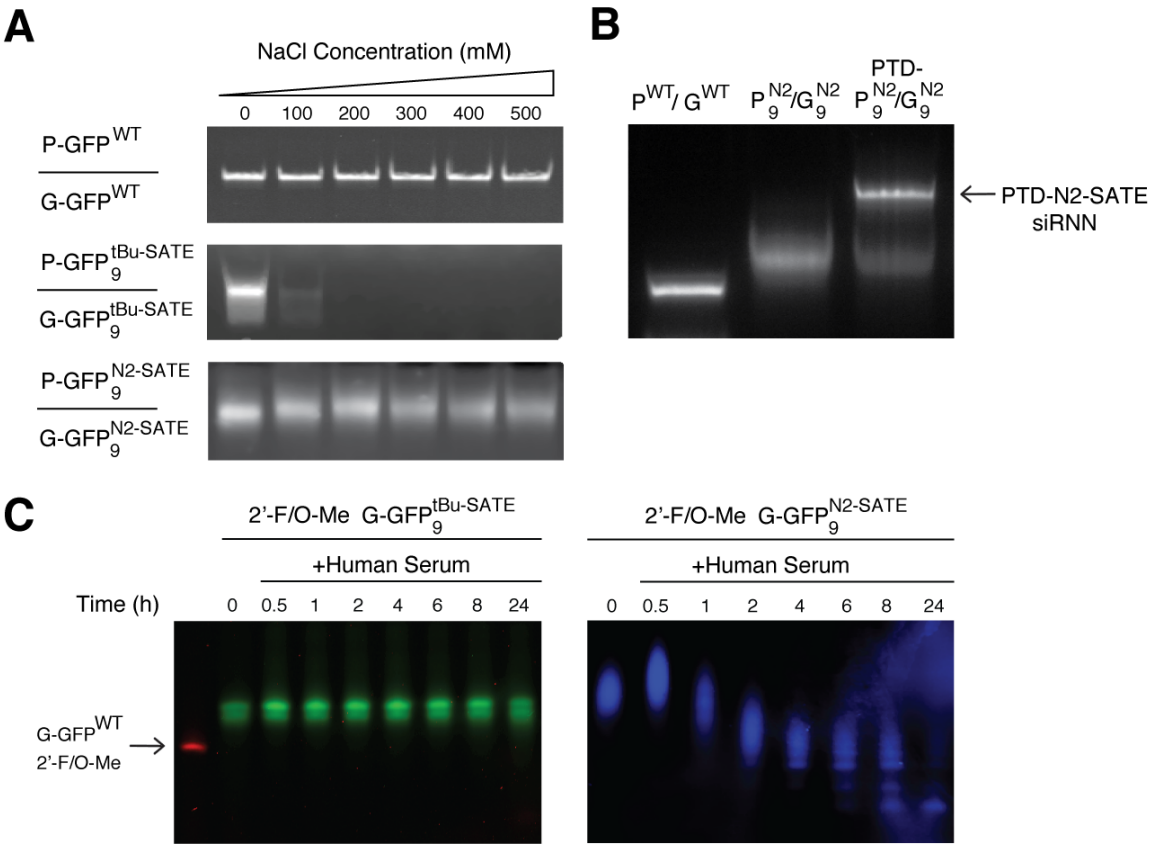

Figure 6.4. Solubility and stability of N2-SATE siRNN oligonucleotides. **A**) Nondenaturing gel analysis of P^{WT}/G^{WT}, $P_9^{tBu\text{-}SATE}/G_9^{tBu\text{-}SATE}$ and $P_9^{N2\text{-}SATE}/G_9^{N2\text{-}SATE}$ oligos in the presence of increasing amounts of NaCl. Note insolubility of tBu-SATE containing oligos in <100 mM NaCl and solubility of N2-SATE siRNN at greater than 500 mM. **B**) Representative example of SDS-PAGE analysis of TAT-N2-SATE siRNN conjugate. Note increasing migration of WT/WT, N2/N2 and PTD-N2/N2 from left to right. **C**) Stability analysis of 2'-F/O-Me 9xSATE or N2-SATE phosphotriester guide strand oligonucleotides incubated in 50% human serum at 37 ^{0}C for indicated times and analyzed on a 15% denaturing gel. 0 indicates starting input. Note stability of tBu-SATE phosphotriester RNN oligonucleotide and instability of N2-SATE phosphotriester RNN.

REFERENCES

Akinc A, Goldberg M, Qin J, et al. Development of lipidoid-siRNA formulations for systemic delivery to the liver. Mol Ther 2009;17:872-9.

Alvarez K, Vasseur JJ, Beltran T, Imbach JL. Photocleavable protecting groups as nucleobase protections allowed the sold-phase synthesis of base-sensitive SATE-prooligonucleotides. J Org Chem 1999;64:6319-6328.

de Fougerolles A, Vornlocher HP, Maraganore J, Lieberman J. Interfering with disease: a progress report on siRNA-based therapeutics. Nat Rev Drug Discov 2007;6:443-53.

Carpino LA, Han GY. 9-Fluorenylmethoxycarbonyl amino-protecting group. The Journal of Organic Chemistry 1972;37:3404.

Eguchi A, Meade BR, Chang YC, et al. Efficient siRNA delivery into primary cells by a peptide transduction domain-dsRNA binding domain fusion protein. Nat Biotechnol 2009;27:567-71.

Elbashir SM, Harborth J, Lendeckel W, Yalcin A, Weber K, Tuschl T. Duplexes of 21-nucleotide RNAs mediate RNA interference in cultured mammalian cells. Nature 2001;411:494-8.

Fields GB. Methods for removing the Fmoc group. Methods in Molecular Biology 1995;35:17-27.

Manoharan M. RNA interference and chemically modified small interfering RNAs. Curr Opin Chem Biol 2004;8:570-9.

Meade BR, Dowdy SF. Exogenous siRNA delivery using peptide transduction domains/cell penetrating peptides. Adv Drug Deliv Rev 2007;59:134-40.

Peyrottes S, Egron D, Lefebvre I, Gosselin G, Imbach JL, Perigaud C. SATE pronucleotide approaches: an overview. Mini Rev Med Chem 2004;4:395-408.

Schroeder A, Levins CG, Cortez C, Langer R, Anderson DG. Lipid-based nanotherapeutics for siRNA delivery. J Intern Med 2010;267:9-21.

Snyder EL, Dowdy SF. Recent advances in the use of protein transduction domains for the delivery of peptides, proteins and nucleic acids in vivo. Expert Opin Drug Deliv 2005;2:43-51.

Tosquellas G, Alvarez K, Dell'Aquila C, et al. The pro-oligonucleotide approach: solid phase synthesis and preliminary evaluation of model pro-dodecathymidylates. Nucleic Acids Res 1998;26:2069-74.

Villard AL, Coussot G, Lefebvre I, Augustijns P, Aubertin AM, Gosselin G, Peyrottes S, Perigaud C. Phenyl phosphotriester derivatives of AZT: variations upon the SATE moiety. Bioorg & Med Chem 2008;16:7321-29.

Whitehead KA, Langer R, Anderson DG. Knocking down barriers: advances in siRNA delivery. Nat Rev Drug Discov 2009;8:129-38.

Zorn C, Gnad F, Salmen S, Herpin T, Reiser O. Deprotection of N-Alloc amines by Pd(0)/DABCO – an efficient method for in situ peptide coupling of labile amino acids. Tetrahedron Letters 2001;42:7049-7053.

CHAPTER 7

CONCLUSIONS AND FUTURE DIRECTIONS

The discovery of RNAi by Fire and Mello and the subsequent observation that RNAi could be induced in human cells following the administration of synthetic siRNA molecules, transformed not only our understanding of gene regulation but also gave us an attractive therapeutic candidate for the intervention of human disease (Fire, et al.1998; Elbashir, et al. 2001). With EC_{50} values in the picomolar range and extreme selectivity for mRNA transcripts based on sequence complementarity, synthetic siRNA molecules remain at the forefront of potential therapeutics for the post-genomic age (Tiemann, et al. 2009). However, at ~14,000 Da and extreme acidity from the 40 phosphodiester backbone charges, naked siRNA molecules have extremely unfavorable pharmacokinetic and cellular delivery properties, being subject to both degradation and kidney filtration following systemic administration (Merkel, et al. 2009). Because of this, a significant amount of effort has been put forth in the last decade to develop safe and efficient siRNA delivery systems to begin to translate the power of RNAi into clinically-relevant settings.

Almost all siRNA delivery systems rely nanoparticle-based formulation strategies, the majority of which were engineered for antisense and gene therapy applications of the previous decade (de Fougerolles, et al. 2007). Generally, nanoparticle-based delivery strategies are composed of cationic lipids and

polymers that condense siRNA molecules into large ~100 MDa structures. This siRNA compaction is sufficient to shield the siRNA from RNase-mediated degradation as well as increase its circulation half-life by altering its biodistribution pattern following *in vivo* administration (Akinc, et al. 2009). Indeed, nanoparticle-based delivery systems have shown promise in multiple pre-clinical models of human disease following the condensation of siRNA molecules with cationic lipids, polymers and peptides (de Fougerolles, et al. 2007).

While some success has been shown, nanoparticle-based delivery strategies have also displayed significant drawbacks including notorioius cytotoxicity to primary cells in culture due to non-natural polymer composition, excessive liver filtration due to particle size requirements, poor *in vivo* diffusion constants and a need for exacting formulation conditions to ensure homogenously-sized particle mixtures (Schroeder, et al. 2010). In order to avoid inherent problems associated with nanoparticle-based siRNA delivery strategies, our laboratory has attempted to engineer soluble siRNA delivery systems without the use of large particle forming polymers. I have done so utilizing a class of small cationic peptides termed Peptide Transduction Domains (PTDs).

PTDs are small, ~8-20 amino acid peptides containing dense cationic residues crucial for cellular uptake. Following conjugation, PTDs have been shown to deliver a wide range of macromolecular cargo including peptides, proteins and charge-neutralized morpholino and PNA antisense oligonucleotides

(Snyder, et al. 2005). Indeed, PTDs are currently being tested in multiple phase I and II clinical trials for myocardial infarct, cancer and pain (Gump, et al. 2007). The cationic charge of the PTD is crucial for its ability to interact with the cell membrane, stimulate macropinocytotic uptake, and traffic and escape from endocytic vesicles (Wadia, et al. 2004). Unfortunately, upon covalent conjugation to siRNA molecules, PTD-siRNA conjugates have no cellular delivery properties resulting from the extremely anionic phosphodiester backbone of the siRNA molecule. Following PTD-siRNA conjugate formation, electrostatic neutralization prevents PTD-mediated uptake by blocking the critical cationic residues from interacting with the cell surface (Meade, et al. 2007).

In an attempt to avoid this electrostatic neutralization and develop soluble, monomeric PTD-siRNA conjugates, I began synthesizing a collection of siRNA oligonucleotides containing bioreversible, phosphodiester-neutralizing modifications. We termed this new class of siRNA oligonucleotides short interfering RiboNucleic Neutrals (siRNN). Theoretically, synthetic neutralization of the phosphodiester backbone would allow for successful PTD-siRNN conjugate delivery. Following cellular internalization, the biolabile phosphodiester-protected siRNN oligos would decompose back to RNAi compatible siRNA oligonucleotides to elicit efficient RNAi responses (Figure 3.1A).

In order to directly test the hypothesis that phosphodiester-neutral siRNA molecules could be delivered following PTD-conjugation, I set up oligonucleotide

synthesis conditions with surrogate non-bioreversible, methyltriester-modified siRNA oligonucleotides (Chapter 3). Using a GFP siRNA sequence as our template, I generated 15x methyltriester guide and passenger strand oligonucleotides ($P_{15}^{Methyl}/G_{15}^{Methyl}$). Following passenger strand aldehyde addition and guide strand cyanine dye (Cy3) addition, this surrogate siRNN molecule contains an overall anionic charge of (-)13 out of the total possible 43 negative phosphodiester charges. Conjugation and cellular treatment of monomer and multimer PTD-HyNic conjugates including TAT-HyNic, 2xTAT-HyNic and 3xTAT-HyNic indicated that the ability of a conjugated PTD to interact with the cell membrane requires the overall charge of the conjugate to be cationic, when simply counting anionic and cationic residues. Indeed, flow cytometry analysis of Cy3 uptake determined that the 2xTAT-siRNN (+3) and the 3xTAT-siRNN (+11) conjugates displayed increasing Cy3 uptake relative to their overall positive charge. This set of experiments not only proved the hypothesis that neutralized siRNA molecules could be delivered following PTD-conjugation but also defined the degree of neutrality that was necessary for successful PTD-siRNN conjugate delivery.

Scanning the literature for small molecule pro-drug phosphate modifications, we settled on the *t*-Butyl-S-Acyl ThioEthyl (*t*-Bu-SATE) moiety that has been shown to aid in the cellular uptake of multiple pro-drug compounds including the HIV reverse transcriptase inhibitor AZT (Peyrottes, et al. 2004). *t*-Bu-SATE phosphate protection allows for extracellular phosphate neutralization

and, following cellular uptake, cytoplasmic thioesterases efficiently process the *t*-Bu-SATE group inducing a two-step decomposition process resulting in a biologically-active charged phosphate compound (Figure 4.1A). Interestingly, tBu-SATE modifications have been attempted on deoxyoligonucleotide tester sequences to enhance the cellular uptake of antisense oligonucleotides. Of the few studies that exist, all reported the same inherent instability of the SATE thioester bond in basic conditions required for oliognucleotide deprotection (Tosquellas, et al. 1998; Guzaev, et al. 2001). Although alternative deprotecting strategies were successful in generating deoxyoligonucleotide tester sequences, to date, there have been no reports of biologically relevant SATE phosphotriester olignucleotides being tested on cells for biological activity as well as no reports of SATE-containing RNA oligonucleotides.

My work with t-Bu-SATE modifications defined the requirements for successful siRNN synthesis and deprotection including: 1) the use of 'Ultramild' 10% DIA/MeOH oligonucleotide deprotection conditions to avoid decomposition of the SATE modification; 2) insertion of RNAi-compatible 2'-F/2'-OMe modifications on SATE-adjacent ribose rings to avoid 2' OH nucleophillic attack and strand scission; and 3) a maximal insertion amount of ~50% due to steric congestion across the major groove of the dsRNA molecule. With these rules in hand, I successfully synthesized, deprotected and purified *t*-Bu-SAT-modified GFP siRNNs. Impressively, transfection of *t*-Bu-SATE siRNNs into cells resulted in intracellular *t*-Bu-SATE cleavage, loading into Ago2, and induction of robust

target-specific RNAi responses. In contrast, control siRNNs containing irreversible phosphotriester linkages were not cleaved or loaded into Ago2, and did not induce RNAi responses. Importantly, this is the first study reporting a new class of biologically active, bioreversible phosphotriester RNAi-inducing molecules (Chapter 4).

Due to the limitation of phosphotriester insertions for *t*-Bu-SATE groups of ~50%, conjugation to highly cationic PTD multimers was needed to create PTD-siRNN conjugates with overall cationic charge. Unfortunately, attempts to conjugate, purify and treat cells with a PTD-siRNN conjugate in a soluble, monomeric form was futile due to extensive hydrophobicity associated with the *t*-Bu-SATE modification. To overcome this hydrophobicity, manipulation of the terminal *t*-butyl group of the SATE phosphotriester was done to increase the overall hydrophilicity of the siRNN oligonucleotide. This was initially attempted by decreasing the carbon content of the t-butyl moiety (Chapter 5). Unfortunately, distal methyl reductions of the t-Bu-SATE to Me- and Et-SATE modifications resulted in a significant decrease in stability during 'Ultramild' oligonucleotide deprotection conditions.

I hypothesized that this mechanism of base-mediated decomposition for Me- and Et-SATE was similar to the two-step decomposition process that occurs following thioesterase cleavage. To alter the kinetics of base-mediated decay and create more stable Me- and Et-SATE distal modifications, proximal methylene group increases were made between the thioester and

phosphotriester groups to decrease the rate of decomposition by altering the efficiency of by-product formation. Indeed, creation of S-Acyl ThioButyl (SATB) linkages sufficiently stabilized the modification for isolation of Me- and Et-SATB siRNN oligonucleotide deprotection. These oligonucleotides displayed RNAi activity in cells in culture comparable to both wildtype phosphodiester siRNA and *t*-Bu-SATE siRNN oligonucleotides. Unfortunately, distal methyl group reduction required proximal methylene group addition, thus the overall hydrophobic character of the phosphotriester modification was not altered. While this series of experiments was an example of the manipulation that can be done to the SATE modification to effect synthetic stability without the loss of biological function, Me- and Et-SATB were not further processed due to a lack of reduction of the overall hydrophobicity of the siRNN oligonucleotide (Chapter 5).

SATE-containing siRNN oligonucleotides possess two fundamental problems for the generation of PTD-siRNN conjugations: 1) due to steric congestion across the major groove, the number of SATE-phosphotriester insertions is limited to ~50% requiring the use of highly cationic PTD multimers for the creation of overall positively-charged PTD-siRNN conjugates; and 2) the hydrophobic nature of the SATE modification results in insolubility in biologically-relevant solutions for both the siRNN and PTD-siRNN conjugates. Due to these two fundamental difficulties, I began the synthesis of Amino-SATE (N-SATE) siRNN oligonucleotides containing terminal primary amines on the SATE moiety (Chapter 6). While the number of insertions onto the backbone of the siRNN

molecule will remain restricted to ~50%, insertion of N-SATE groups should theoretically act as a 2-for-1 modification; decreasing the anionic charge by insertion of a phosphotriester-modification and also imparting a cationic charge from the primary amine. Thus, an ~50% inserted N-SATE siRNN would require conjugation to less cationic PTD multimers compared to the t-Bu-SATE siRNN due to the donation of cationic charges from the primary amines. Additionally, installation of primary amines should also positively affect the solubility of siRNN oligonucleotides in aqueous solutions.

Phosphoramidite and oligonucleotide synthesis of N-SATE modifications requires the use of amine protection in order to prevent any unwanted size chain reactions. Importantly, amine-protecting groups must also be orthogonal with phosphoramidite and oligonucleotide synthesis conditions as well as possessing the capability of undergoing deprotection in conditions compatible with SATE-phosphotriester stability. After scanning multiple primary amine protection strategies, I settled on Alloc-N-SATE protection due to its ability to be successfully deprotected in the presence of a palladium catalyst to generate primary amine-containing N-SATE siRNN oligonucleotides. Indeed, maximally-modified N-SATE siRNN were efficiently synthesized, shown to induce robust RNAi activity in cells in culture, and finally, displayed significant increases in solubility compared to the SATE siRNNs in biological-relevant solutions and solutions of high ionic strength (Chapter 6). Currently, PTD conjugation reactions

are underway with N-SATE siRNN oligonucleotides to test the ability of PTD-siRNN conjugates to be a viable siRNA delivery platform.

Work with the N-SATE modification defined certain characteristics for primary amine installation on the SATE phosphotriester including: 1) increasing the distance of the terminal primary amine from the thioester group positively influences the stability to 'Ultramild' basic deprotection conditions; 2) primary amine protecting groups must be capable of deprotection in non-basic solutions due to the significant instability of a naked N-SATE to basic conditions; and 3) careful handling following N-SATE siRNN generation is necessary as N-SATE phosphotriesters appear to undergo spontaneous decomposition in standard biological media.

Technically, while I have successfully generated N-SATE siRNN oligonucleotides, the yield loss associated with the current deprotection steps is potentially rate-limiting for the future of N-SATE siRNN olignucleotide generation. This yield loss can be attributed to a couple of factors including: 1) the need to purify full-length Alloc-N-SATE oligonucleotides prior to palladium catalysis due to reversal events that occur during 'Ultramild' 10% DIA/MeOH deprotection; and 2) yield loss associated with palladium-mediated deprotection and subsequent purification following RP-HPLC direct injection. To overcome these technical difficulties, we are currently engineering UV light-sensitive protecting groups for nucleobase, N-SATE and wildtype phosphodiester protection. The benefit of UV-sensitive protecting groups would be the ability to have a one-pot reaction step

for efficient oligonucleotide and N-SATE deprotection, avoiding the use of 10% DIA/MeOH and the multi-step purification process that is necessary to generate N-SATE siRNN with the current protocol. Indeed, recent results have demonstrated the ability to generate UV-sensitive N-SATE siRNN oligonucleotides and successfully deprotect primary amines following exposure to UV light (data not shown).

Of more immediate concern however, is the instability of N-SATE modifications following addition to biological media. Current negative results of PTD-siRNN conjugate induction of RNAI are difficult to interpret due to the decomposition occurring with the N-SATE phosphotriester upon addition to cells in biological media. Interestingly, this decomposition has been only shown to occur in common biological medias including DMEM, MEM and RPMI while not occurring in water or phosphate buffers at pH 7.2. A potential mechanism for N-SATE spontaneous decomposition results from intramolecular nucleophilic attack of the primary amine onto the adjacent thioester and subsequent decay to the phosphodiester (Figure 7.1A). While this reaction is not occurring in water or phosphate buffers at pH 7.2, this decomposition could also be due to some common nucleophile used in biological media. I am currently analyzing N-SATE stability in various biological media components as well as engineering minimal nutrient media assaying both N-SATE stability and cellular viability.

Lastly, in an attempt to engineer around the instability of the N-SATE modification while still retaining enhanced solubility properties, we have begun

synthesis of Pyrrolidine N-SATE (NP-SATE) phosphoramidites and oligonucleotides (Figure 7.2B). Theoretically, NP-SATEs should be more stable than N-SATEs in biological media due to sterics associated with the pyrrolidine ring. Indeed, recent results indicate the higher stability of NP-SATEs to oligonucleotide deprotection conditions indicating a potential increased stability in biological media (data not shown). Currently, olignucleotide synthesis is being undertaken to determine the ability of NP-SATE to act as bioreversible, neutralizing modifications for successful PTD-siRNN delivery.

In conclusion, my thesis work has shown: 1) the first complete synthesis and purification of RNA oligonucleotides containing bioreversible, phosphotriester modifications; 2) the first example of intracellular, biological conversion of SATE phosphotriester-modifications on any oligonucleotide (RNA or DNA); and 3) the first example of any bioreversible, phosphotriester containing oligonucleotide (RNA or DNA) to elicit a phenotypic cellular response. Moreover, during the course of my studies, I have successfully synthesized, deprotected, purified and biologically assayed siRNN oligonucleotides with over 20 different bioreversible phosphotriester variations, seven of which required the design, synthesis and deprotection of orthogonal protecting groups compatible with overall siRNN integrity. Importantly, this work represents an entirely novel siRNA synthetic route to generate monomeric siRNA pro-drug templates to overcome inherent problems associated with current liposome and nanoparticle siRNA therapeutic

strategies and potentially opens the door to an entirely new field of developing RNAi therapeutics.

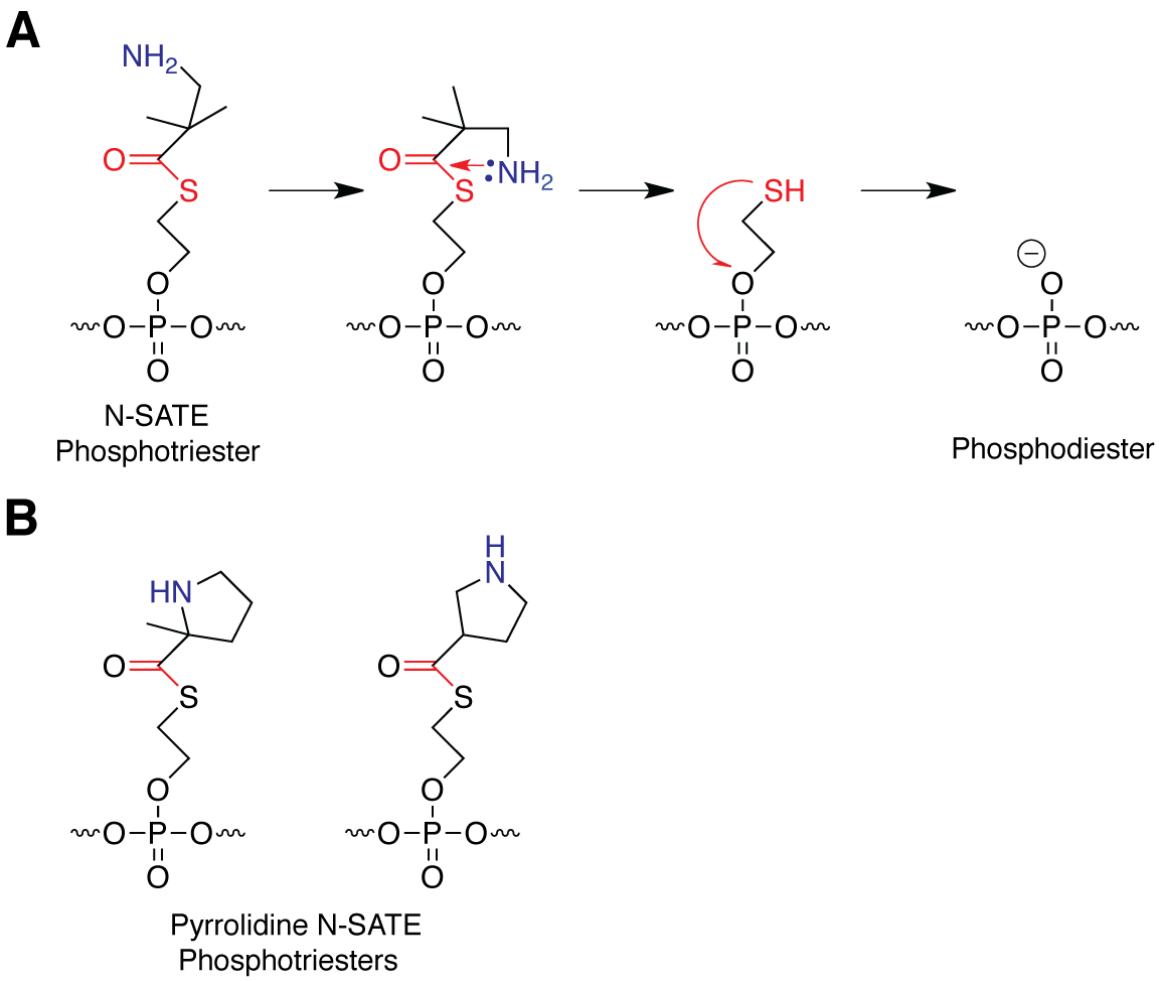

Figure 7.1. Proposed decomposition mechanism for N-SATE phosphotriesters. A) Theoretical scheme for N-SATE decomposition mechanism. Intramolecular nucleophilic attack results in thioester decomposition and phosphodiester conversion. **B**) Structure of Pyrrolidine N-SATE (NP-SATE) phosphotriesters to avoid intramolecular decay of N-SATEs.

REFERENCES

Akinc A, Goldberg M, Qin J, et al. Development of lipidoid-siRNA formulations for systemic delivery to the liver. Mol Ther 2009;17:872-9.

de Fougerolles A, Vornlocher HP, Maraganore J, Lieberman J. Interfering with disease: a progress report on siRNA-based therapeutics. Nat Rev Drug Discov 2007;6:443-53.

Elbashir SM, Harborth J, Lendeckel W, Yalcin A, Weber K, Tuschl T. Duplexes of 21-nucleotide RNAs mediate RNA interference in cultured mammalian cells. Nature 2001;411:494-8.

Fire A, Xu S, Montgomery MK, Kostas SA, Driver SE, Mello CC. Potent and specific genetic interference by double-stranded RNA in Caenorhabditis elegans. Nature 1998;391:806-11.

Gump JM, Dowdy SF. TAT transduction: the molecular mechanism and therapeutic prospects. Trends Mol Med 2007;13:443-8.

Guzaev AP, Bhat B, Balow G, Manoharan M. Synthesis of chimeric oligonucleotides containing internucleosidic phosphodiester and S-pivaloylthioethyl phosphotriester residues. Nucleosides Nucleotides Nucleic Acids 2001;20:1015-8.

Meade BR, Dowdy SF. Exogenous siRNA delivery using peptide transduction domains/cell penetrating peptides. Adv Drug Deliv Rev 2007;59:134-40.

Merkel OM, Librizzi D, Pfestroff A, Schurrat T, Behe M, Kissel T. In vivo SPECT and real-time gamma camera imaging of biodistribution and pharmacokinetics of siRNA delivery using an optimized radiolabeling and purification procedure. Bioconjug Chem 2009;20:174-82.

Peyrottes S, Egron D, Lefebvre I, Gosselin G, Imbach JL, Perigaud C. SATE pronucleotide approaches: an overview. Mini Rev Med Chem 2004;4:395-408.

Schroeder A, Levins CG, Cortez C, Langer R, Anderson DG. Lipid-based nanotherapeutics for siRNA delivery. J Intern Med 2010;267:9-21.

Snyder EL, Dowdy SF. Recent advances in the use of protein transduction domains for the delivery of peptides, proteins and nucleic acids in vivo. Expert Opin Drug Deliv 2005;2:43-51.

Tiemann K, Rossi JJ. RNAi-based therapeutics-current status, challenges and prospects. EMBO Mol Med 2009;1:142-51.

Tosquellas G, Alvarez K, Dell'Aquila C, et al. The pro-oligonucleotide approach: solid phase synthesis and preliminary evaluation of model pro-dodecathymidylates. Nucleic Acids Res 1998;26:2069-74.

Wadia JS, Stan RV, Dowdy SF. Transducible TAT-HA fusogenic peptide enhances escape of TAT-fusion proteins after lipid raft macropinocytosis. Nat Med 2004;10:310-5.